Title

Inflammasome regulation of adaptive immunity

Author

Deets, Katherine

Publication Date

2021

Peer reviewed|Thesis/dissertation

Inflammasome regulation of adaptive immunity

By

Katherine Deets

A dissertation submitted in partial satisfaction of the

requirements for the degree of

Doctor of Philosophy

in

Molecular & Cell Biology

in the

Graduate Division

of the

University of California, Berkeley

Committee in charge:

Professor Russell E. Vance
Professor Ellen A. Robey
Professor David H. Raulet
Professor Shauna Somerville

Fall 2021

Inflammasome regulation of adaptive immunity

Katherine Deets

Abstract

Inflammasome regulation of adaptive immunity

By

Katherine Deets

Doctor of Philosophy in Molecular & Cell Biology

University of California, Berkeley

Professor Russell E. Vance, Chair

The innate immune system detects pathogens and initiates adaptive immune responses. Inflammasomes are central components of the innate immune system, but whether inflammasomes provide sufficient signals to activate adaptive immunity is unclear. In this dissertation, I present the work I have done using a genetic mouse model system that allowed me to simultaneously express the model antigen ovalbumin (Ova) and activate the NAIP–NLRC4 inflammasome in specific cells throughout the mouse.

Chapter One begins with an introduction to innate and adaptive immunity. I then provide an overview of inflammasome activation, followed by a discussion of what is currently known about how inflammasomes influence adaptive immunity. This section discusses the roles inflammasome-driven lytic cell death (termed pyroptosis) might play in antigen release, evidence for inflammasome activation driving $CD4^+$ and $CD8^+$ T cell responses, and instances where inflammasome activation appears to inhibit adaptive immunity. This chapter closes with evidence for inflammasomes influencing adaptive immunity in vaccines, anti-tumor immunity, and autoimmunity. Overall, Chapter One provides a foundation for appreciating why we need better understanding of the role inflammasome activation plays in driving adaptive immune responses.

In Chapter Two, I present my early doctoral work, where I began to explore what role(s) NAIP–NLRC4 inflammasome activation might have on adaptive T cell immunity. Here I introduce the OvaFla mouse model previously, which was described by the Vance lab. These mice use the Cre-Lox system to inducibly express a fusion protein containing Ova antigen and the 166 amino acid C-terminal of flagellin, which will activate NAIP–NLRC4 but not an alternative flagellin sensor called TLR5. For experiments in this chapter, I crossed these “OvaFla” mice with mice containing a tamoxifen-inducible Cre driver, Cre-ER^{T2}, that results in systemic OvaFla expression following tamoxifen administration. I found that systemic OvaFla can drive cross priming of $CD8^+$ T cells in both WT and NLRC4-deficient mice. However, because Cre-ER^{T2} is expressed throughout the mouse, we remain unsure where and how this cross priming is occurring. I did determine, however, that signaling through the IL-18R on cross presenting cells is not required for $CD8^+$ T cell activation. One potential benefit to the

OvaFla Cre-ER^{T2} system is that localized tamoxifen application can be used to drive a more focused Cre expression. Additionally, bone marrow-derived cells from these mice retain the ability to activate OvaFla, which may be useful for future *in vitro* studies. In all, the work presented in this chapter provides some initial insights into the OvaFla Cre-ER^{T2} system, with suggestions on how they may be a useful tool for others.

Chapter Three describes the bulk of my doctoral work, which specifically focused on activation of the NAIP–NLRC4 inflammasome in intestinal epithelial cells (IECs). NAIP–NLRC4 activation in these cells results in IEC pyroptosis, followed by an expulsion of the IEC into the intestinal lumen. One of my original hypotheses was that pyroptosis, which is mediated by the pore-forming protein Gasdermin D, provides an opportunity for cytosolic antigen to escape into the underlying lamina propria. In the lamina propria, the antigen is theoretically available to be cross-presented on dendritic cells (DCs), which can then drive antigen-specific CD8$^+$ T cell activation. To test this hypothesis, I crossed the OvaFla mice with the Villin-Cre-ER^{T2} mice, thereby creating animals where tamoxifen administration results in robust OvaFla expression in IECs. These OvaFla Villin-Cre-ER^{T2} mice were crossed onto Gasdermin D-, ASC-, and NLRC4-deficient backgrounds.

In support of my hypothesis, my work showed that IEC-derived antigens can be cross presented to CD8$^+$ T cells *in vivo*, but we were surprised to find that this cross presentation occurred in both WT and NLRC4-deficient OvaFla mice. Additionally, Gasdermin D-mediated pyroptosis played only a partial role in CD8$^+$ T cell cross-priming. My project then shifted to understanding whether there were any mechanistic differences in antigen cross-presentation between inflammatory conditions (NLRC4-dependent) and steady state (NLRC4-independent). By using two separate genetic knockout mouse lines, I found that cross presentation of IEC antigens during non-inflammatory conditions (in NLRC4-deficient mice) relies on a subset of classical DCs (cDCs) that require the *Batf3* transcription factor (cDC1s)—these findings align with previously published data. However, in the presence of inflammasome activation, a *Batf3*-independent cDC population (likely cDC2s) can cross present IEC-derived antigen. Altogether, these data provide a better understanding of the complex interactions between IECs, DCs, and CD8$^+$ T cells in the gut.

In Chapter Four, I close my dissertation with a discussion on some of the remaining questions generated from my work. These questions center around the mechanism(s) of antigen acquisition functional maturation of the cross presenting cDCs.

In all, my dissertation work has provided a stripped-down approach to understanding how inflammasome activation influences adaptive immunity. Unlike previous studies that rely on infection models, the OvaFla system allowed me to selectively activate the NAIP–NLRC4 inflammasome and uncover a *Batf3*$^+$ cDC1-independent pathway of IEC antigen cross presentation.

Table of Contents

Abstract 1

Table of Contents i

Acknowledgements iii

Chapter One: Introduction 1

1.1 Introduction to innate and adaptive immunity 1
1.1.1 Innate immunity 1
1.1.2 Adaptive immunity 2
1.1.3 Innate activation of adaptive immunity 3

1.2 The immune system at epithelial barrier surfaces 5

1.3 Inflammasomes and adaptive immunity 5
1.3.1 Overview of inflammasomes 5
1.3.2 Fate of pyroptotic cell antigens 8
1.3.3 Antigen release from pyroptotic epithelial cells 9
1.3.4 Inflammasomes and $CD4^+$ T cell responses to pathogens 10
1.3.5 Inflammasomes and $CD8^+$ T cell responses to pathogens 11
1.3.6 Impairment of adaptive responses by inflammasomes 12
1.3.7 Inflammasome activation by vaccines 13
1.3.8 Inflammasomes and the adaptive response to cancer 14
1.3.9 Broader roles of pyroptosis in cancer immunity 15
1.3.10 Inflammasomes and Autoimmunity 16

1.4 Concluding remarks 17

Chapter Two: Following the $CD8^+$ T cell response in OvaFla Cre-ER^{T2} system 18

2.1 Introduction 18

2.2 Results 19
2.2.1 Genetic system for systemic OvaFla production activates NAIP–NLRC4 19
2.2.2 OT-I T cell response in OvaFla Cre-ER^{T2} mice 21
2.2.3 Neonatal chimeras as a potential tool to reduce the number of OvaFla producing cells in the Cre-ER^{T2} system 23
2.2.4 Concentration of OvaFla expressing cells in OvaFla Cre-ER^{T2} system 25
2.2.5 Irradiation bone marrow chimeras with OvaFla Cre-ER^{T2} mice 32
2.2.6 No role for the IL-18 receptor on cross-priming following NAIP–NLRC4 activation 34

2.3 Discussion 36

Chapter Three: Inflammasome activation leads to cDC1 independent cross-priming of CD8 T cells by epithelial cell derived antigen 38

3.1 Introduction 38

3.2 Results 38
3.2.1 IECs undergo pyroptosis prior to expulsion following NAIP–NLRC4 activation 38
3.2.2 Genetic system for NAIP–NLRC4 activation in IECs 40
3.2.3 $CD8^+$ T cell activation by epithelial antigens 45
3.2.4 Cross-presentation of IEC antigens 50
3.2.5 NAIP–NLRC4 activation drives *Batf3*$^+$ cDC1-independent cross presentation 55
3.2.6 cDCs are required for cross-presentation of IEC derived antigen 63

3.3 Discussion 67

Chapter Four: Remaining questions and final thoughts 71

4.1 What are the NAIP–NLRC4-dependent signals that drive *Batf3*-independent cross priming of IEC antigens? 71

4.2 How are antigens from steady-state IECs acquired by *Batf3*-dependent cDC1s? How are antigens from pyroptotic IECs acquired by *Batf3*-independent cDCs? 71

4.3 Are the cross-primed OT-I T cells activated in the presence and absence of NAIP–NLRC4 activation functionally similar? Are they able to protect from future challenge with SIINFEKL-expressing pathogens? 72

4.4 Final thoughts 73

Materials and Methods 74

References 83

Acknowledgements

It takes a village to raise a scientist. It should be obvious that behind any individual's success is a long list of supportive friends, family, and colleagues, but we rarely take the opportunity to consider all the help we've received and thank everyone that has been there for us. Writing the extensive list of acknowledgements that follows here gave me the chance to pause and reflect on the people that have had a positive impact on my life as a scientist. After a long, emotional six and a half years, I found that these acknowledgements act at the cathartic capstone to my time as a PhD student at UC Berkeley.

Before I acknowledge the wonderful friends and family that have carried me through, I need to start by recognizing that a lot of my success is also due to the privileges I have as a white, cis, able-bodied, US-born individual from a middle-class family. Although I cycled through many career interests early in life, I never experienced any fear or uncertainty about my future because of my race, my physical abilities, or my family's income or immigration status. I was almost always able to find a face that looked like mine among a group of athletes, musicians, physicians, or scientists. And with only two clear exceptions—a male orthopedic surgeon and a male college professor—no one ever told me I couldn't achieve my dreams. My parents had enough money that I could pursue most of my interests, and they had enough free time to come to nearly every competition, performance, and parent-teacher conference. Growing up, I took these privileges for granted. Only now when I look back do I start to understand how much I have benefit from being a white, middle-class citizen in an often racist, classist, ableist, nationalistic country.

These privileges served me throughout my graduate career as well. Nobody ever questioned whether I was a doctoral student or whether I belonged in a campus building at night. I never felt fear in the presence of a University of California police officer or fear that I would be deported from this country. I did not have any financial dependents or major medical bills. I never needed to jump through any hoops to make sure my work and learning spaces were accessible to my needs. There were no language or cultural barriers for me to overcome, and I felt comfortable being my true self around my colleagues. Although I worked incredibly hard to earn my PhD, I must acknowledge that there are many others who needed to work much harder to reach the same finish line.

My family has been a large source of support during my journey to obtaining a PhD. My parents Mary and Tony, and my two sisters Gena and Anna, have always had an endless amount of faith in me, and for that I cannot thank them enough.

Although my sisters and I are distant in age and miles, we will always share that unique sibling bond. I thank Anna for being such a strong supporter of women in STEM and for always appealing to my inner nerd. I also appreciate that she's one of those rare people that always backs whatever crazy ideas I have, no questions or judgement. I thank Gena for being one of my biggest cheerleaders throughout my life, whether I appreciated it in the moment or not. We have been through a lot together, but at the end of the day, knowing that she will always be there for me is a gift for which I can never say Thank You enough.

I thank my dad for the obsessive curiosity he passed down to me. I am forever inspired by the wide array of interests he has in the world around him, and I deeply cherish our long conversations about meteorology, geology, and everything in between. He is also one of the few people in my life that understands many of my idiosyncrasies and how they make me who I am. His understanding and support mean the world to me.

My mom has earned a special set of acknowledgements. From her I have learned to be kind, patient, and genuine, even in the face of adversity. There was a time in 2013 when nobody thought she would be around to watch me even apply to graduate programs, let alone sit in the audience for my dissertation finishing talk several years later. But damn she is one of the most persistent, strong-willed people I have ever met, and so I can tell her Thank You here in these acknowledgements and know that she will be reading them for many more years to come. Her unconditional love and support have gotten me through tough many times, and I face my future knowing that she will always be there for me.

Following my family, I owe a considerable amount of gratitude to my best friend and partner Ben LaFrance. We met while I was interviewing for the UC Berkeley MCB program, and he has been enthusiastically supporting my dreams ever since. Ben is one of the most present, kind, and generous people I have ever spent time with. As already mentioned, I have a lot of idiosyncrasies, including a thought process that can be very difficult to follow on a good day. But Ben has shown me more patience and understanding than possibly anyone else I've met, and he genuinely loves me for who I am. His support as a friend, partner, and adventure companion kept me afloat throughout graduate school, and I feel so damn lucky to have him in my life. I really cannot thank him enough for all the love and kindness he has shared with me.

I have many other friends to thank as well. People say misery loves company, and the misery of graduate school has given me the gift of some of the best company I could ever ask for. Over the last six and a half years, I have collected a group of the most supportive, wonderful humans, and I hope our friendships last long past the memories of thesis committee meetings and those terrible pizza lunches on Graduate Student Appreciation Day.

One of my most cherished friendships from my time at UC Berkeley is that with Shally Margolis. We began our journey together as a pair of opposites that shared a rotation in the Portnoy lab, but we forged a bond in the Vance Lab Bistro, and Shally quickly became the fun, spirited, outgoing Ying to my grumpy old Yang. As my baymate, classmate, and close friend, she has been there for me nearly every day, through all of the really fun and really terrible experiences I've had in the last six and a half years. I genuinely do not know if I would have survived graduate school without her eternal patience and willingness to listen, and I don't think I could have thrived without her unbreakable spirit and endless support.

For my life outside of science, I have been lucky to share the support of one of the most awesome, badass people I've ever met, Laura Nocka. My love of physical activity has long been an important foundation for my mental health, and Laura has become one of my all-time favorite co-conspirators. She's a rare find in that she is

always down to anything, anytime, and she will never complain about something being too easy, too hard, or too boring. I am so thankful that a chance meeting in the climbing gym has led to what I hope will be a lifelong friendship, no matter where we end up.

When I'm not in lab or outside, the third slice of my life occurs at home, where I have also been extremely lucky to build treasured, long-lasting friendships. I began my time in Berkeley at the Hariharmon House with Sam Fernandez, Ryan Muller, and Kurtresha Worden. I could not have asked for a more kind and humbly brilliant group of people to start graduate school with. I owe Kurtresha an extra big Thank You for putting up with me as a housemate for another three and a half years on Ward St. Having a safe space at home to laugh, relax, and air my grievances made the daily stresses of life in graduate school much easier to bear.

I would also like to acknowledge the friends I made and all the other folks I worked with during my four years as an editor for the *Berkeley Science Review*. I often joked that the BSR gave me "something other than science to complain about", but I am confident that my experiences with the magazine helped me build communication and management skills that will benefit me for years to come. I am especially grateful for the friendship I forged with my classmate and fellow editor Hayley McCausland. Our comradery began as a misery-loves-company connection, but Hayley quickly became part of my crucial support network, and she will always be one of my favorite Berkeley people.

I have many other friends and non-lab colleagues that I need to thank for the support they gave me during my time at UC Berkeley. Shally and I shared our small 2015 Immunology & Pathogenesis sphere with two other classmates, Erik Van Dis and Nick Lind. The four of us supported each other as we studied for classes and our Qualifying Exams, as we struggled through the doldrums of third, fourth, and fifth year, as our projects let us down again and again, and as the SARS-CoV-2 pandemic pulled the rug out from under our feet. I am also thankful for the support and friendship from my classmate and fellow Seattleite Mathew Summers—Go Hawks! And for the kindness and camaraderie from both Victoria Chevee and Ellie Bondra. There is also a very special place in my heart for my badass climbing friend Josh Cofsky. These people, and many more, have filled my time at UC Berkeley with love and support, and I am so grateful to each and every one of them.

I have also received a tremendous amount of love and support from my dear friends Dom and Caitlin Castanzo. I consider myself lucky that they came as a package deal with my partner Ben, and they have opened their door and hearts to me as well. Nearly every Wednesday for the last few years, they have provided me with a home cooked meal and a place to relax, and I cannot thank them enough for their friendship.

Along with Dom and Caitlin, my relationship with Ben also brought his wonderful parents, Dan and Kay LaFrance, into my life. They are two unbelievably awesome and caring people, and they have become a cherished second family to me.

Last—but certainly not least—on my list of close non-lab friends that I need to acknowledge are Katie Wieliczkiewicz and Jasmine Davis. These two amazing ladies are my best friends from college, and they have managed to stick it out with me since we graduated together nearly 10 years ago. They have always provided me with a judgement-free space to tell stupid stories, complain about anything and everything, or brag about something petty.

One of the best choices I made as a graduate student at UC Berkeley was to join the Vance lab, and I owe a tremendous amount of gratitude to everyone that I shared time with while I was there. The lab always felt like an extended family to me. I know that I am incredibly fortunate to have such a kind, fun, and scientifically and emotionally supportive environment to work in each and every day, and I look forward to staying connected with everyone for years to come.

I need to say a very, very big Thank You to my first mentor of graduate school, Bella Rauch. As a postdoc in the Vance lab, she immediately made me feel like I had a home away from home in the Bay Area, and she continues to support me as a close friend and colleague to this day from her badass PI position at the Oregon Health & Science University. I am especially grateful for how she has taught me to have faith in myself as a scientist. It is far too easy to get caught up in scientific failures and negativity, but Bella always provides a clear and realistic-yet-hopeful perspective that helps me stay focused. I am thankful beyond words for her support over the last six years, and I hope to replicate her mentorship qualities as I become a postdoc myself.

Another former Vance lab postdoc, Patrick Mitchell, also played an important role in helping me become a competent and confident scientist. I'd like to thank him specifically for the kindness and patience he gave me—even during the times I rambled on about mouse T cells or the gel doc printer paper. I am also especially grateful for the unique scientific perspectives he brought to the lab as a virologist trained in host-pathogen evolution. These perspectives helped push the Vance lab research in new and exciting directions, and they were a large driver behind my decision to pursue a postdoc position in the Elde lab. I am also thankful that Patrick was also always there to sooth my Seattle homesickness—Go Hawks!

I'd also like to say Thank You for all of the friendship, support, and laughs I received from former postdoc Lívia Yamashiro. As I slipped into the weary, jaded phase of my PhD project, Lívia became a crucial confidante of mine that was always there to share a smile or an appropriately timed eye roll. She listened to my concerns and complaints, whether they were trivial or not, and provided faith and hope when my own ran dry. I appreciate all of the time we got to spend together and look forward to staying in touch.

Aside from Shally, I believe I owe Justin Roncaioli the most amount of thanks for putting up with my shenanigans day in and day out. Because our bench and desk space faced one another, Justin was subject to all of my verbal processing (and accidental kicking), and he handled it with patience and kindness. I am grateful for our many long discussions that spanned from intestinal immunity and mouse husbandry to politics and the effects of White privilege. He also played a vital role in maintaining the strong sense of community held among the Vance lab grad students over the last few years.

There is a long list of other Vance lab people I need to thank. Kristen Witt and Elizabeth Turcotte are two amazingly kind graduate students that are always willing to lend an ear, even when they themselves were bogged down by science and life. Former postdoc Jordan Price has been a gift that keeps on giving through his humor and honest career advice. As the lab's flow cytometry and confocal microscopy know-it-all—and the only other Vance lab member that cares much for adaptive immunity—postdoc Dmitri Kotov became a highly valued source of knowledge and scientific advice for me the last few years. I'd like to thank former postdoc Andrew Sandstrom, another beloved

Seattleite (Go Hawks), for his role as the patient biochemist friend to this cellular immunologist. The Vance lab's newest graduate student Janet Peace Babirye has become a quick friend, and I appreciate her humor and patience as I hone my mentorship skills with her. I am thankful for the tenacity of Brenna Remick and Marian Fairgrieve, who had the unfortunate timing of joining the lab as new grad students in the depths of the pandemic. Moritz Gaidt has provided me with a lot of thoughtful feedback and has also been kind enough to share his unbelievably adorable son Justus and his wife Julia with our lab over the last few years.

I also need to thank the Vance lab grad students from my early days. Jeannette Tenthorey and Randilea Nichols Doyle helped induct me and Shally into the Vance lab culture. I owe Randilea an extra Thank You for helping me get started on the OvaFla project. Daisy Ji provided a lot of sage graduate student advice and served as proof that it is possible to make a stunning comeback after being scooped. Justin De Leon showed me that scientists can be both serious and fun, and I owe him a bonus Thank You for teaching me the art of ribbing Russell and Greg Barton (Go Hawks!).

There are two other Vance lab members that I need to give a special set of acknowledgements to. They are (now former) lab manager Peter Dietzen and former mouse technician (now lab manager) Roberto Chavez. Peter undertook the daunting task of maintaining peace and order in the large, mildly chaotic, and often rambunctious Vance lab, and he somehow always came out the other side smiling. He put up with a lot of my crap and usually took my nagging and grumbling in stride. I very genuinely appreciate Peter's years of patience and laughter. Roberto also gifted me with years of patience and kindness. As the keeper of our mouse colony, he very likely deserves the biggest slice of credit for my PhD project. I cannot overstate how indebted I am to the hours and hours of time he saved me by helping maintain my vast array of mice and dealing with the constant comings and goings of OLAC. I am so grateful for his hard work, organization, good communication, and genuinely easygoing personality. I also need to add a shout-out to Roberto's replacement, Joceline Morales. She has done a terrific job at filling Roberto's shoes, and I really appreciate the work she is currently doing to help maintain my mouse colony as my project ramps down.

I also owe many thanks to the other folks involved in keeping my mouse colony up and running. I had the privilege of working closely with two very smart, driven, and wonderful undergraduates, Andy Contreras and Ashley Chu. Learning the ins and outs of mouse husbandry and genotyping is a daunting task for any person, but taking on that responsibility as an underclassman with little biology background is especially challenging. Both Andy and Ashley far exceeded my expectations and were a genuine pleasure to worth with. I enjoyed being able to watch them both learn and grow as students and am thankful to have had them in my life. I also owe many, many thanks to a few key OLAC staff members. It can be difficult to find (and keep) good technicians in the animal facilities, but Terrance Thompson, Ricky Victoriano, and Caroline Kim were three genuinely amazing technicians I was lucky enough to work with at UC Berkeley. I really appreciated their continual efforts and kindness day in and day out. I'd also like to thank facility supervisors Richard Duru and Markshaun Fields. Markshaun gets an extra shout-out for rescuing me from a locked door on a weekend. And I'd like to say Thank You to Vet Staff member Dr Kelly Jensen for her kindness, patience, and genuine desire to help keep our animals safe and healthy.

I need to give another set of acknowledgements to some key I&P mentors and colleagues outside of the Vance lab. I feel fortunate to have had such a fun, brilliant, and supportive community throughout my graduate school experience.

Greg Barton and his lab have provided a tremendous amount of intellectual and emotional support to me. Greg often acts as a second advisor to the Vance lab trainees and provides a much needed outside opinion when I or others are stumped with some technical issue or confusing data. He is also a genuinely fun person to have around and is patient enough to let the Vance lab push his buttons from time to time (but sorry about the googly eyes on the family photo, Greg). I also need to thank some specific folks from the Barton lab. Aloe Stanbery gave me a lot of guidance early in my graduate school career and provided a safe place for me to come cry when I was deep in QE hell. Victoria Rael and Shaina Carroll have both become much needed sounding boards for my many random ideas and sanity checks. I am beyond grateful for their friendship, especially over this last year and a half. I am also grateful that I got to know Gaby Reiner, first as a social friend, and then as a much-respected scientific colleague. I'd like to thank Kathleen Pestal as well. It was a fun coincidence that she and I ended up in the Barton and Vance labs together, and I really appreciate her willingness to answer my questions and help me troubleshoot dozens of annoying technical issues. I also owe former Barton lab manager Beth Russell many Thank Yous for all of the help she provided me, especially as I was learning the ropes of the LSA mouse house. And I'd like to thank the Barton lab as a whole for acting as a second family to the Vance lab and joining us in endless memorable shenanigans.

I need to acknowledge several other faculty members that helped me along throughout my time at UC Berkeley. A very big Thank You goes to my Thesis Committee, including David Raulet, Ellen Robey, and Shauna Somerville. David and Ellen both played a critical role in helping me and Russell learn our way through antigen presentation and T cell immunity. Many of their suggestions proved to be key in moving my project forward. And as an expert in plant-microbial interactions, Shauna's outside opinion was especially helpful when it came to identifying obvious questions or issues that we overlooked. I'd like to thank Sarah Stanley for being a wonderful mentor that I knew I could always trust when tough question or dilemma arose. I thank Laurent Coscoy for his guidance as my first year advisor and as an instructor of record while I was a GSI for MCB150 and MCB55. I also need to thank Dan Portnoy for his mentorship when I rotated in his lab, Kaoru Saijo for her kindness, Michel DuPage for many good scientific discussions, and Nilabh Shastri for sharing his time, reagents, and extensive knowledge of antigen presentation.

I'd like to give a special acknowledgement to Professor Robert Beatty. Teaching has always been a passion of mine, and I learned a lot from Robert over the three semesters I worked with him as a GSI. I am especially grateful that he nominated me for the Outstanding Graduate Student Instructor award I received.

It is also important that I acknowledge the time and effort given by some key staff members whose support and guidance helped me throughout my time at UC Berkeley. These folks include the GAO staff of past and present: Hannah Bottger, Hannah Bloom, Carlos Garcia, Berta Perra, Eric Buhlis, and Carina Galicia. I thank our building manager Barbara Duncan and all of the custodial staff for doing everything they can to keep the inhabitants of LSA safe. I also owe a lot of thanks to the Cancer Research

Laboratory Flow Core staff Hector Nolla and Alma Valeros. And a big Thank You to the Berkeley Imaging Facility staff Steve Ruzin and Denise Schichnes.

I want to close my acknowledgements by thanking all of the academic mentors that have helped me reach the finish line of my PhD. Each one has played a significant role in supporting my scientific career, and I wouldn't be where I am today without them.

As cliché as it is, my love for science really began to materialize in elementary school. My fifth and sixth grade teacher, Mrs. (Debbie) Foreman, has a passion for teaching science and math that is unparalleled, and she gave an incredible amount of support and encouragement to every single one of her students. As I graduate now from 23rd grade, Mrs. Foreman remains one of my most respected mentors, and I am so thankful to still have her in my life as a wonderful neighbor and family friend.

The next milestone on my path into science occurred while I was an undergrad at Seattle University. I entered college as a pre-med psychology student, but I had a small meltdown my sophomore year when I realized I would never be the A-plus student I thought I needed to be. I was lucky enough to take an introduction to immunology course with Professor Carolyn Stenbak the following year, and she enthusiastically supported my newfound love for biology by suggesting I apply to a research position in her virology lab. My experiences working with Dr Stenbak set the foundation for my career in scientific research and continue to drive my professional interests to this day. I am incredibly grateful for her mentorship and guidance and can never say Thank You enough. I also need to add a quick shoutout to my original supporting cast of labmates: Chris Hagan, Jeremiah Grams, and Jacqui Wallis.

The generosity of Dr Jessica Hamerman at the Benaroya Research Institute provided a crucial bridge for me between undergraduate research and the research technician position that would ultimately guide me to graduate school. Jess was kind enough to let me volunteer in her lab with then-graduate student Matt Buechler. I learned a lot from Jess and Matt in a short time and am especially grateful for their continued mentorship after I left to take a paid position at the University of Washington.

My time in the immunology department at UW paved my pathway to graduate school, and for that I owe Dr Pam Fink a bottomless amount of gratitude. I worked with her as a research technician and lab manager for almost three years, and during that time she showed me an indescribable amount of generosity, kindness, patience, and mentorship. Pam supported my growth not only because it supported her lab but also because she wanted to see me succeed. She held me to a high standard and provided guidance when I fell short. She also genuinely cared about my wellbeing—I will always remember the time she helped me clean gravel out of my arm after I crashed my bike on my way into lab. I am incredibly grateful for the support she gave me then and the support she continues to give me today. I am also thankful for the support I received from other members of the Fink lab. Amy Berkley, Lauren Higdon, and Travis Friesen all provided an incredible amount of guidance, patience, and kindness as I fumbled my way through learning mouse work and flow cytometry. They taught me numerous lab techniques, and Amy and Lauren graciously let me help them with their research projects. I also owe a big Thank You to Mike Bevan. I learned a lot of immunology from him and leaned heavily on his work on cross presentation for my PhD project. I am so

grateful for my time spent in the immunology department at UW and for all of the people that helped me while I was there.

And finally, I need to acknowledge the guidance and mentorship I received from Russell Vance. I have enough friends in science to know that Russell is somewhat of a unicorn when it comes to PIs—he is a very talented and successful scientist, yet he is also incredibly thoughtful, generous, patient, easygoing, and perhaps most impressive of all, present. I feel very fortunate to have had a graduate mentor that was always willing to make the time to meet with me, and he gave me the just right balance of guidance and freedom. He is a tough critic, but that toughness has helped me learn how to ask informative questions, generate logical hypothesis, and clearly communicate my thoughts, ideas, and findings with others. I cannot thank Russell enough for his role as my PhD advisor, and I look forward to having his support as a mentor and colleague for the rest of my scientific career.

Thank you again to everyone for all of the time and energy you have given to support me on my journey to earning a PhD.

Chapter One: Introduction

1.1 Introduction to innate and adaptive immunity

An immune system allows organisms to survive and thrive in our microbe-filled world. While all living organisms possess some form of innate immunity—which recognizes and responds to a broad range of microbial-associated molecules and activities—jawed vertebrates additionally possess a highly-specific, lymphocyte-based adaptive immune system (Brubaker et al., 2015; Hirano et al., 2011). Together, the innate and adaptive immune systems can provide both immediate and long-term protection from viruses, bacteria, fungi, protists, and parasitic worms.

1.1.1 Innate immunity

The mammalian innate immune system is comprised of a body's barrier surfaces, molecules and secretions found at these surfaces, and a collection of specialized innate immune cells. The barrier surfaces (discussed below) include the gastrointestinal tract, respiratory tract, blood-brain barrier, urogenital tract, and skin. The innate immune cells reside within most tissues throughout the body and include dendritic cells (DCs), macrophages, neutrophils, mast cells, eosinophils, basophils, and a collection of innate lymphoid cells (ILCs) (Sonnenberg and Hepworth, 2019), which includes natural killer (NK) cells (Figure 1.1). These innate immune features work together to provide the first line of defense against invading microbes.

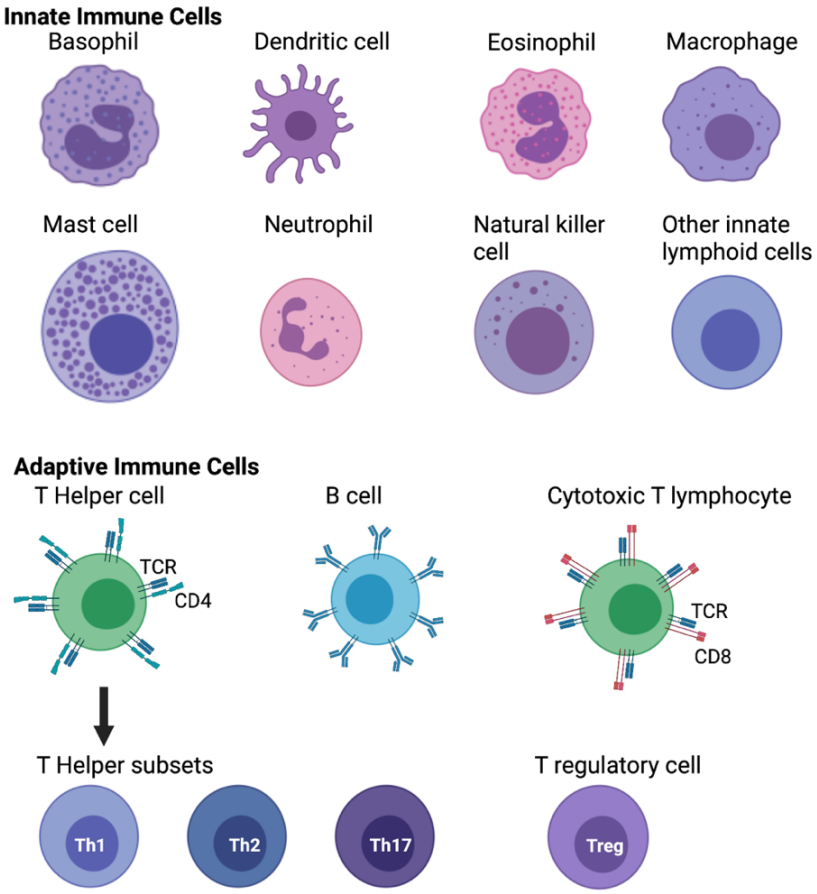

Figure 1.1 Illustration of immune cells from the innate (top) and adaptive (bottom) immune systems.

One of the fundamental concepts in mammalian innate immunity is based on interactions between “pathogen-associated molecular patterns” (PAMPs) and various cell-associated “pattern recognition receptors” (PRRs) (Janeway, 1989). Although PAMP-PRR interactions are not limited to disease-causing microbes, they allow the cells of the innate immune system to rapidly distinguish molecules that are “self” (e.g., enzymes produced in the liver, hemoglobin on a red blood cell, etc.) from those that are “non-self” (e.g., bacterial flagellin, viral proteins, etc.). Dozens of PRRs have been identified over the last 30 years, and they can be found intracellularly and extracellularly across many different cell types (Brubaker et al., 2015). The understanding of innate immunity has recently expanded beyond the PAMP-PRR model to consider how additional aspects of an infection, such as the microbe’s location, replication, or other host-manipulating activities, might influence how the innate immune system responds (Stuart et al., 2013; Vance et al., 2009).

The ideal outcome of an innate immune response is elimination of the invading pathogen, though the strategy can vary. Some of the potential elimination tools include consumption and degradation of the pathogen (phagocytosis) (Gordon, 2016; Uribe-Querol and Rosales, 2020) programmed death of infected cells (Jorgensen et al., 2017), and production and release of small molecules like anti-microbial peptides (Lazzaro et al., 2020) or components of the complement cascade (Reis et al., 2019). The innate immune system also uses a vast array of signaling molecules (cytokines and chemokines) to communicate the type and location of response needed from various cells around the body (Holdsworth and Gan, 2015; Hughes and Nibbs, 2018; Liu et al., 2021). Ultimately, however, innate immunity may be insufficient to contain and remove an infection (Beachboard and Horner, 2016; Odendall and Kagan, 2017), so another key outcome of the innate immune response is to activate cells of the adaptive immune system.

1.1.2 Adaptive immunity

The mammalian adaptive immune system is comprised of two groups of lymphocytes: B cells and T cells. T cells are further divided into cytotoxic T lymphocytes (CTLs), various types of T helper (T_H) cells, and T regulatory (T_{REG}) cells (Figure 1.1). There is also a group of so-called “unconventional” T cells (Godfrey et al., 2015), though they function largely as innate immune cells and will not be discussed here. Both B and T cells arise from progenitors generated in the bone marrow; however, newly formed T cell progenitors rapidly migrate to the thymus, where they undergo important selection and maturation processes (Kurd and Robey, 2016). B cells undergo their maturation process in the bone marrow (Wang et al., 2020b). The majority of these mature lymphocyte groups then migrate throughout the spleen and lymph nodes, where they await activation.

Unlike cells of the innate immune system, B and T cells have clonally distinct surface receptors that recognize short, unique amino acid sequences (antigens), with each of the receptors on an individual cell recognizing the same antigen. The main component of the B cell receptor (BCR) is an immunoglobulin molecule, also known as an antibody. The BCR can bind either soluble or membrane-bound antigens, and antigen binding leads to the activation and clonal expansion of the B cell. The majority of B cell clones will become plasma blasts, which secrete large quantities of antibodies

for rapid defense against an invading pathogen (Wang et al., 2020b). The remainder of B cell clones will become plasma cells. Plasma cells provide long-term memory and quickly activate if they encounter the antigen again in the future. The T cell receptor (TCR), conversely, will only bind antigens presented on the major histocompatibility complex (MHC) at the surface of another cell. If the TCR of a naïve T cell encounters its cognate antigen-MHC with the appropriate co-stimulatory signals (discussed below), the T cell will undergo activation and clonal expansion (Conley et al., 2016; Hwang et al., 2020). While innate immune cells can respond within minutes to hours of the start of an infection, adaptive B and T cells responses take five to nine days to mount a full response the first time they see a pathogen.

Each of the different T cell subsets mentioned above has distinct effector functions that it carries out upon activation. CTLs follow cytokine and chemokine signals to move into infected tissues and kill infected cells (Halle et al., 2017). T_H cells, whose roles are tailored based on the activating signals they receive, provide cytokines to direct the inflammatory functions of B cells, CTLs, and innate immune cells (Bhattacharyya and Feng, 2020; Zhu, 2018). T_{REG} cells suppress immune responses and are necessary to maintain immune tolerance (Li et al., 2020). Like B cells, a subset of activated T cells will become long-lived memory cells that are ready to respond rapidly if the same pathogen is encountered in the future (Nguyen et al., 2019; Samji and Khanna, 2017).

1.1.3 Innate activation of adaptive immunity

Innate immune responses help initiate and shape the adaptive immune responses mediated by T and B cells (Iwasaki and Medzhitov, 2015; Janeway, 1989). While many cells are capable of presenting antigens to T cells, DCs—and to a lesser extent, macrophages (Bernhard et al., 2015; Muntjewerff et al., 2020) and B cells (Hua and Hou, 2020; Morris et al., 1994; Rubtsov et al., 2015)—are considered “professional” antigen presenting cells (APCs) because of their ability to simultaneously provide the “3 signals” required for T cell activation (Cantrell, 2015; Chudnovskiy et al., 2019) (Figure 1.2).

In a simplified 3-signal model, the first signal to activate T cells is provided by TCR recognition of an MHC-bound antigen, and signal 2 is co-stimulation provided by the professional APC. Signal 3 is provided by inflammatory cytokines, derived from innate immune activation, which may act directly on the T cell and/or indirectly by increasing co-stimulatory molecules on the APC (Curtsinger and Mescher, 2010; Jain and Pasare, 2017). B cells are activated by antigen via T cell-dependent or -independent mechanisms (Cyster and Allen, 2019).

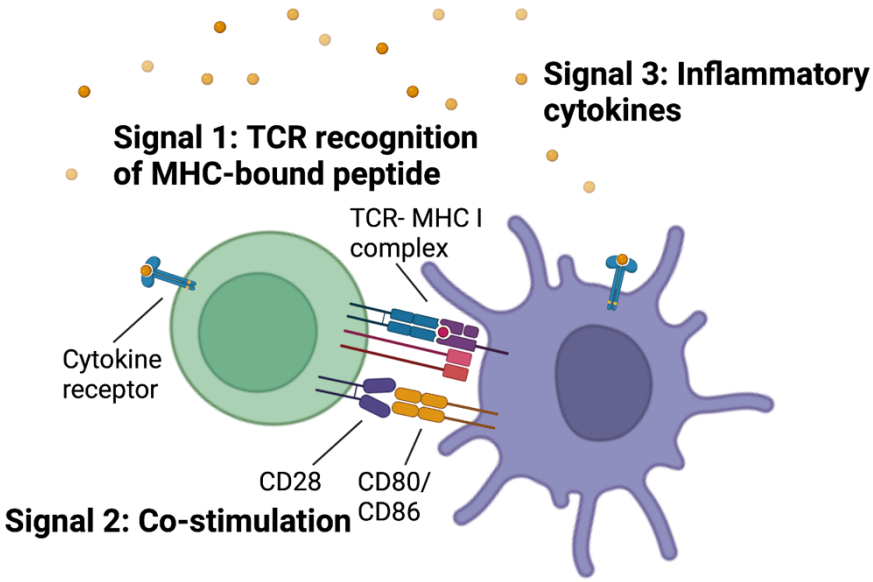

Figure 1.2. Illustration of the three-signal model of naïve T cell activation.

Cells can present both endogenous- and exogenous-derived antigens on their MHC molecules (Blum et al., 2013). Exogenous antigens taken up by APCs are predominantly processed and presented on MHC class II to T_H cells, which express CD4 on their cell surface. Conversely, endogenous antigens—typically derived from pathogens within the cytosol of the cell—are processed and presented on MHC class I to CTLs, which express CD8 on their surface. One notable exception to these two "classical" presentation pathways is the ability of some cells, largely type 1 conventional DCs (cDC1s) (Gutierrez-Martinez et al., 2015; Murphy and Murphy, 2021) and certain macrophages (Muntjewerff et al., 2020), to shuttle exogenous antigen through the MHC class I presentation pathway in a process termed "cross presentation" (Bevan, 1976; Cruz et al., 2017; Gros and Amigorena, 2019). These cross-presented antigens are often derived from dead infected cells (discussed below in 'Fate of Pyroptotic Antigens'), and the process is thought to help generate a CTL response against viral (Enders et al., 2020; Helft et al., 2012; Ng et al., 2018) and bacterial (Kaufmann and Schaible, 2005; Patel and Sad, 2016) pathogens that do not directly infect the cross-presenting APC. Cross presentation may also have an important role in anti-tumor immunity (Fu and Jiang, 2018; Noubade et al., 2019).

DCs are able to provide activating co-stimulation once they have encountered an inflammatory stimulus (Fitzgerald and Kagan, 2020; Iwasaki and Medzhitov, 2015). The requirement for an inflammatory stimulus in T cell activation serves as a checkpoint to assure the presented antigen is derived from a pathogen and not self (ElTanbouly and Noelle, 2021)—although co-stimulatory molecules are still engaged in many autoimmune diseases (Adams et al., 2016; Bluestone and Anderson, 2020). To date, the majority of studies on DC maturation have focused on ligand recognition by TLRs (Fitzgerald and Kagan, 2020), and so questions remain about other potential DC maturation signals, such as the inflammatory cytokines IL-1α/β (Pang et al., 2013) and IL-18 (Li et al., 2004) that are often released following inflammasome activation.

1.2 The immune system at epithelial barrier surfaces

Epithelial barrier surfaces are unique from other immune tissues in that they sit at the interface between the sterile inside of an organism and the surrounding microbe-filled world. This constant exposure means that epithelial cells must fulfill many roles at once. In addition to their non-immune functions (e.g., secretion, air exchange, nutrient acquisition, etc.), they also provide a physical barrier, maintain a homeostatic relationship with commensals (Coates et al., 2019; Palm et al., 2015), and recognize and respond to a variety of microbial signals (Constant et al., 2021; Larsen et al., 2020). One group of innate immune sensors that was recently revealed to have a crucial role in barrier defense are the inflammasomes (Churchill et al., 2021; Palazon-Riquelme and Lopez-Castejon, 2018), which are discussed in detail below.

Additionally, many adaptive immune cells interact with epithelial barriers. These include the classical lymphocytes outlined above, as well as non-classical lymphocytes, such as innate lymphoid cells, MAIT cells, γδT cells, and iNKT cells.

1.3 Inflammasomes and adaptive immunity

Inflammasomes are key components of the innate system, involved in the response to most pathogens. However, their role of in the adaptive immune response remains poorly understood (Deets and Vance, 2021; Evavold and Kagan, 2018).

1.3.1 Overview of inflammasomes

Inflammasomes comprise a heterogeneous group of cytosolic multi-protein complexes whose function is to detect infectious or noxious stimuli and serve as a platform to activate specific pro-inflammatory caspase proteases, most notably caspase-1, but also including caspase-8, caspase-11 (in mice), and caspase-4/5 (in humans). Each distinct inflammasome contains a unique sensor protein that mediates responsiveness to specific stimuli (Broz and Dixit, 2016; Lamkanfi and Dixit, 2014; Rathinam and Fitzgerald, 2016).

Despite the diversity of their signaling inputs, inflammasomes all converge on a shared set of signaling outputs (Figure 1.3). In particular, active caspase-1 cleaves and activates three key substrates: pro-interleukin (IL)-1β, pro-IL-18, and gasdermin-D. Cleavage of gasdermin-D—one member of a small family of gasdermin proteins—releases its N-terminal domain, which oligomerizes to form pores in the plasma membrane. These pores induce a lytic form of cell death, called pyroptosis. Though traditionally classified as an ‘apoptotic’ caspase, caspase-8 can also be activated by inflammasomes (Antonopoulos et al., 2015; Goncalves et al., 2019; Karki et al., 2015; Man et al., 2013; Masumoto et al., 2003; Rauch et al., 2017) and can mediate both IL-1β (Schneider et al., 2017) and gasdermin-D cleavage (Chen et al., 2019; Orning et al., 2018; Sarhan et al., 2018). The “non-canonical” caspases-4/5/11 inflammasomes are activated directly by lipopolysaccharide (LPS), or downstream of guanylate-binding proteins (GBPs) (Hagar et al., 2013; Kajiwara et al., 2014; Pilla et al., 2014; Santos et al., 2018; Shi et al., 2014), and are able to cleave gasdermin-D (Kayagaki et al., 2015; Shi et al., 2015) as well as pro-IL-1β /18 with variable efficiency (Bibo-Verdugo et al., 2020; Ramirez et al., 2018; Santos et al., 2020; Wandel et al., 2020). Caspase-4/5/11 activation can also lead indirectly to caspase-1-mediated IL-1β/18 cleavage because

gasdermin-D pore formation results in potassium efflux, a signal that triggers NLRP3 inflammasome and caspase-1 activation (Yi, 2020). As a consequence of the extensive redundancy among inflammatory caspases downstream of inflammasomes, *Casp1* deficiency is often insufficient to eliminate inflammasome signaling, an experimental challenge for studies that seek to link inflammasomes and adaptive immunity.

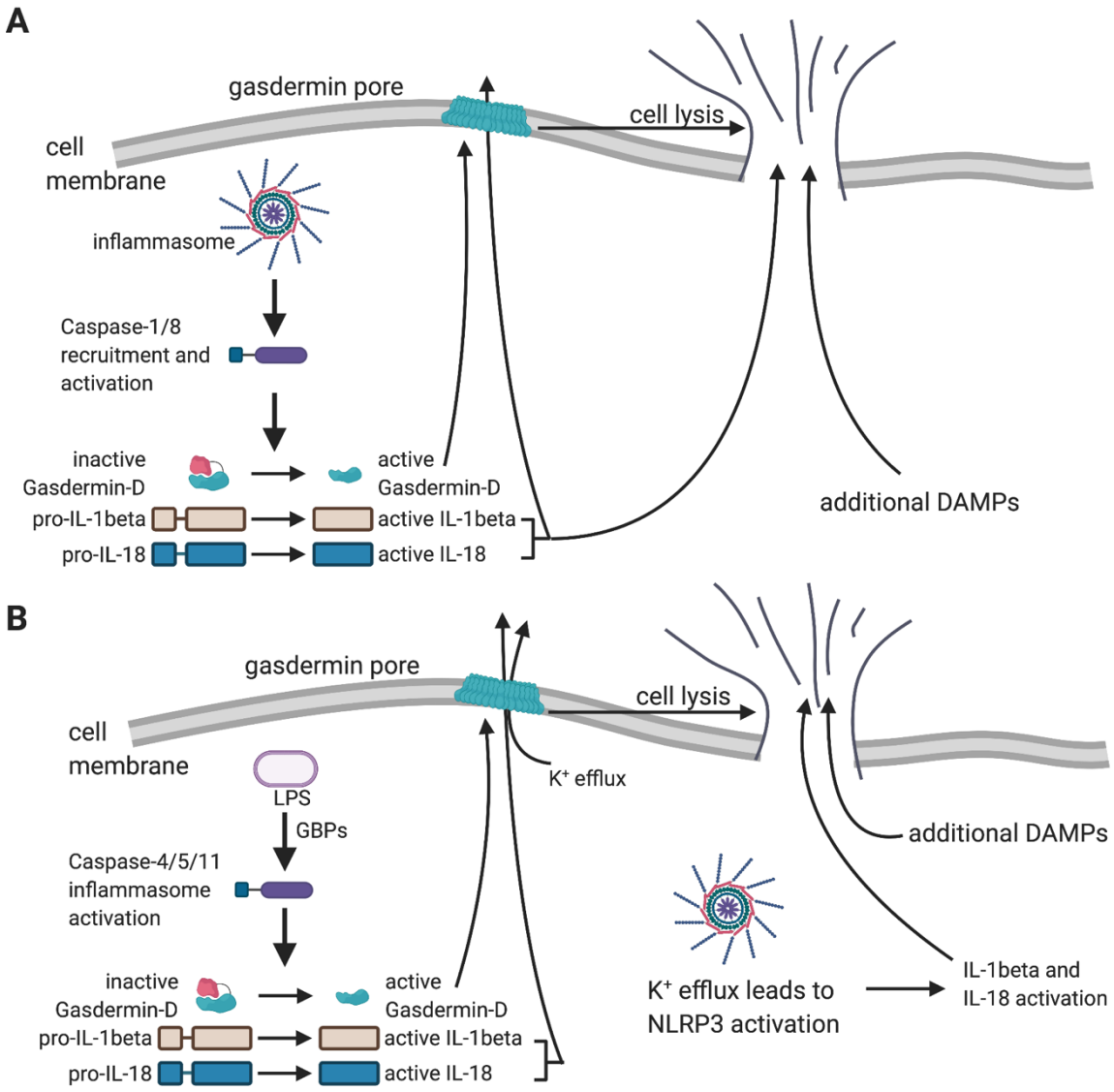

Figure 1.3. Mechanisms of canonical (**A**) and non-canonical (**B**) inflammasome activation.

Pyroptotic cell death can also release other inflammatory molecules, sometimes called “damage-associated molecular patterns” or DAMPs (de Vasconcelos and Lamkanfi, 2020). Among the best characterized of these is IL-1a, which, unlike IL-1β, does not require caspase-1 processing for its activity. Other inflammatory mediators released from pyroptotic cells include DNA, HMGB1, ATP, uric acid, and eicosanoid lipid mediators (de Vasconcelos et al., 2019; Lamkanfi et al., 2010; von Moltke et al., 2012), though the importance of these factors in inflammasome-dependent responses

often remains unclear. Pyroptosis can also facilitate the extracellular release of antigens, with or without concomitant cell death, depending on the cell type or degree of activation (de Vasconcelos and Lamkanfi, 2020). Thus, an interesting feature of inflammasome activation as compared to other innate stimuli (e.g. Toll-like receptors, TLRs) is that it can potentially provide signal 1 and 2/3 in concert (Figure 1.4). Importantly, IL-1β and other DAMPs can be released as a consequence of any form of cell death, including necrosis triggered by injury or secondary to apoptosis; thus, a specific requirement for inflammasomes can be difficult to observe experimentally.

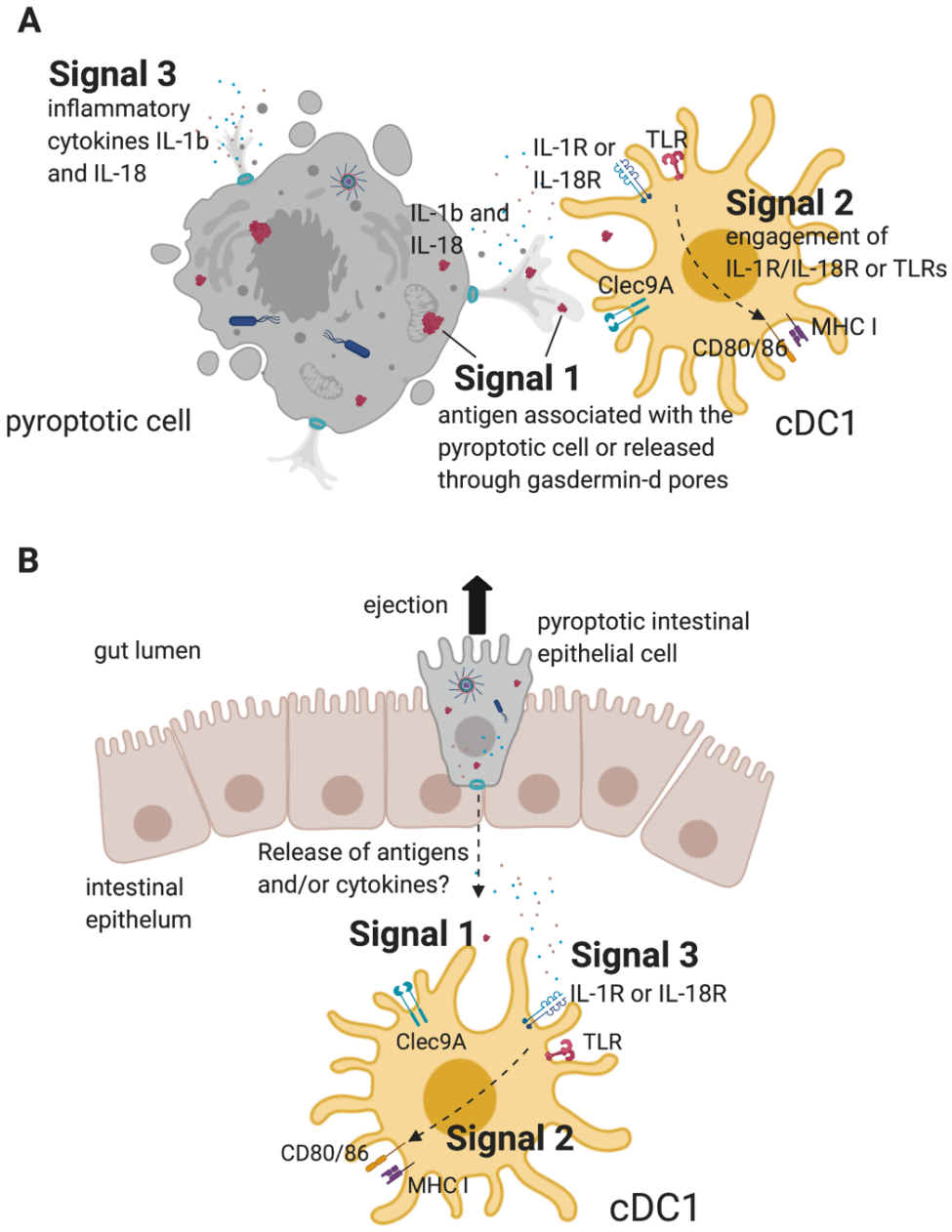

Figure 1.4. Proposed mechanisms of how inflammasome activation and pyroptosis in cells such as macrophages (**A**) or IECs (**B**) might provide antigen and inflammatory signals to mature cross-presenting DCs.

Inflammasome-independent pathways for release of bioactive IL-1a/β/-18 (Netea et al., 2015) also means that the effects of IL-1R (which binds both IL-1a and IL-1β) or IL-18R deficiency cannot necessarily be ascribed to inflammasomes. Moreover, in most experimental contexts, inflammasome activation is accompanied by activation of other innate pathways, most notably TLRs, which can respond to many of the same agonists as inflammasomes (e.g., LPS, DNA, RNA or flagellin). The presence of these additional signals can obscure the contributions of inflammasomes. It is rare that a study addresses whether inflammasome activation alone—in the absence of other innate signals—is sufficient to initiate an adaptive immune response.

1.3.2 Fate of pyroptotic cell antigens

Pyroptotic cells are a potential source of both inflammatory cytokines and antigens, but most studies of inflammasomes in adaptive immunity focus selectively on IL-1β and IL-18, likely due to the difficulty of tracking pyroptotic cell-derived antigens *in vivo*. In principle, antigens from pyroptotic cells might follow several distinct fates (Figure 1.4). For example, smaller cytosolic proteins are rapidly released in a soluble form through gasdermin pores (de Vasconcelos et al., 2019; DiPeso et al., 2017). In cases where pyroptosis results in overt cell lysis, larger protein complexes (e.g., tetrameric lactate dehydrogenase LDH) are released via plasma membrane ruptures. Release of soluble antigens may not be optimal for initiating adaptive responses, as such antigens would be rapidly diluted and might not be delivered to an APC along with the pathogen-associated molecular patterns (PAMPs) or DAMPs needed to stimulate APC maturation for optimal T cell priming (Gutierrez-Martinez et al., 2015).

However, inflammasome activation and gasdermin-D activation do not always trigger overt cell lysis (Chen et al., 2014; Evavold et al., 2018; Gaidt et al., 2016), and in addition, larger or cell-associated antigens might be retained even in lysed pyroptotic cells. One recent study using fluorescent *Salmonella typhimurium* reported that pyroptotic cells retain living bacteria in pore-induced intracellular traps (PITs) (Jorgensen et al., 2016b). The cytoskeletal structures present in the pyroptotic cell corpse traps bacteria until the dead cell is eaten, or efferocytosed, by phagocytes (Davis et al., 2019; Jorgensen et al., 2016a; Jorgensen et al., 2016b). Efferocytosis is orchestrated by molecular signals which recruit phagocytes and initiate consumption of the cell corpse (Boada-Romero et al., 2020). The removal of dead cells is important for avoiding autoimmunity and maintaining homeostasis, but infected dead cells can also provide antigen to initiate adaptive immunity, including cDC1-mediated cross-priming of $CD8^+$ T cells (Boada-Romero et al., 2020; Cruz et al., 2017; Cummings et al., 2016; Penteado et al., 2017; Torchinsky et al., 2009). Cross-presentation of lytic cell-associated antigen is at least partially mediated by the CLEC9A (DNGR-1) receptor on cDC1s (Ahrens et al., 2012; Cueto et al., 2019; Schulz et al., 2018; Zelenay et al., 2012; Zhang et al., 2012). CLEC9A recognizes myosin II-associated filamentous (F)-actin, which becomes exposed during necroptosis and secondary necrosis (Ahrens et al., 2012; Zhang et al., 2012). F-actin is also likely exposed following pyroptosis, implying antigen retained inside pyroptotic cells may be accessible to DCs for cross-priming of $CD8^+$ T cells, but more work is needed to understand how DCs interact with pyroptotic cells.

To address the *in vivo* role of inflammasome activation in DC maturation and antigen presentation, one recent study infected mice with a strain of *Listeria monocytogenes* that secretes flagellin into the host cytosol and thus robustly activates the NAIP–NLRC4 inflammasome. The authors found that flagellin-secreting *Listeria* induced the maturation of more cDC1s relative to wild-type *Listeria* at 24 h post infection (Theisen and Sauer, 2017). It is possible that the inflammatory nature of pyroptosis drives maturation of uninfected DCs, as other studies have found that IL-1α/β (Pang et al., 2013) and IL-18 (Li et al., 2004) may have a role in maturing DCs. Following *in vivo Listeria* infection, the antigen abundance on a per-cell basis was neither impaired nor enhanced by inflammasome activation, and, in agreement with earlier findings (Sauer et al., 2011), the authors saw no apparent decrease in overall $CD8\alpha^+CD11c^+$ DC numbers in the spleen (Theisen and Sauer, 2017). However, flagellin-secretion and inflammasome activation overall impaired the adaptive response to *Listeria*. The authors suggest that the unique inflammatory signal of pyroptosis may inhibit $CD8^+$ T cell activation (discussed below), but other explanations are possible. Overall, it remains unclear whether inflammasome activation promotes or perhaps impairs the concerted delivery of maturation signals and antigens to DCs for optimal presentation to T cells.

1.3.3 Antigen release from pyroptotic epithelial cells

Although inflammasome activation is most often studied in macrophages and other hematopoietic cells, inflammasome activity in non-hematopoietic cells might also contribute to adaptive immunity. The role of inflammasomes in intestinal epithelial cells (IECs) has been the subject of several recent studies, although it has been decades since IECs were first discovered to produce IL-1β (Radema et al., 1991) and IL-18 (Takeuchi et al., 1997). Many of the currently identified inflammasomes have now been found to play a role in IEC barrier immunity (Lei-Leston et al., 2017; Palazon-Riquelme and Lopez-Castejon, 2018). In general, IEC-residing inflammasomes are thought to play two crucial roles in barrier immunity: they provide early innate immune sensing of cytosolic pathogens, and in the case of at least some inflammasomes, they can rapidly eliminate invading pathogens by triggering IEC pyroptosis (Churchill et al., 2021).

Antigens from apoptotic IECs appear capable of driving regulatory T cell differentiation in the gut (Cummings et al., 2016). Additionally, a subset of cDC1s can cross-present IEC-derived antigen to activate $CD8^+$ T cells in the mesenteric lymph node (Cerovic et al., 2015). Such results indicate that IEC-derived antigens play a role in $CD4^+$ and $CD8^+$ effector T cell responses under inflammatory conditions. However, the lytic nature of inflammasome-induced pyroptosis is distinct from non-lytic apoptosis and raises the important questions of how antigens in pyroptotic IECs would be delivered to APCs for presentation and whether effector T cell responses might be influenced by inflammatory cytokines and lipid mediators (Rauch et al., 2017; von Moltke et al., 2012) uniquely released during pyroptosis of IECs.

IECs express multiple inflammasomes, of which the NAIP–NLRC4 inflammasome has been studied in most detail (Lei-Leston et al., 2017; Winsor et al., 2019). The NAIP–NLRC4 inflammasome is robustly activated in IECs following infection with gut pathogens such as *Salmonella*, *Shigella*, or *Citrobacter rodentium*, resulting in pyroptosis and subsequent expulsion of infected cells into the gut lumen (Mitchell et al., 2020; Nordlander et al., 2014; Rauch et al., 2017; Sellin et al., 2014). Although

expulsion of infected IECs reduces pathogen invasion, it might also hinder adaptive responses by limiting the delivery of pathogen antigens to underlying APCs in the lamina propria. *In vivo* and time-lapse organoid studies indicate that pyroptotic IECs undergo cell lysis while still present in the epithelial monolayer, and in addition, high concentrations of IEC-derived IL-18 are found in the serum of mice following IEC-specific NAIP–NLRC4 activation (Rauch et al., 2017). These findings raise the possibility that pyroptosis of IECs may enhance adaptive responses by the release of antigen and other inflammatory signals to underlying DCs, prior to IEC expulsion.

1.3.4 Inflammasomes and CD4$^+$ T cell responses to pathogens

The influence of inflammasome activation on CD4$^+$ T cells has largely been studied in the context of three main effector subsets: T helper type 1 (T_H1) in response to intracellular pathogens, T_H2 in response to extracellular parasites, and T_H17 in response to extracellular bacteria and fungi. Signaling through the IL-1R—in conjunction with IL-6R or IL-23R—on a CD4$^+$ T cell generally drives T_H17 induction, while IL-18R signaling—in conjunction with IL-12R signaling—promotes T_H1 immunity and potentially suppresses a T_H2 response (Chung et al., 2009; Deng et al., 2019; Dostert et al., 2013; Harrison et al., 2015; Mantovani et al., 2019; Yasuda et al., 2019). Engagement of these cytokine receptors on differentiated CD4$^+$ T cells also drives non-cognate effector function during various bacterial infections (Jain et al., 2018; Pham et al., 2017; Srinivasan et al., 2007). Because there are both inflammasome-dependent and -independent sources for IL-1β and IL-18 during an infection (Netea et al., 2015), and because infections trigger many innate immune signals, it is difficult to determine whether inflammasome activation is necessary or sufficient for driving CD4$^+$ T cell polarization and effector function.

Salmonella potently activates several inflammasomes, including NAIP–NLRC4, NLRP3, and caspase-11(Aachoui et al., 2013; Broz et al., 2010a), and triggers a robust, polyclonal T_H1 response in infected individuals (McSorley, 2014). However, few studies have addressed the link between inflammasome activation and the adaptive immune response against this pathogen. IL-18R-driven activation of non-cognate T_H1 cells appears to play a significant role in *Salmonella* clearance *in vivo*, and the relative abundance of these effector T cells is reduced by half in the absence of both NLRC4 and NLRP3 (O'Donnell et al., 2014; Pham et al., 2017; Tourlomousis et al., 2020). Importantly, previous studies show that mice deficient in both of these inflammasomes have no detectable serum IL-18 following *S. typhimurium* infection (Broz et al., 2010a). Thus, these data suggest a direct link between inflammasome activation and non-cognate T_H1 responses. There is evidence that inflammasome activation promotes CD4$^+$ T cell immunity against other bacterial pathogens as well, including T_H17 immunity against *Legionella pneumophila* (Trunk and Oxenius, 2012) and T_H1 immunity against *Anaplasma phagocytophilum* (Pedra et al., 2007). Caspase-1 has also been shown to be required for robust T_H1 interferon-g (IFN-γ) production during influenza A virus (IAV) infection (Ichinohe et al., 2009), but further research is required to identify the inflammasome responsible for this effect.

As with studies of bacterial and viral infections, studies exploring the influence of inflammasome activation on anti-fungal T_H1 and T_H17 immunity focus almost exclusively on the role of inflammatory cytokines (van de Veerdonk et al., 2015). NLRP3-, ASC-,

and caspase-11-deficient mice have fewer T_H1 and T_H17 cells, and increased disease burden, after infection with the fungal pathogen *Paracoccidioides brasiliensis* (Feriotti et al., 2017; Ketelut-Carneiro et al., 2015; Ketelut-Carneiro et al., 2019). However, the underlying mechanisms are unclear. One group, using intravenous infections, found that NLRP3-dependent IL-18 drives a T_H1 response, while caspase-11-dependent IL-1β drives a T_H17 response (Ketelut-Carneiro et al., 2019). A separate study, using intratracheal infections, proposed that NLRP3-dependent pro-inflammatory cytokines inhibit the influx of regulatory T (T_{reg}) cells that express IL-4 and transforming growth factor-b (TGF-b) into the lung and thereby favors a T_H1–T_H17 response (Feriotti et al., 2017). These mechanisms are not mutually exclusive, and a better understanding of how inflammasome activation at different sites of infection influences T_{reg} cells is an important avenue for future studies.

The relationship between inflammasomes and adaptive immunity is even less obvious with protozoan parasite infections, which activate a variety of inflammasomes and induce a strong T_H1 response (Engwerda et al., 2014; Zamboni and Lima-Junior, 2015). Infection with the intracellular protozoan *Trypanosoma cruzi*, the causative agent of Chagas disease, activates NLRP3 (Silva et al., 2013), but whether inflammasome activation has a role in driving $CD4^+$ T cell immunity is complicated by the heterogeneity of parasite strains and host responses. One recent study showed that *T. cruzi*-infected caspase-1–caspase-11-deficient mice have significantly fewer T_H1 and T_H17 cells compared to wild-type mice, but the T cell response occurs independently of NLRP3 (Paroli et al., 2018). These results may implicate another inflammasome in sensing *T. cruzi*, though it should also be noted that inflammasome-independent caspase-1 was recently found to promote T_H17 differentiation *in vivo* (Gao et al., 2020). Interestingly, NLRP3 does seem to influence parasite-triggered adaptive immunity at the gut mucosal barrier. A study with *Tritrichomonas musculis*—whose closest human ortholog, *Dientamoeba fragilis*, has a debatable role in inflammatory bowel disease (IBD) (Rostami et al., 2017)—shows that NLRP3-derived IL-18 can drive anti-parasitic T_H1 and T_H17 immunity, which may in turn influence host susceptibility to future infections and intestinal inflammation (Chudnovskiy et al., 2016). Further studies may illuminate the role of inflammasomes in the gut microbiome–inflammasome–T cell axis. Overall, inflammasomes appear to promote T_H1 and T_H17 $CD4^+$ T cell immunity, but work remains to build a comprehensive mechanism that includes cytokines, antigen, eicosanoids, and other DAMPs.

1.3.5 Inflammasomes and $CD8^+$ T cell responses to pathogens

IL-18 enhances the proliferation and survival of effector $CD8^+$ T cells and drives antigen-independent IFN-γ production from memory cytotoxic T lymphocytes (CTLs) (Cox et al., 2013; Kupz et al., 2012). Additionally, as discussed above, antigens from pyroptotic cells may cross-prime $CD8^+$ T cells. However, few studies have specifically addressed whether inflammasome activation is necessary or sufficient for $CD8^+$ T cell immunity.

One study found that the NAIP–NLRC4 inflammasome is required for non-cognate activation of memory $CD8^+$ T cells in response to injection of heat-killed *Salmonella* (HKST) (Kupz et al., 2012). $CD8^+$ T cell activation was greatly reduced in the absence of IL-18, which was produced by $CD11c^+$ cells. Selective depletion of

cross-presenting cDC1s with cytochrome *c* injection also greatly reduced the $CD8^+$ T cell response. These results suggest flagellated bacteria stimulate inflammasome-dependent release of IL-18 by cross-presenting DCs, and this IL-18 then drives non-cognate activation of memory $CD8^+$ T cells. However, recent data indicate that cross-presenting DCs transcriptionally suppress inflammasomes to promote their survival and preserve their T cell-activating function (Erlich et al., 2019; McDaniel et al., 2020). Thus, another subset of $CD11c^+$ cells, such as macrophages, might be the source of IL-18 following HKST injection.

Several groups have explored the influence of inflammasome activation on the $CD8^+$ T cell response to IAV. The AIM2 and NLRP3 inflammasomes are reported to be activated by IAV (Ichinohe et al., 2010; Zhang et al., 2017), and may provide innate protection (Allen et al., 2009; Thomas et al., 2009), but appear not to be required for primary or memory $CD8^+$ T cell formation during influenza infection (Ichinohe et al., 2009; Lee et al., 2016; Thomas et al., 2009). However, one study found that mice deficient in ASC, caspase-1, or the IL-1R had significantly reduced $CD8^+$ T cell activation and nasal immunoglobulin A (IgA) responses relative to wild-type and NLRP3-deficient mice (Ichinohe et al., 2009). IL-1R signaling on DCs has been shown to promote influenza-specific $CD8^+$ T cell activation (Pang et al., 2013), yet it remains unclear which inflammasome(s) could be important for driving adaptive immunity to IAV. AIM2 is an unlikely candidate, as another group recently showed that AIM2 deficiency does not affect the activation of $CD4^+$ or $CD8^+$ T cells or the titers of influenza-specific IgG (Zhang et al., 2017). In all, the role of inflammasomes in providing antigens or inflammatory cytokines to activate $CD8^+$ T cells deserves additional study with a broader range of pathogens.

1.3.6 Impairment of adaptive responses by inflammasomes

While inflammasome activation is often thought to enhance adaptive immunity following infection, there are also instances in which inflammasomes impair adaptive immunity. As mentioned above, intravenous immunization with flagellin-secreting *L. monocytogenes* that strongly engages the NAIP–NLRC4 inflammasome results in a diminished memory $CD8^+$ T cell response (Sauer et al., 2011). In a follow-up study, the authors hypothesize that inflammasome-derived prostaglandin E_2, which is thought to suppress CTL responses (Ahmadi et al., 2008), may dampen the *Listeria*-specific $CD8^+$ T cell response (Theisen and Sauer, 2017). Another recent study found that a strain of *S. typhimurium* expressing a modified flagellin that evades NAIP–NLRC4 recognition induced a stronger T_H1 response and provided better protective immunity than wild-type *S. typhimuirum* (Tourlomousis et al., 2020). Inflammasome activation might impair adaptive immunity through the loss of soluble antigens or via pyroptosis of crucial immune cell populations, e.g., dendritic cells (McDaniel et al., 2020) or T cells (Doitsh et al., 2010; Johnson et al., 2020; Linder et al., 2020; Monroe et al., 2014), though it is difficult to test these hypotheses *in vivo*.

Humoral immunity to certain pathogens may be negatively impacted by inflammasome activation as well. One study used recombinant FliC proteins that selectively activated TLR5 or NAIP–NLRC4 to determine the effects of these innate sensors on anti-FliC antibody formation *in vivo* (Li et al., 2016). The authors found that NAIP–NLRC4 engagement diminished IgG titers, possibly through the pyroptosis-

dependent loss of F4/80$^+$ macrophages, though the results were not confirmed with NAIP–NLRC4-deficient mice. A separate report showed that NLRC4-deficient mice have higher IgG titers than wild-type mice following infection with *C. rodentium* (Nordlander et al., 2014). One explanation for this finding is that there is a trade-off between limiting bacterial burdens and the amount of available antigen. Another possibility is that inflammasome-dependent IL-18 promotes T_H1 differentiation at the expense of T follicular helper cells, which are critical for productive B cell responses. Similar T_H1 skewing may negatively impact anti-parasite responses. A study using the gastrointestinal helminth *Trichuris* showed that NLRP3-dependent IL-18 production hinders the protective T_H2 responses required to control infection (Alhallaf et al., 2018). Taken together, these data suggest a complex interplay between inflammasomes and adaptive immunity and imply that negative effects of inflammasome activation can sometimes outweigh any positive effects on adaptive immunity.

1.3.7 Inflammasome activation by vaccines

Similar to their role during natural infections, inflammasomes may be activated by vaccine components (Suschak et al., 2015) and boost responses through the pyroptotic release of antigens and inflammatory cytokines (Seydoux et al., 2018; Smedberg et al., 2014). However, few studies specifically address the contribution of inflammasomes to vaccine-elicited immunity.

One early area of interest was a potential role for the NLPR3 inflammasome in the efficacy of alum, one of the few adjuvants approved for human use. However, though alum does activate NLRP3 (Eisenbarth et al., 2008; Li et al., 2008), neither NLRP3 nor its downstream signaling components are required for alum adjuvanticity (Franchi and Nunez, 2008; McKee et al., 2009; Wen and Shi, 2016). Another potential role for NLRP3 in vaccine-elicited immunity emerged from a study using a newly designed TLR4 agonist, glucopyranosyl lipid adjuvant (GLA), combined with squalene oil-in-water emulsion (SE). A GLA-SE-adjuvanted recombinant protein vaccine stimulated antigen-specific CD4$^+$ T cells and B cells in a manner dependent on NLRP3, ASC, IL-1R signaling, and extracellular ATP (an NLRP3 agonist) (Seydoux et al., 2018).

Another potential adjuvant of recent interest is the oxidized phospholipid oxPAPC, a DAMP found in dying cells (Chang et al., 2004; Imai et al., 2008). When co-administered with LPS, oxPAPC appears to “hyperactivate” DCs by inducing caspase-11-mediated IL-1β secretion (Zanoni et al., 2016). These DCs trigger robust IFN-γ and T_H17 production from antigen-specific CD4$^+$ T cells *in vitro* and were also recently found to induce long-lived anti-tumor immunity *in vivo* (Zhivaki et al., 2020). It is important to note that the effects of OxPAPC are context-dependent, as pre-treatment of cells with OxPAPC can inhibit caspase-11 (Chu et al., 2018; Zanoni et al., 2016) or boost DC-derived IL-10 to suppresses IL-1β production (Muri et al., 2020).

Flagellin has also been studied as a potential adjuvant, though only a handful of flagellin-based vaccines have made it into early-phase clinical trials (Cui et al., 2018). Flagellin-based vaccines are typically intended to engage TLR5 but might also activate NAIP–NLRC4 if the flagellin reaches the cytosol. Multiple studies have addressed whether NAIP–NLRC4 is necessary or sufficient for adjuvant activity (Ahmed et al., 2010; Garaude et al., 2012; Knudsen et al., 2013; Nystrom et al., 2013; Smedberg et al., 2014; Tran et al., 2019; Vijay-Kumar et al., 2010). In one example, a potential role

for NAIP–NLRC4 in vaccine adjuvant activity was uncovered using a recombinant modified vaccinia virus Ankara (rMVA) that encodes both flagellin and ovalbumin. After intranasal immunization, NLRC4 promoted ovalbumin (OVA)-specific $CD8^+$ T cell responses in the lung, as well as anti-OVA antibody titers in bronchoalveolar lavage (BAL) fluid (Sanos et al., 2017). Similar effects were also seen in the intestines of these mice, suggesting that NAIP–NLRC4 activation can drive T and B cell responses at multiple mucosal sites (Sanos et al., 2017). Conversely, a recent influenza vaccine study using flagellin-expressing virus-like particles shows a minimal role for NAIP–NLRC4 in providing protective immunity, though it is unclear how much of the membrane-anchored flagellin reaches the cytosol in this model (Ko et al., 2019).

The above findings suggest that inflammasome activation can be desirable in vaccine-elicited immunity, though further work to determine how inflammasome activation and pyroptosis influence antigen delivery, T cell costimulation, and B cell activation is needed.

1.3.8 Inflammasomes and the adaptive response to cancer

As is seen for inflammation in general, inflammasome-induced immune activation has been found to be both pro- and anti-tumorigenic, depending on the context. For example, gain-of-function mutations in NLRP1 lead to skin hyperplasia and increased cancer susceptibility (Zhong et al., 2016), whereas NLRP3-driven natural killer (NK) cells kill metastatic colorectal cancer cells (Dupaul-Chicoine et al., 2015). Although inflammasomes primarily exert their effects on tumorigenesis via activation of innate immunity, whether or not inflammasomes also play a role in the adaptive response to cancer is an active area of investigation. Many questions remain, including: how are inflammasomes activated in different tumor types? does pyroptotic release of tumor-associated antigens or cytokines influence adaptive immunity? and, do tumor cells evolve mechanisms to avoid inflammasome activation and pyroptosis?

Early studies addressing inflammasome activation and adaptive immunity showed that NLRP3-mediated IL-1β release is required for cross-priming anti-tumor $CD8^+$ T cell responses in several subcutaneous tumor models (Ghiringhelli et al., 2009). A more recent report—building on work demonstrating that exogenous IL-1β delivery enhances antigen-dependent $CD8^+$ T cell immunity (Ben-Sasson et al., 2013a; Ben-Sasson et al., 2013b; Garaude et al., 2012; Lin et al., 2016)—specifically examines the role of IL-1β in adoptive cell-based immunotherapy. The authors found that systemic administration of IL-1β drives effector function of antigen-specific $CD8^+$ T cells and increases $CD8^+$ T cell numbers in peripheral tissues through enhanced cell trafficking and survival (Lee et al., 2019). Others have also shown that IL-1β boosts anti-tumor $CD8^+$ T cells following anti-CTLA4 monoclonal antibody therapy (Segovia et al., 2019). IL-18 signaling was also recently reported to promote polyfunctional anti-tumor $CD8^+$ T cells (Zhou et al., 2020a).

There are also reports of inflammasome-derived IL-1β suppressing anti-tumor T cell responses. Using two different models of pancreatic ductal adenocarcinoma (PDA), one group recently found that NLRP3-driven IL-1β—produced by the tumor stroma and ductal epithelium—leads to an immunosuppressive environment characterized in part by upregulation of M2-polarized tumor-associated macrophages (TAMs) and a decrease in anti-tumor $CD8^+$ T cells (Das et al., 2020). These findings support earlier

data showing that blockade of NLRP3-dependent IL-1β decreases T cell-suppressive M2 TAMs in the PDA tumor microenvironment (Daley et al., 2017).

IL-1β also appears to inhibit anti-tumor T cell responses by driving an influx of myeloid-derived suppressor cells (MDSCs) (Daley et al., 2017; Das et al., 2020; Theivanthiran et al., 2020; van Deventer et al., 2010). Using an inducible melanoma model, one group reported that knocking down NLRP3 in melanoma cells prior to implantation reduced MDSC recruitment and tumor volume and increased the relative number of tumor-infiltrating $CD8^+$ T cells when combined with anti-PD-1 immunotherapy. Pharmaceutical NLRP3 inhibition had a similar effect (Theivanthiran et al., 2020). The heterogeneity of different cancers likely accounts for the disparate effects of inflammasome activation on T cell-mediated tumor immunity, and a more detailed understanding is necessary to assess whether inflammasomes are a viable target for anti-cancer therapies.

1.3.9 Broader roles of pyroptosis in cancer immunity

Gasdermin proteins are found to be increased or decreased across various tumor types—including gastric, colorectal, skin, lung, esophageal, breast, and esophageal cancers (Xia et al., 2019). In several cases, gasdermin activation and pyroptosis are triggered independent of inflammasomes. For example, it was recently found that caspase-3, which normally induces apoptosis, can also cleave and activate gasdermin-E to induce pyroptotic killing of tumor cells *in vivo* following treatment with a variety of chemotherapy drugs (Wang et al., 2017). Because many tumors are resistant to apoptosis, these findings suggest pyroptosis could be exploited to kill tumor cells. In fact, recent work shows that $CD8^+$ T cells can kill tumor cells by inducing gasdermin-mediated (but inflammasome-independent) pyroptosis (Wang et al., 2020a; Xi et al., 2019; Zhang et al., 2020; Zhou et al., 2020b). One study found that both CTL- and NK cell-derived granzyme B, which is released into the cytosol of target cells, cleaves and activates gasdermin-E, leading to tumor pyroptosis and induction of anti-tumor CTLs (Zhang et al., 2020). Another study found that granzyme A, released by NK cells and CTLs, can trigger pyroptosis via cleavage of tumor cell gasdermin-B (Zhou et al., 2020b). In both cases, the mechanism(s) by which pyroptosis leads to anti-tumor immunity deserves more study, and in particular, whether antigen and/or cytokine release by pyroptotic cells is critical for the anti-tumor effects.

A recent study used an antibody-drug conjugate containing active gasdermin-A3 to induce pyroptosis in murine mammary tumors (Wang et al., 2020a). Both intravenous and intra-tumoral injections lead to tumor regression, and the rejection was dependent on both $CD4^+$ and $CD8^+$ T cells. The authors found that blocking IL-1β also inhibited tumor regression and hypothesized that IL-1β plays a role in driving these T cell responses. However, the above study with gasdermin-E did not find an increase in IL-1β following tumor pyroptosis (Zhang et al., 2020), implying that other pyroptosis-derived signals may also have an effect on anti-tumor immunity. While it is still unclear whether targeting inflammasome-dependent pyroptosis could also induce tumor-specific adaptive immune responses, the idea that pyroptosis is immunogenic opens exciting new possibilities in cancer immunotherapy.

1.3.10 Inflammasomes and Autoimmunity

When considering the roles of inflammasome activation in autoimmunity, it is important to make a distinction between autoimmune diseases, which are driven by self-reactive B or T cells, and autoinflammatory diseases, which are not. Gain-of-function inflammasome mutations cause several rare autoinflammatory diseases—e.g., Muckle Wells Syndrome, Familial Mediterranean Fever, Cryopyrin-Associated Periodic fever Syndrome, and other inflammasomopathies (Harapas et al., 2018)—but there is currently little evidence of pathogenesis being driven by autoantibodies or self-reactive T cells in either patients or animal models of these inflammasomopathies (Brydges et al., 2009; Harapas et al., 2018; Meng et al., 2009; Nichols et al., 2017). Several studies, however, implicate inflammasomes in driving autoantigen-specific adaptive immunity (Tartey and Kanneganti, 2020). Unfortunately, the often chronic, self-perpetuating nature of autoimmune diseases makes it difficult to distinguish whether inflammasome activation is causing autoimmunity or merely reacting to the disease state. Additionally, several autoimmune diseases appear to involve multiple inflammasomes, further complicating experiments to understand their role in adaptive immunity.

Experimental autoimmune encephalomyelitis (EAE), the mouse model for multiple sclerosis, is largely driven by myelin specific $CD4^+$ T cells. In at least some instances, NLRP3 plays a role in disease induction and progression (Inoue et al., 2012), but the exact mechanisms of NLRP3 activation and subsequent effects on the pathological $CD4^+$ T cell responses are incompletely understood. One study suggested the existence of two sub-types of EAE, only one of which was driven by NLRP3 (Gris et al., 2010; Inoue et al., 2012). It has been proposed that NLRP3 contributes to EAE via a feed-forward mechanism whereby $CD4^+$ T cell-derived granulocyte-macrophage colony stimulating factor (GM-CSF) enhances inflammasome-mediated IL-1β production, and IL-1β in turn signals through the IL-1R on $CD4^+$ T cells to increase GM-CSF production (Barclay and Shinohara, 2017). Others have reported that T cell-intrinsic inflammasome activation either promotes (Martin et al., 2016) or diminishes (Braga et al., 2019) EAE disease severity. Mice deficient in cholesterol-25-hydroxylase exhibit heightened inflammasome activation and increased IL-17A-producing T cells and exacerbated EAE (Reboldi et al., 2014). More recently, it was shown that gasdermin-D is largely responsible for $CD4^+$ T cell mediated EAE (Li et al., 2019). Gasdermin-D deficiency in peripheral myeloid cells decreased disease progression and dampened the differentiation and activation of T_H1 and T_H17 cells in central nervous system.

NLRP3 has also been implicated in the development of type 1 diabetes (T1D) in both humans and mice (Carlos et al., 2017; Liu et al., 2017; Motta et al., 2015). Loss of NLRP3—whose activation promoted the proliferation, differentiation, and trafficking of diabetogenic Th1s into the pancreatic islets—delayed onset of diabetes in the spontaneous nonobese diabetic (NOD) mouse model (Hu et al., 2015). Though the underlying mechanism of NLRP3 activation is still elusive, it is interesting that bone marrow chimera experiments showed NLRP3 functioned primarily in radio-resistant (non-hematopoietic) cells. Although speculative, NLRP3 activation in islet cells (also seen in humans (Lebreton et al., 2018)) might expose self-antigens that drive disease. Inflammasome-driven pyroptosis may also be a source of self-antigens and inflammatory signals that drive auto-antibodies associated with systemic lupus

erythematosus (Qiu et al., 2019), another autoimmune disease with ties to inflammasome activation (Lu et al., 2017; Shin et al., 2013; Zhao et al., 2013).

Inflammatory bowel disease (IBD), which includes Ulcerative Colitis and Crohn's disease, is a T cell-mediated autoimmune disease thought to be driven by dysregulated innate and adaptive immune responses at the intestinal barrier. NLRP3, NLRP6, and NLRP1 have all been implicated in IBD progression; however, firm conclusions are impossible given the lack of an animal model that fully recapitulates human IBD (Choy et al., 2017; Tye et al., 2018). NLRP3 activation was recently shown to induce colitis-protective T_{reg} cells (Yao et al., 2017), yet blocking NLRP3 activity also appears to reduce or prevent IBD (Gong et al., 2018; Mak'Anyengo et al., 2018). There is further confusion surrounding the role of IL-18 in T cell-mediated IBD. Reports show IL-18R signaling on T cells either hinders (Holmkvist et al., 2016; Mak'Anyengo et al., 2018) or advances (Guan et al., 2019) disease progression in various IBD models. A better understanding of the interplay between gut microbes, intestinal inflammasomes, and adaptive immunity may shed light on the complicated etiologies behind IBD.

1.4 Concluding remarks

While there is growing evidence that inflammasome activation influences adaptive immunity under a variety of settings, many questions remain regarding when, where, and how these components of the immune system interact. As discussed above, key outstanding questions include: do pyroptotic cells act as a source of foreign or self-antigen? If so, how is that antigen presented to stimulate adaptive responses? Is inflammasome activation sufficient to trigger the adaptive immune response during an infection? What additional signals downstream of inflammasomes influence adaptive responses, and what determines whether their effects are positive or negative? A better grasp of these issues, and awareness that inflammasome responses in humans can differ from those seen in mice, is critical for the therapeutic targeting of inflammasomes in complex human diseases such as autoimmunity or cancer.

Chapter Two: Following the CD8$^+$ T cell response in OvaFla Cre-ER^{T2} system

2.1 Introduction

To investigate how inflammasome activation might influence adaptive immunity, we focused on the NAIP–NLRC4 inflammasomes, which specifically respond to flagellin (via NAIP5/6) or bacterial type III secretion system proteins (via NAIP1/2) (Kofoed and Vance, 2011; Rauch et al., 2016; Zhao et al., 2016; Zhao et al., 2011). Although most inflammasomes require the adaptor protein Apoptosis-associated Speck-like protein containing a Caspase-activation and recruitment domain (ASC) to recruit and activate pro-Caspase-1, NLRC4 is able to bind and activate pro-Caspase-1 directly—though ASC (encoded by the *Pycard* gene) has been found to enhance the production of IL-1β and IL-18 (Broz et al., 2010a; Broz et al., 2010b; Mariathasan et al., 2004). Cleavage of Gasdermin D does not require ASC following NAIP–NLRC4 activation (He et al., 2015; Kayagaki et al., 2015; Shi et al., 2015).

As discussed above, most studies to date have evaluated the effect of inflammasome activation on adaptive immunity in the context of infections. Though they are physiologically relevant, microbial infections are also complex to analyze since they engage multiple innate receptors, including TLRs. It thus remains unknown whether inflammasome activation alone provides sufficient co-stimulatory signals to initiate an adaptive response, and if so, which inflammasome-containing cell populations can drive this response. In addition, the fate of antigens after inflammasome activation remains poorly understood.

To address the role of inflammasome-induced cell death in antigen presentation and subsequent activation of CD8$^+$ T cells, we used a genetic mouse model in which an Ovalbumin (Ova)-Flagellin (Fla) fusion protein is inducibly expressed in various cell types throughout the mouse (Nichols et al., 2017). The OvaFla fusion protein provides a model antigenic epitope (SIINFEKL) to activate specific CD8$^+$ (OT-I) T cells (Hogquist et al., 1994), concomitant with the activation of the NAIP–NLRC4 inflammasome by a C-terminal fragment of flagellin that does not activate TLR5. This genetic system has the advantage of selectively activating inflammasome responses in the absence of exogenous or pathogen derived TLR ligands, allowing us to address the sufficiency of inflammasome activation for adaptive responses.

Because cells that die under inflammatory conditions can be efferocytosed and scavenged for antigen to present to the adaptive immune system (Boada-Romero et al., 2020; Davis et al., 2019; Jorgensen et al., 2016a; Jorgensen et al., 2016b), we hypothesized that OvaFla expression in WT mice, but not mice lacking NLRC4, would drive a cross-primed CD8$^+$ T cell response (Figure 1.4). However, we instead found that cross presentation of Ova peptide occurred both in the presence and absence of NAIP–NLRC4 activation. These findings suggest that inflammasome activation may have a minimal impact on CD8$^+$ T cell cross priming. It is also possible that there are parallel NLRC4–dependent and –independent cross presentation pathways.

2.2 Results

2.2.1 Genetic system for systemic OvaFla production activates NAIP–NLRC4

To study the effects of NAIP–NLRC4 activation on adaptive immunity, we took advantage of a previously established mouse model (Nichols et al., 2017) that allows for Cre-inducible and cell type-specific NAIP–NLRC4 activation (Figure 2.1). These mice harbor an OvaFla gene fusion that encodes a non-secreted chicken ovalbumin protein—a model antigen—fused to the C-terminal 166 amino acids of flagellin that functions as an agonist of NAIP–NLRC4 but not TLR5 (Nichols et al., 2017). The OvaFla gene is inserted within the constitutively expressed *Rosa26* locus, downstream of a floxed transcriptional stop cassette and upstream of an IRES-GFP cassette.

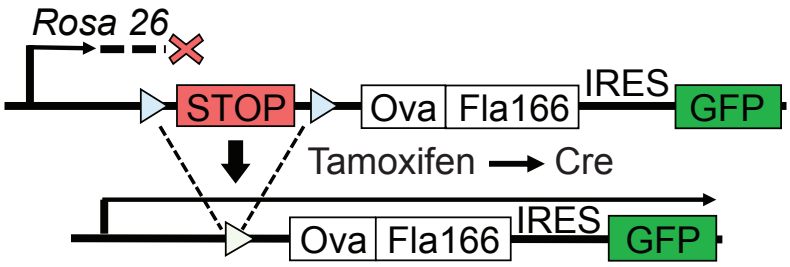

Figure 2.1. Illustration of the OvaFla gene cassette on the *Rosa 26* locus. The cassette contains full-length ovalbumin, flagellin with a C-terminal truncation at amino acid 166, and an IRES-GFP. When OvaFla mice are crossed to mice containing the tamoxifen-inducible Cre-ER^{T2}, tamoxifen administration results in Cre-controlled excision of the stop cassette and expression of the OvaFla fusion protein and GFP throughout the mouse.

To simulate the onset of infection, we crossed the OvaFla mice to the R26-CreER^{T2} mouse line (hereafter OvaFla Cre-ER^{T2}), which allows for tamoxifen-controlled expression of OvaFla in nearly any cell type throughout the mouse (Ventura et al., 2007)(Jax strain 008463). It is important to note, however, that NLRC4 and the various NAIPs are not expressed in all cells. They are highly expressed in macrophages and IECs (ImmGen), so we assumed that these would be dominant sites of NAIP–NLRC4 activation in the OvaFla Cre-ER^{T2} mice following tamoxifen administration. However, we have not directly confirmed that in the work presented below.

Tamoxifen is typically administered in a corn oil emulsion through oral gavage or intraperitoneal injection. Previous work from our lab found that corn oil contains trace bacterial contaminants that activate TLR signaling (Nichols, 2017). Thus, to avoid confounding effects of TLR activation, and to isolate the specific effects of inflammasome activation, we administered tamoxifen orally through a commercially available tamoxifen-containing chow. Mice were fed *ab libitum*. To determine if tamoxifen chow administration resulted in robust NAIP–NLRC4 activation in the OvaFla Cre-ER^{T2} mice, we placed the mice on a tamoxifen chow diet for 25 days and collected serum from the mice each week to measure IL-18—a known product of NAIP–NLRC4 activation. There was minimal IL-18 production in the WT OvaFla Cre-ER^{T2} mice prior to

beginning the tamoxifen diet (Figure 2.2). By day 7 on the diet, the WT but not *Nlrc4*$^{-/-}$ mice were producing significant amounts of IL-18, and these levels remained high through day 13. By day 25, some WT mice still had measurable systemic IL-18. Because the mice remained on tamoxifen for the entire experiment, we cannot determine whether IL-18 was continuously produced over the 25-day period, though the decrease by day 25 suggest that it is not. Notably, neither the WT nor *Nlrc4*$^{-/-}$ mice showed any signs of disease throughout the time course (not shown). We know from previous work that NAIP–NLRC4 activation in IECs leads to rapid weight loss, hypothermia, and eventually death in mice (Rauch et al., 2017; von Moltke et al., 2012), so we hypothesize that the Cre-ER^{T2} system might not result in robust OvaFla expression in IECs.

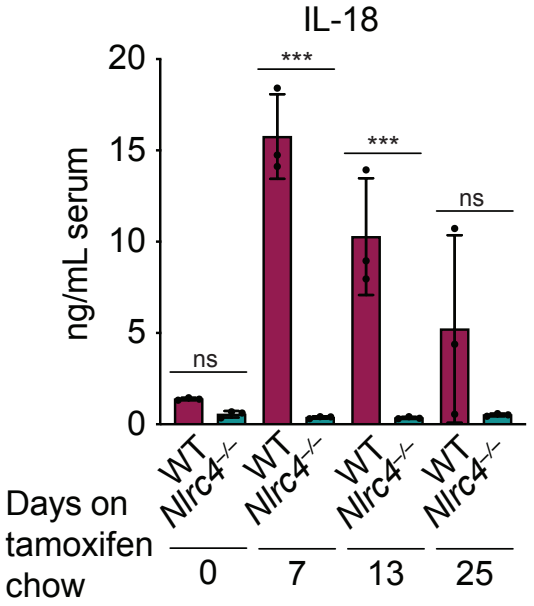

Figure 2.2. Tamoxifen administration results in systemic IL-18 production in WT but not *Nlrc4*$^{-/-}$ OvaFla Cre-ER^{T2} mice. ELISA-based quantification of IL-18 levels in WT and *Nlrc4*$^{-/-}$ OvaFla Cre-ER^{T2} mice over a 25-day course of tamoxifen chow. Data are from a single experiment, and each dot represents an individual mouse. Data shown as mean ± SD. Significance calculated using one-way ANOVA and Tukey's multiple comparisons test (*$p < 0.05$, **$p < 0.01$, ***$p < 0.001$).

2.2.2 OT-I T cell response in OvaFla Cre-ER^{T2} mice

We used congenically marked (CD45.1^{+}) SIINFEKL-specific OT-I T cells to track the CD8^{+} T cell response following tamoxifen administration in the OvaFla Cre-ER^{T2} mice. OT-Is were harvested from the spleens and mesenteric lymph nodes of OT-I *Rag2*$^{-/-}$ mice. These cells were labeled with CellTrace Violet, and 1×10^{6} cells were intravenously transferred into each OvaFla Cre-ER^{T2} mouse. The mice were kept on tamoxifen chow for five days following the adoptive transfer, and at day five, the mice were euthanized, and their peripheral lymph nodes (pLNs) and spleens were analyzed for OT-I T cell proliferation, activation, and relative numbers.

We found that there was a significant increase in the relative number of OT-Is in the pLNs of WT OvaFla Cre-ER^{T2} mice over the OvaFla only controls (Figure 2.3A). Additionally, the OT-Is in the WT OvaFla Cre-ER^{T2} mice had undergone significantly more divisions in their pLNs and spleen relative to the OvaFla only mice (Figure 2.3B). However, there was no clear difference in the OT-I activation status between these two groups (Figure 2.3C). Without a true negative control (e.g., B6 or Cre-ER^{T2} only), it is difficult to determine if the OT-Is in the OvaFla only controls are responding to a low level of cognate peptide (thus suggesting that the OvaFla transgene is somewhat "leaky") or if they are proliferating independently of TCR signaling. If the latter is true, the lack of a difference in OT-I T cell activation between WT OvaFla Cre-ER^{T2} mice and the OvaFla only mice suggests that NAIP–NLRC4 activation is not sufficient to fully activate CD8^{+} T cells.

In an interesting contrast, the OT-Is in the *Nlrc4*$^{-/-}$ OvaFla Cre-ER^{T2} mice were not significantly different from the WT or OvaFla-only control mice in relative number (Figure 2.3A), yet they had undergone more divisions (Figure 2.3B) and showed an increase in activation (Figure 2.3C) relative to the OvaFla only controls. We were surprised to see OT-I activation in the *Nlrc4*$^{-/-}$ OvaFla Cre-ER^{T2} mice because the lack of inflammasome-driven inflammation should make SIINFEKL appear more like a self-antigen. However, it is possible that constitutively expressed peptide can drive OT-I activation, though we predict that these cells will eventually become anergic (Kurts et al., 1996; Kurts et al., 1997; Liu et al., 2007; Vezys et al., 2000).

Overall, these data show that, following tamoxifen administration, OT-Is adoptively transferred into WT and *Nlrc4*$^{-/-}$ OvaFla Cre-ER^{T2} mice encounter their cognate antigen and divide, regardless of NAIP–NLRC4 activation.

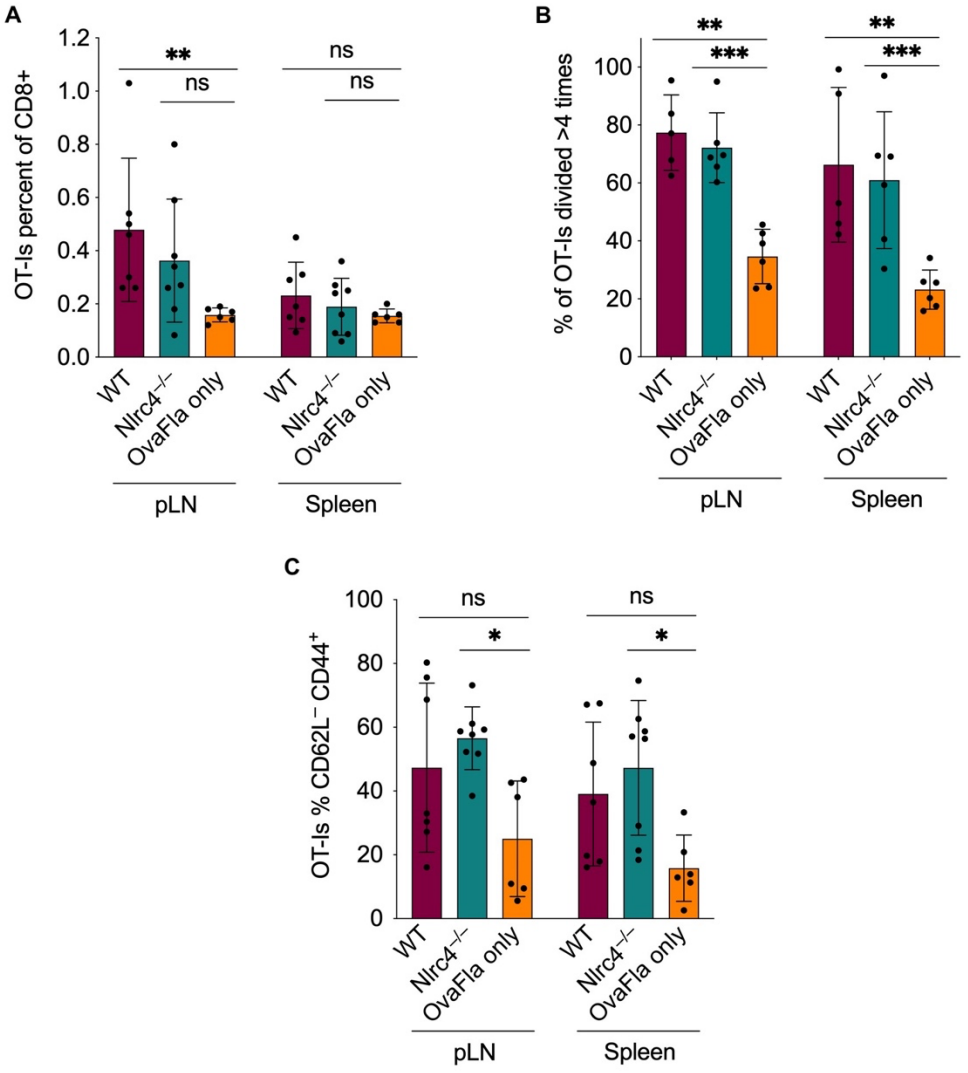

Figure 2.3. OvaFla production in Cre-ER^{T2} mice results in OT-I T cell proliferation and activation. **A.** Quantification of OT-Is as a percent of total CD8$^+$ T cells in the peripheral lymph nodes and spleens of the indicated OvaFla Cre-ERT2 mice. **B.** Percent of OT-Is that have divided at least five times in the peripheral lymph nodes and spleens of the mice from A. **C.** Percent of OT-Is that are CD62L$^-$CD44$^+$ in the peripheral lymph nodes and spleens of the mice from A. Data are pooled from three biological replicates, and each dot represents an individual mouse. Data shown as mean ± SD. Significance calculated using one-way ANOVA and Tukey's multiple comparisons test (*$p < 0.05$, **$p < 0.01$, ***$p < 0.001$).

2.2.3 Neonatal chimeras as a potential tool to reduce the number of OvaFla producing cells in the Cre-ER^{T2} system

One concern we had with the OvaFla Cre-ER^{T2} mice was that a potentially large number of cells could be producing OvaFla throughout the mouse following tamoxifen treatment. Since most cytosolic infections begin with relatively few infected (antigen-carrying) cells, we were interested in finding a way to reduce the number of OvaFla producing cells. To do so, we created neonatal chimeras, which generate adult mice with a donor cell frequency of less than 10% (Durkin et al., 2008). We transferred 3×10^6 bone marrow stem cells from WT OvaFla Cre-ER^{T2}, *Nlrc4*$^{-/-}$ OvaFla Cre-ER^{T2}, or OvaFla only mice into three-day old B6 neonates and confirmed engraftment by PCR amplification of the OvaFla transgene in peripheral blood (data not shown).

When the mice were 11 weeks of age, we transferred 1×10^6 OT-I T cells and put the mice on a tamoxifen chow diet. After five days, we euthanized the mice and harvested the pLNs and spleen. Unfortunately, there was no difference in the relative number (Figure 2.4A) or activation (Figure 2.4B) of OT-Is across any of the mice. There was a significant but modest increase in the percent of OT-Is that had divided in the spleen between the *Nlrc4*$^{-/-}$ OvaFla Cre-ER^{T2} mice and the mice that did not receive any bone marrow stem cells (Figure 2.4C), but there were no other clear differences in OT-I division between mouse groups. There was a large data spread in this neonatal chimera experiment, and so it is possible that boosting the numbers of mice could create a better separation between the experimental and control groups.

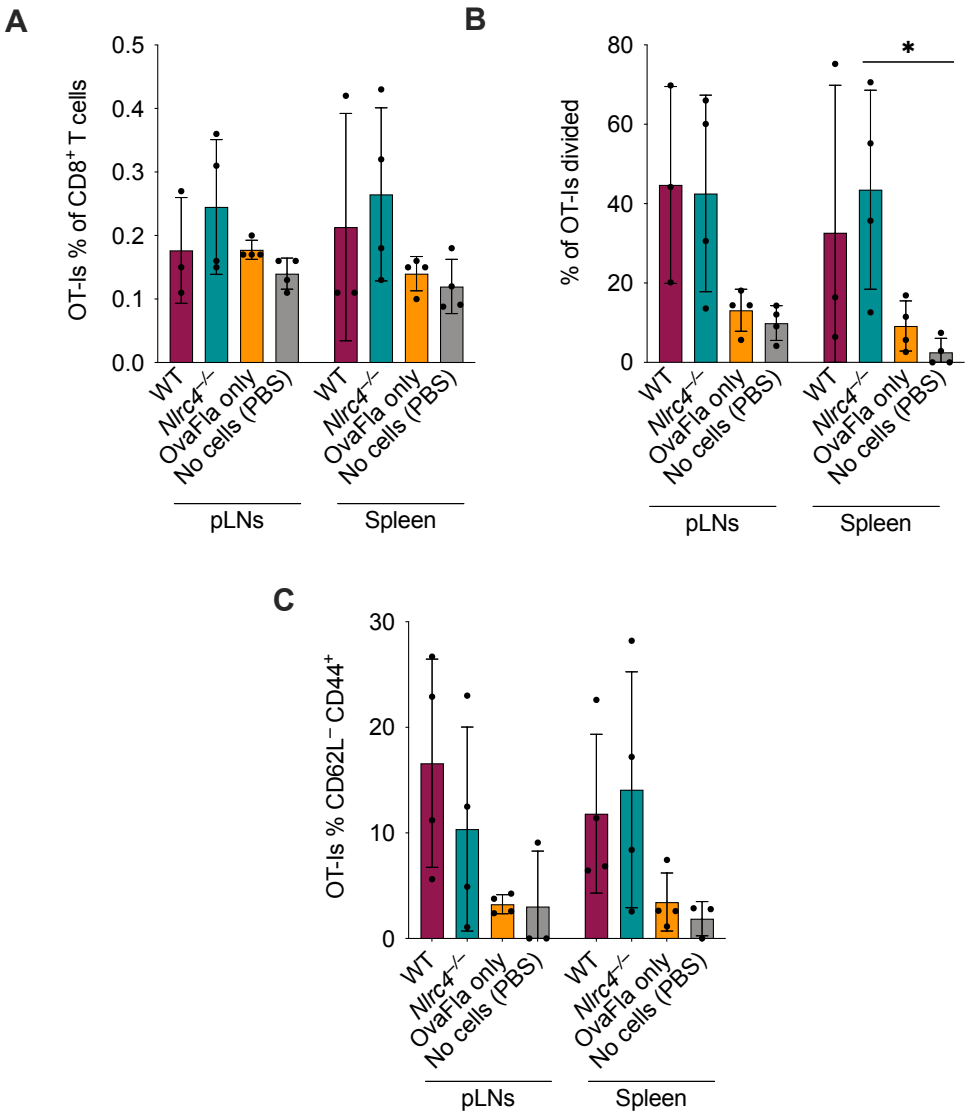

Figure 2.4. Neonatal chimeras as a potential tool to reduce the number of OvaFla producing cells in the Cre-ER^{T2} system. **A.** Quantification of OT-Is as a percent of total CD8$^+$ T cells in the peripheral lymph nodes and spleens of chimeric mice that received bone marrow from the indicated OvaFla Cre-ER^{T2} lines at three days post birth. **B.** Percent of OT-Is that have divided in the peripheral lymph nodes and spleens of the mice from A. **C.** Percent of OT-Is that are CD62L$^-$CD44$^+$ in the peripheral lymph nodes and spleens of the mice from A. Data are from a single experiment, and each dot represents an individual mouse. Data shown as mean ± SD. Significance calculated using one-way ANOVA and Tukey's multiple comparisons test (*p < 0.05).

2.2.4 Concentration of OvaFla expressing cells in OvaFla Cre-ER^{T2} system

Although the neonatal chimeras allowed us to decrease the overall number of OvaFla-producing cells, the OvaFla production is still likely spread systemically throughout the mouse. Since most infections begin in a localized site, we sought to concentrate the source of OvaFla expression *in vivo*. To do so, we tried two different general approaches.

The first approach was to transfer different cell types from WT and *Nlrc4*$^{-/-}$ OvaFla mice naïve B6 mice. In one experiment, we transferred peritoneal macrophages from OvaFla mice. All of the recipient B6 mice were then given 1×10^6 OT-I T cells and placed on tamoxifen chow for five days. On day five, the mice were euthanized and spleen, peripheral lymph nodes, and peritoneal lavage were harvested. While we were able to recover OT-Is in all recipient mice, there was no clear increase in their relative number between the experimental groups and the B6 control (Figure 2.5A). Interestingly, the majority of the splenic OT-Is in the mice that received WT and *Nlrc4*$^{-/-}$ OvaFla Cre-ER^{T2} peritoneal macrophages had divided, indicating that these cells had encountered their cognate antigen. There was also a clear, but insignificant, increase in OT-I division between these groups and the B6 controls (Figure 2.5B).

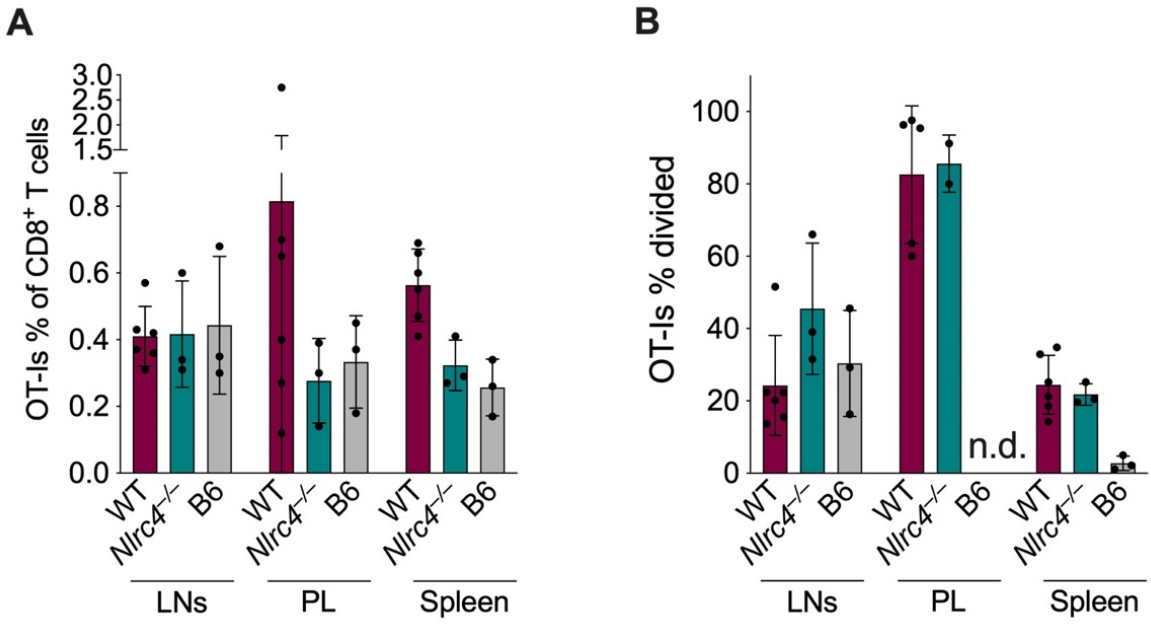

Figure 2.5. Peritoneal macrophage transfer from OvaFla Cre-ER^{T2} mice. **A.** Quantification of OT-Is as a percent of total CD8$^+$ T cells in the peripheral lymph nodes, peritoneal lavage, and spleen of B6 mice that received peritoneal macrophages from the indicated mouse lines. **B.** Percent of OT-Is that have divided in the peripheral lymph nodes, peritoneal lavage, and spleen of B6 mice that received peritoneal macrophages from the indicated mouse lines. Data are from a single experiment, and each dot represents an individual mouse. Data shown as mean ± SD. n.d. indicates no data for that condition.

In a second experiment, bone marrow-derived DCs (BMDCs) were made from WT and *Nlrc4*$^{-/-}$ mice and transferred subcutaneously into naïve B6 hosts. The advantage of BMDCs is that we can test their ability to produce OvaFla *in vitro* by treating the cells with 4-OHT and performing a B3Z assay. The B3Z assay uses a highly sensitive T cell hybridoma expressing an MHC I–SIINFEKL specific TCR (Karttunen et al., 1992). TCR signaling in these cells activates expression of β-galactosidase following recognition of the Ova peptide presented on H2-K^{b}. When treated with different concentrations of 4-OHT, BMDCs from *Nlrc4*$^{-/-}$ OvaFla mice produced measurable levels of SIINFEKL peptide (Figure 2.6A). There was no apparent SIINFEKL in the WT OvaFla mice, though we hypothesize this to be because these cells undergo rapid pyroptosis. We transferred untreated BMDCs into recipient B6 mice, and then gave each mouse 1×10^{6} OT-I T cells followed by five days of tamoxifen chow. On day five, the mice were euthanized, and the spleens and peripheral lymph nodes were collected. Although there was no clear difference in relative number of OT-Is between mouse groups (Figure 2.6B), the mice that received BMDCs from WT OvaFla mice had significantly more OT-Is in their pLNs relative to the mice that received *Nlrc4*$^{-/-}$ BMDCs (Figure 2.6C). Additionally, the OT-Is in the pLNs and spleens of these mice had undergone a significant number of divisions when compared with the Cre only controls (Figure 2.6D). These data suggest that NAIP–NLRC4 activation in a localized subset of cells can drive proliferation of antigen-specific CD8^{+} T cells.

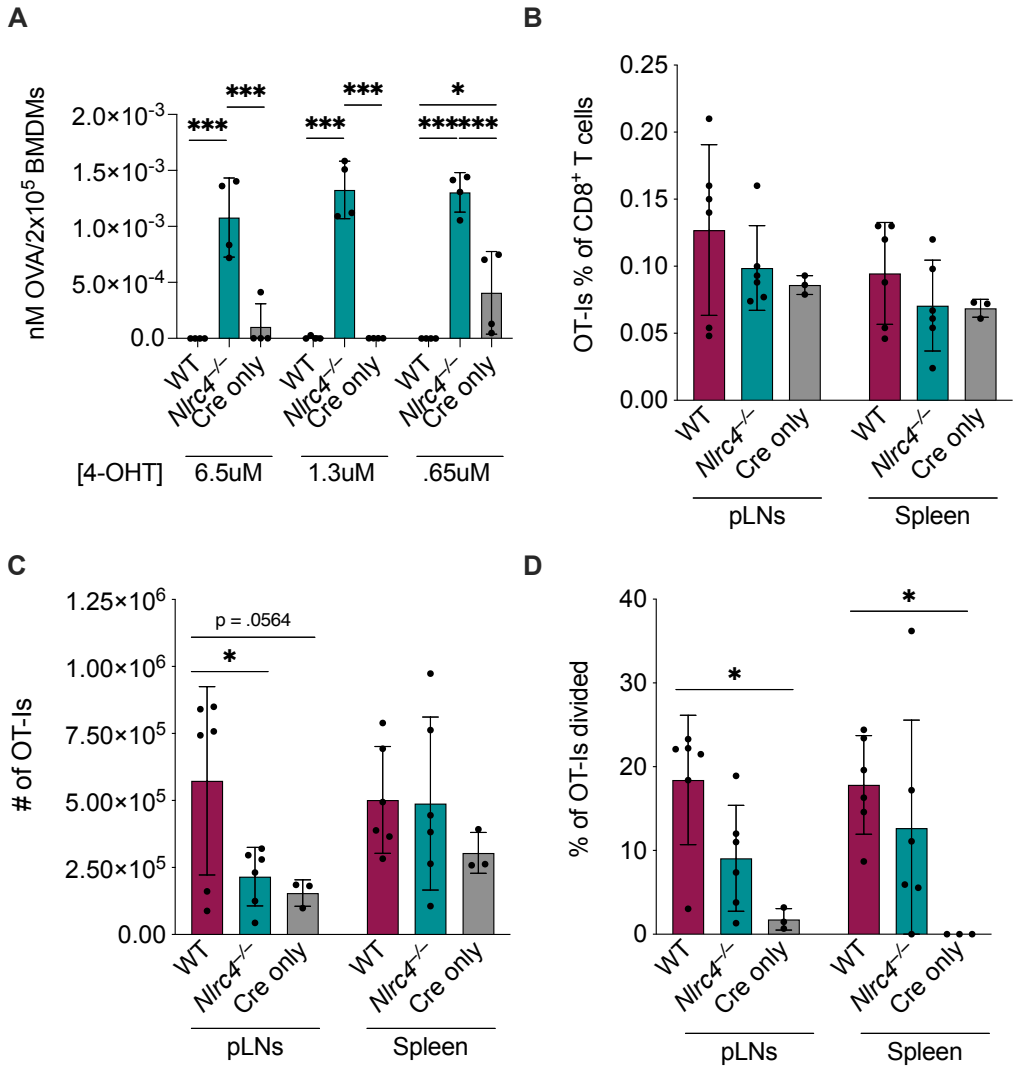

Figure 2.6. BMDC transfer from WT OvaFla Cre-ER^{T2} mice results in significant OT-I proliferation. **A.** Quantification of SIINFEKL peptide presented on BMDCs from the OvaFla mouse lines following treatment with the indicated amounts of 4-OHT **B.** Quantification of OT-Is as a percent of total CD8$^+$ T cells in the peripheral lymph nodes, peritoneal lavage, and spleen of B6 mice that received peritoneal macrophages from the indicated mouse lines. **C**. Total number of OT-Is. **D.** Percent of OT-Is that have divided in the peripheral lymph nodes, peritoneal lavage, and spleen of B6 mice that received peritoneal macrophages from the indicated mouse lines. Data are from a single experiment, and each dot represents an individual mouse. Data shown as mean ± SD. Significance calculated using one-way ANOVA and Tukey's multiple comparisons test (*$p < 0.05$, **$p < 0.01$, ***$p < 0.001$).

Our second general approach to localize the OvaFla expressing cells *in vivo* involved topical application of 4-hydroxytamoxifen (OHT) (Sigma, Cat # SML1666-1ML)—the tamoxifen derivative that binds the estrogen receptor—to the ears of OvaFla Cre-ER^{T2} mice. The goal here was to selectively activate NAIP–NLRC4 in an area that drains to the cervical lymph nodes (cLNs), which would ideally localize an adaptive immune response. In these experiments, mice were given 1×10^6 OT-I T cells, and then one ear received 100μg of 4-OHT dissolved in ethanol (EtOH), while the other remained untreated as a contralateral control (Figure 2.7A). The cLNs from each side, as well as the spleen, were harvested five days later and analyzed for OT-I proliferation and activation.

In the first experiment, we compared mice that received 4-OHT with mice that received EtOH as a control. There was no difference in the relative (Figure 3.4B) or total number (Figure 2.7C) of OT-Is in any tissue examined between these two groups of mice. However, the OT-Is in the cLNs from the painted ear of mice that received 4-OHT were significantly more activated (Figure 2.7D) and had undergone more divisions (Figure 2.7E) when compared to the mice that received EtOH. The splenic OT-Is in the 4-OHT treated mice were also more activated than those in the EtOH mice (Figure 2.7D). These data show we can induce OvaFla production in the Cre-ER^{T2} system through topical application of 4-OHT.

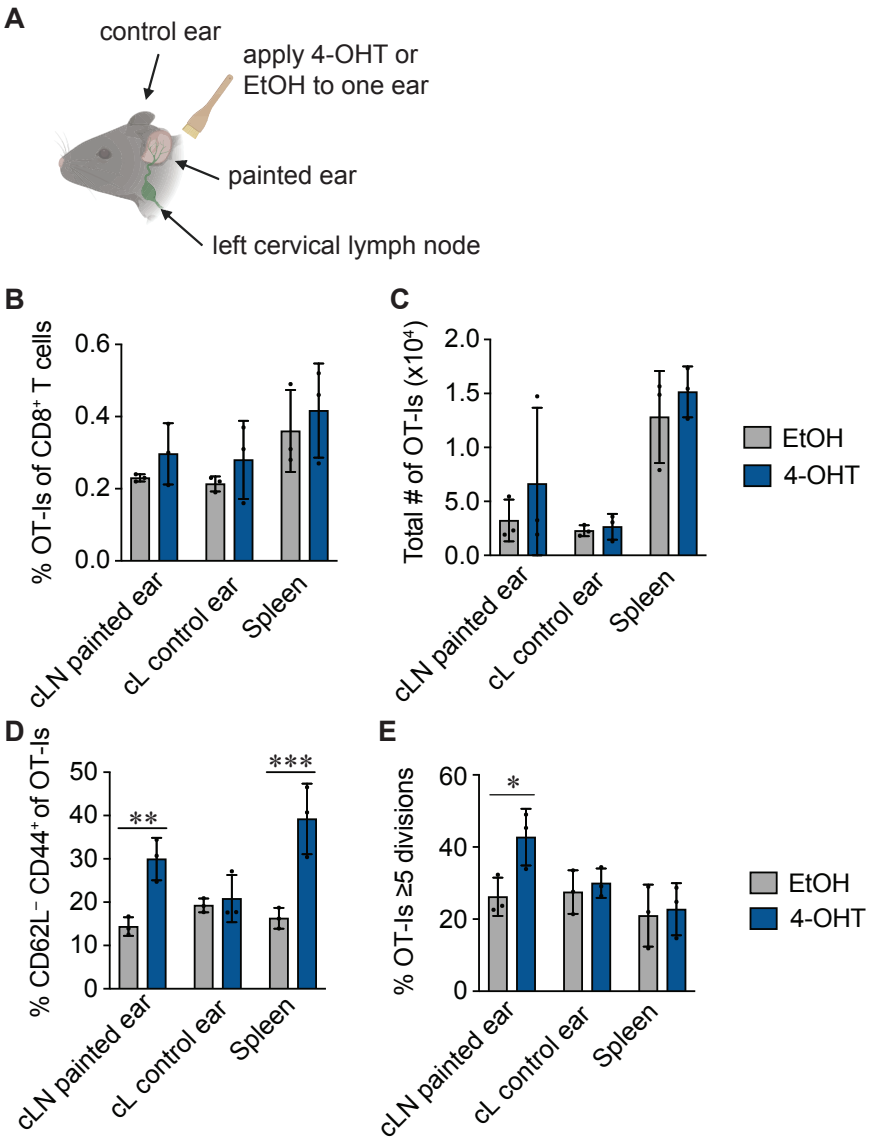

Figure 2.7. Topical application of 4-OHT results in OT-I activation in WT OvaFla Cre-ER^{T2} mice. **A.** Illustration of the experimental setup, where 100μg of 4-OHT or an EtOH control was applied to the left ear of each mouse following OT-I transfer. cLNs from the ipsilateral (treated) and contralateral (un-treated) ear were harvested, along with the spleen, five days later, and analyzed for OT-I activation and proliferation. **B.** Quantification of OT-Is as a percent of total CD8$^+$ T cells in each tissue. **C.** Total number of OT-Is. **D.** Percent of OT-Is that have divided. **D.** Percent of OT-Is that are CD62L$^-$ CD44$^+$. **E.** Percent of OT-Is that have divided five our more times. Data are from a single experiment, and each dot represents an individual mouse. Data shown as mean ± SD. Significance calculated using one-way ANOVA and Tukey's multiple comparisons test (*p < 0.05, **p < 0.01, ***p < 0.001).

In the second experiment, we followed the same protocol outlined in Figure 2.7A and compared OT-Is in WT OvaFla Cre-ER^{T2} mice with those in *Nlrc4*$^{-/-}$ OvaFla Cre-ER^{T2} mice and Cre-ER^{T2} only mice. We found relatively more OT-Is in all three tissues of the WT and *Nlrc4*$^{-/-}$ mice when compared to Cre-only control mice (Figure 2.8A). These OT-Is had also divided significantly more times (Figure 2.8B) and had a higher percent of activation (Figure 2.8C) relative to the controls. Additionally, in the WT mice, there was a significant increase in relative OT-I numbers (Figure 2.8A) and their division (Figure 2.8B) in the cLNs from the painted ear relative to the cLNs from the unpainted ear. In all, these data suggest that topical application of 4-OHT can be a successful method of creating localized NAIP–NLRC4 activation using the Cre-ER^{T2} system.

From the above experiments, it appears that localization of OvaFla production is possible with further optimization. These and similar experiments, such as transfer of bone marrow macrophages or DCs derived from OvaFla Cre-ER^{T2} mice, might improve the use of the OvaFla Cre-ER^{T2} system as a tool for studying the effects of NAIP–NLRC4 activation on adaptive immunity.

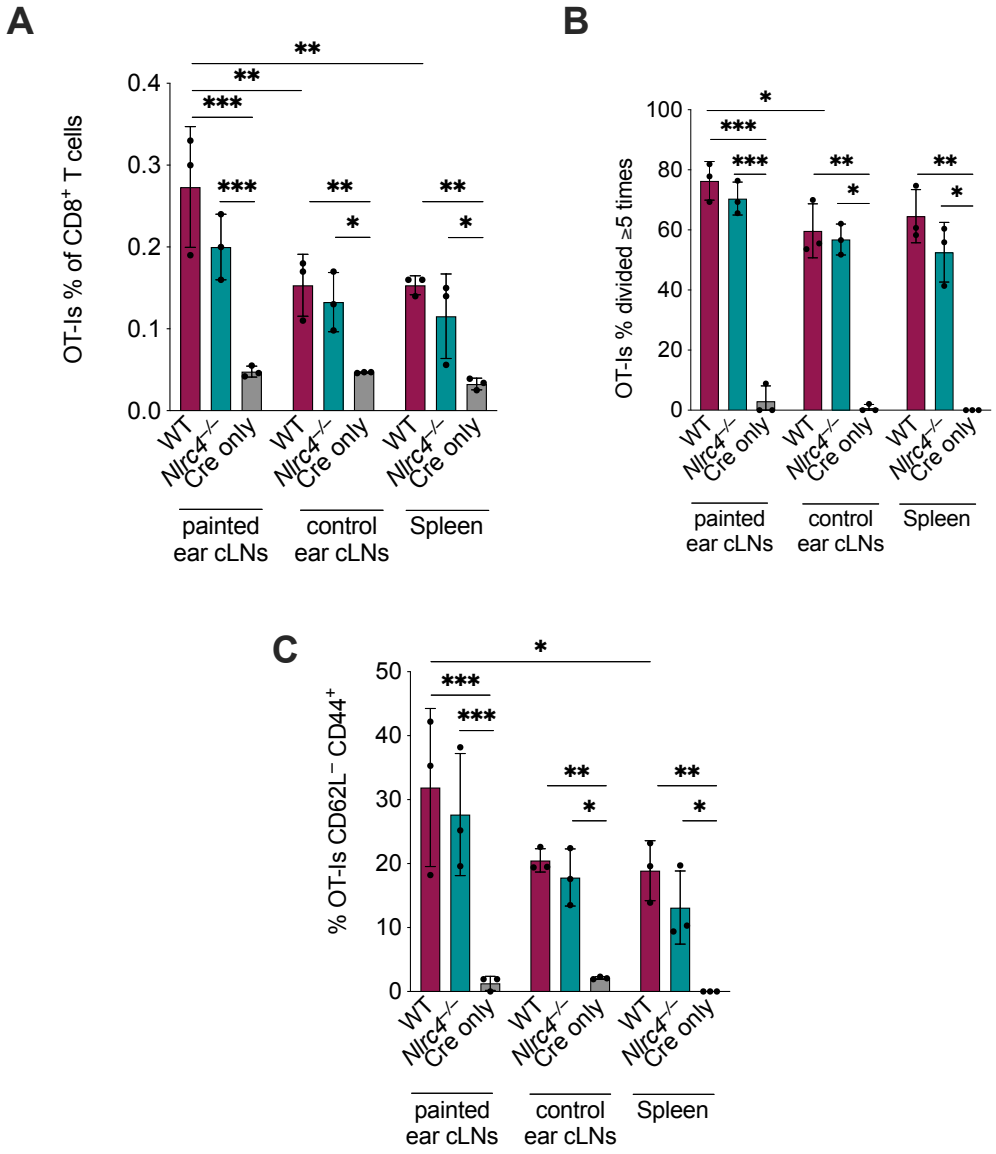

Figure 2.8. Topical application of 4-OHT results in similar OT-I proliferation and activation between WT and *Nlrc4*$^{-/-}$ OvaFla Cre-ERT2 mice. **A.** Quantification of OT-Is as a percent of total CD8^{+} T cells in the cLNs from the painted and control side, as well as the spleen from the indicated mouse lines. **B.** Percent of OT-Is that have divided in the in the cLNs from the painted and control side, as well as the spleen from the indicated mouse lines. **C.** Percent of OT-Is that are CD62L^{-} CD44^{+} in the cLNs from the painted and control side, as well as the spleen from the indicated mouse lines. Data are from a single experiment, and each dot represents an individual mouse. Data shown as mean ± SD. Significance calculated using one-way ANOVA and Tukey's multiple comparisons test (*p < 0.05, **p < 0.01, ***p < 0.001).

2.2.5 Irradiation bone marrow chimeras with OvaFla Cre-ER^{T2} mice

Throughout the above experiments, we regularly saw similar levels of OT-I proliferation and activation between the WT and *Nlrc4*$^{-/-}$ OvaFla mice. We hypothesize that OvaFla expressing cells in the *Nlrc4*$^{-/-}$ mice accumulate cytosolic OvaFla because they are not undergoing NAIP–NLRC4-mediated pyroptosis. Because all nucleated cells express MHC I, which is used to present cytosolic peptides, it is possible that the OvaFla-producing cells in the *Nlrc4*$^{-/-}$ mice are directly presenting SIINFEKL to the OT-Is. To test this hypothesis, we took advantage of the H-2K^{bm1} mouse model that contains a seven base pair mutation in the gene encoding K^{b} (Schulze et al., 1983). The bm1 mutation renders K^{b} unable to bind the Ova-derived OT-I agonist peptide, SIINFEKL (Nikolic-Zugic and Bevan, 1990). We bred H-2K^{bm1} mice to each of our OvaFla lines to establish mice that make OvaFla but are incapable of directly presenting the SIINFEKL peptide (H-2K^{bm1+} OvaFla Cre-ER^{T2} mice, referred to here as bm1^{+} OvaFla Cre-ER^{T2} mice). We then generated bone marrow chimeras using bm1^{+} OvaFla Cre-ER^{T2} mice as lethally irradiated recipients that were reconstituted with WT H-2K^{b} bone marrow from B6 CD45.1 donors. In this experimental setup, adoptively transferred OT-I T cells will only see their cognate antigen if it is cross presented from OvaFla-producing cells.

After five days of tamoxifen chow, we found relatively more OT-Is in the mesenteric lymph nodes of the bm1^{+} WT OvaFla Cre-ER^{T2} mice when compared to the bm1^{+} OvaFla only mice (Figure 2.9A), though the total number of OT-Is between these groups of mice was not significantly different (Figure 2.9B). However, of the OT-Is present in both the mesenteric lymph nodes and the spleen of the bm1^{+} WT mice, a significantly higher proportion of them were CD62L^{-}CD44^{+} relative to the bm1^{+} OvaFla only control (Figure 2.9C). Although the differences are minor, and the experiment is lacking a true negative control (e.g., Cre only), these data suggest that NAIP–NLRC4 expression—in some unknown cell type(s)—is driving the cross-priming of OT-I CD8^{+} T cells. We found similar results when we compared OT-I proliferation and activation between the bm1^{+} *Nlrc4*$^{-/-}$ OvaFla Cre-ER^{T2} mice and the bm1^{+} OvaFla only control. The bm1^{+} *Nlrc4*$^{-/-}$ mice had significantly more OT-Is in both relative (Figure 2.9A) and absolute (Figure 2.9B) numbers in the mesenteric lymph nodes. The OT-Is were also more activated (Figure 2.9C, D). These data indicate that cross presentation is also occurring in the bm1^{+} *Nlrc4*$^{-/-}$ OvaFla Cre-ER^{T2}, which is surprising given our assumption that cells in these mice are not undergoing OvaFla-induced cell death. Perhaps homeostatic turnover of these cells is sufficient to release antigen for cross presentation in the OvaFla system.

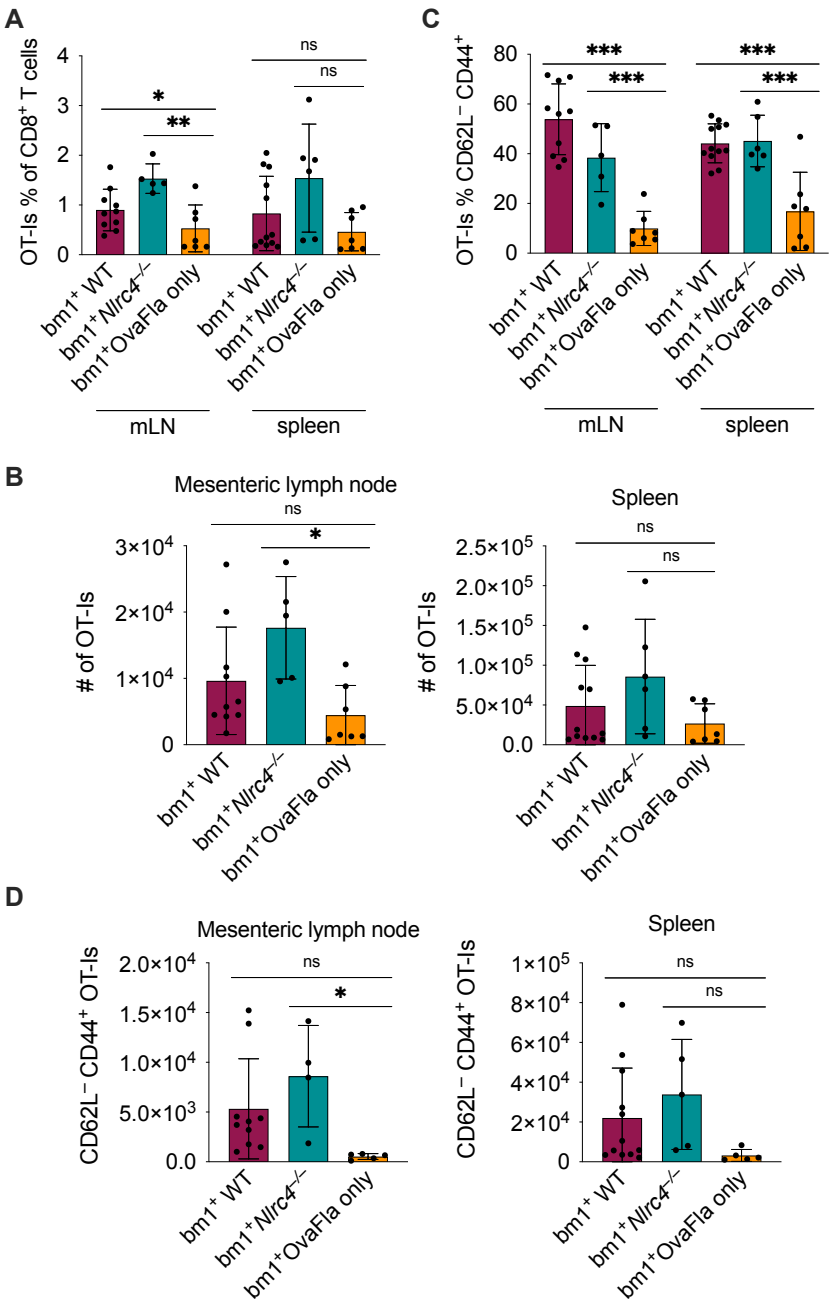

Figure 2.9. SIINFEKL is cross presented to OT-Is in chimeric bm1$^+$ OvaFla Cre-ER^{T2} mice. **A.** OT-Is as a percent of total CD8$^+$ T cells in the mLNs and spleens of the indicated bm1$^+$ OvaFla Cre-ERT2 mice after five days on tamoxifen chow. **B.** Total number of OT-Is in the mLNs (left) and spleens (right) of the mice from A. **C.** Percent of OT-Is that are CD62L$^-$CD44$^+$ in the mice from A. **D.** Total number of CD62L$^-$CD44$^+$ OT-Is in the mLNs (left) and spleens (right) of the mice from A. Data are pooled from two biological replicates, and each dot represents an individual mouse. Data shown as mean ± SD. Significance calculated using one-way or two-way ANOVA and Tukey's multiple comparisons test (*p < 0.05, **p < 0.01, ***p < 0.001).

2.2.6 No role for the IL-18 receptor on cross-priming following NAIP–NLRC4 activation

The bm1^{+} OvaFla Cre-ER^{T2} chimera system allows us to study the APC population(s) responsible for cross-priming the OT-I CD8^{+} T cells. One of the many questions we have regarding this cross-priming is: What inflammatory molecules are driving APC maturation to provide the three signals (antigen presentation, co-stimulation, inflammatory cytokines) required to activate naïve T cells (Figure 1.2)? Another group has shown that IL-18 can drive the upregulation of co-stimulatory molecules on cultured cells (Li et al., 2004). Because we know NAIP–NLRC4 activation leads to relatively high levels of systemic IL-18, we hypothesized that this inflammatory cytokine might play a role in cross presentation in the OvaFla Cre-ER^{T2} mice.

To test this hypothesis, we again generated irradiation bone marrow chimeras with bm1^{+} WT and bm1^{+} *Nlrc4*$^{-/-}$ OvaFla Cre-ER^{T2} as hosts. This time, we transferred bone marrow from either B6 mice or from IL-18R$^{-/-}$ mice. If IL-18 signaling is driving maturation of the SIINFEKL cross presenting APCs, we expect a decrease in OT-I proliferation and activation in mice that received IL-18R$^{-/-}$ bone marrow relative to B6 bone marrow. However, we did not observe any difference in relative (Figure 2.10A) or absolute (Figure 2.10B) OT-I numbers between these groups of mice. There was also no difference in the proliferation (Figure 2.10C) or activation (Figure 2.10D). These data demonstrate that IL-18R signaling on APCs is not required for the cross-priming of OT-I T cells in the OvaFla Cre-ER^{T2} mice.

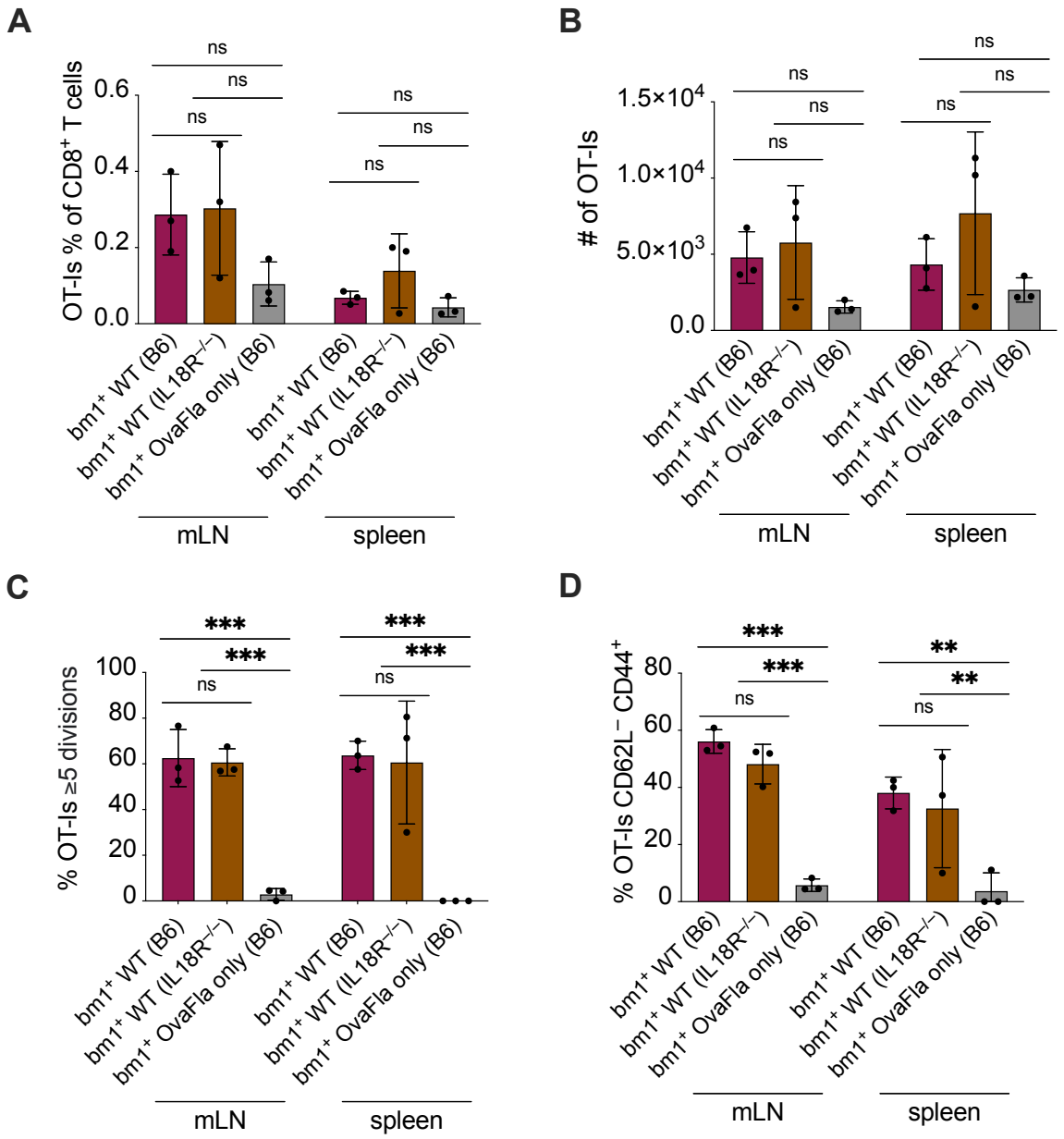

Figure 2.10. The IL-18R on APCs is not required for cross priming OT-I T cells in WT OvaFla Cre-ER^{T2} mice. **A.** OT-Is as a percent of total CD8$^+$ T cells in the mLNs and spleens of the indicated bm1$^+$ OvaFla Cre-ER^{T2} mice after five days on tamoxifen chow. **B.** Total number of OT-Is in the mLNs and spleens of the mice from A. **C.** Percent of OT-Is that have divided at least five times. **D.** Percent of OT-Is that are CD62L$^-$CD44$^+$ in the mice from A. Data are from a single experiment, and each dot represents an individual mouse. Data shown as mean ± SD. Significance calculated using one-way or two-way ANOVA and Tukey's multiple comparisons test (*p < 0.05, **p < 0.01, ***p < 0.001).

2.3 Discussion

The goal of the OvaFla Cre-ER^{T2} mouse system was to address the question of how NAIP–NLRC4 activation influences the generation of CD8$^+$ T cell immunity. Because OvaFla expression is temporally controlled through tamoxifen chow administration, we could adoptively transfer Ova peptide-specific OT-I CD8$^+$ T cells into these mice and assess OT-I T cell proliferation and activation following OvaFla production. We used IL-18 production as a readout of NAIP–NLRC4 activation and confirmed that tamoxifen chow induces systemic IL-18 in an NLRC4-dependent manner (Figure 2.2). We also found that OvaFla production results in OT-I T cell proliferation and activation in both WT and *Nlrc4*$^{-/-}$ OvaFla Cre-ER^{T2} mice (Figure 2.3). These data suggest that the CD8$^+$ T cell response is independent of NAIP–NLRC4 activation; however, it remains possible that the OT-Is are being activated through separate NLRC4-dependent and -independent mechanisms (see Chapter Three).

Because the Cre-ER^{T2} system results in potentially high levels of systemic OvaFla expression, we searched for an experimental approach that would reduce or localize the OvaFla-producing cells within the mouse. We first tried to reduce the overall number of cells capable of making OvaFla by generating neonatal chimeras in which B6 mice were given bone marrow stem cells from WT and *Nlrc4*$^{-/-}$ OvaFla Cre-ER^{T2} mice (Figure 2.4). Unfortunately, this experiment yielded variable OT-I activation that did not differ significantly from the control mice who received no stem cells. We next attempted to localize the OvaFla producing cells to better mimic a physiological immune response. For the first approach, we transferred peritoneal macrophages or BMDCs from WT and *Nlrc4*$^{-/-}$ OvaFla Cre-ER^{T2} mice into B6 hosts. For the peritoneal macrophages, there was no clear increase in OT-I activation in either of these mouse groups over the B6 controls (Figure 3.5). However, there were a significant number of dividing OT-Is in mice that received BMDCs from WT OvaFla mice (Figure 3.6). For the second approach, we chose to localize the tamoxifen administration by applying 4-OHT to the ears of WT and *Nlrc4*$^{-/-}$ OvaFla Cre-ER^{T2} mice (Figures 3.7, 3.8). These experiments yielded OT-I proliferation and activation that were significantly higher than in control mice, suggesting that topical tamoxifen application may be a useful approach to localizing OvaFla production.

From the initial OT-I T cell experiments, we were surprised to see OT-I activation and proliferation in the *Nlrc4*$^{-/-}$ OvaFla Cre-ER^{T2} mice, as the OvaFla-expressing cells in these mice, are not producing inflammatory signals or undergoing pyroptosis. We hypothesized that the OT-I activation may be a result of cells directly presenting the SIINFEKL peptide on their MHC I. To eliminate direct presentation, we used the H-2K^{bm1} mouse model to create a scenario where OT-Is can only see their cognate antigen if it is cross-presented (Figure 2.9). Surprisingly, we still found OT-I cross priming in both the WT and *Nlrc4*$^{-/-}$ OvaFla Cre-ER^{T2} mice. These data suggest that NAIP–NLRC4 activation may play a negligible role in cross presentation, or as discussed in Chapter Three, there may be parallel pathways of inflammasome-dependent and -independent cross presentation.

Finally, we took advantage of the bm1$^+$ OvaFla Cre-ER^{T2} system to test the hypothesis that IL-18R signaling might drive antigen cross presentation following NAIP–NLRC4 activation. We compared chimeric bm1$^+$ OvaFla Cre-ER^{T2} mice that received

either B6 bone marrow or IL-18R$^{-/-}$ bone marrow and found no difference in OT-I proliferation or activation between these mice (Figure 2.10), though it is important to note that this experiment does not rule out a role for IL-18R signaling on the OT-I T cells themselves. The bm1^{+} OvaFla Cre-ER^{T2} chimeric system can still be used to test the role of other inflammatory signals, such as IL-1β.

Overall, these experiments show that both systemic and localized OvaFla expression can drive cross priming of OT-I CD8^{+} T cells. It remains unclear if there are two separate NLRC4-dependent and -independent mechanisms for cross presentation, or if NAIP–NLRC4 activation instead has no role in CD8^{+} T cell cross priming. One approach to determine if the former is true is to dissect the mechanism(s) of antigen presentation following OvaFla production. Unfortunately, systemic antigen production in the OvaFla Cre-ER^{T2} mice likely leads to OvaFla expression and NAIP–NLRC4 activation in different cell types throughout the mouse. These different cell types (for example, alveolar macrophages versus IECs) may engage different cross-presenting APCs, thus making it difficult to experimentally test the individual roles of these APCs in CD8^{+} T cell cross priming in the presence or absence of NAIP–NLRC4 activation. The bone marrow chimera experiments with bm1^{+} OvaFla Cre-ER^{T2} mice (Figure 2.9) suggest that the antigen being cross presented is derived from non-hematopoietic, or other radioresistant, cells. Work from our lab and others found that NAIP–NLRC4 can be robustly activated in IECs (Rauch et al., 2017; Sellin et al., 2014), and other recent work has begun to uncover the mechanisms of IEC-derived antigen presentation. Therefore, we decided to move the OvaFla system to an IEC-specific Cre driver and focus on the question of whether NAIP–NLRC4 activation in IECs has a role in CD8^{+} T cell cross priming.

Chapter Three: Inflammasome activation leads to cDC1 independent cross-priming of CD8 T cells by epithelial cell derived antigen

3.1 Introduction

NAIPs and NLRC4 are highly expressed in IECs, where they provide defense against enteric bacterial pathogens including *Citrobacter* (Nordlander et al., 2014), *Salmonella* (Fattinger et al., 2021; Hausmann et al., 2020; Rauch et al., 2017; Sellin et al., 2014) and *Shigella* (Mitchell et al., 2020). Inflammasome-driven IEC expulsion appears to be a major mechanism by which NAIP–NLRC4 provides innate defense against enteric pathogens. However, it is not currently known how NAIP–NLRC4 activation, pyroptosis, and IEC expulsion influence the availability of IEC-derived antigens and what impact this has on the adaptive immune response. Conceivably, expulsion of pyroptotic epithelial cells may result in the loss of antigen, thereby hindering adaptive immunity, or alternatively, pyroptosis may promote the release of epithelial or hematopoietic cell antigens to APCs to activate adaptive immunity. Indeed, even at steady state in the absence of inflammasome activation and pyroptosis, it remains unclear how antigens present in IECs are delivered to APCs to stimulate adaptive immune responses, or whether perhaps IECs can directly activate T cells (Chulkina et al., 2020; Heuberger et al., 2021; Liu and Lefrancois, 2004; Nakazawa et al., 2004). cDC1s are thought to acquire apoptotic bodies from IECs and shuttle the cell-associated antigens through the MHC II pathway to drive a tolerogenic $CD4^+$ T cell response under homeostatic conditions (Cummings et al., 2016; Huang et al., 2000). These cells were also recently shown to induce $FoxP3^+CD8^+$ T_{regs} through the cross presentation of IEC-derived tissue specific antigens (Joeris et al., 2021). Additionally, in the context of inflammation, a subset of migratory cDC1s have been shown to also take up IEC-derived antigen to activate $CD8^+$ T cells; however, it remains unclear how these cDC1s acquire IEC-derived antigen.

Because NAIP–NLRC4 activation can result in IEC pyroptosis prior to the expulsion of IECs from the epithelium (Rauch et al., 2017), we hypothesized that cell lysis could release antigen basolaterally, which could then be taken up by cDC1s and cross-presented to $CD8^+$ T cells. To test this hypothesis, we used the OvaFla genetic mouse model described in Chapter Two, which couples expression of the model antigen Ovalbumin (Ova) with expression of the C-terminal fragment of flagellin (Fla) that selectively activates NAIP5/6 and not TLR5. To temporally control NAIP–NLRC4 activation and OvaFla production in IECs, these OvaFla mice were bred to a tamoxifen-inducible IEC-specific Cre driver. Our results suggest the existence of distinct NLRC4-dependent and NLARC4-independent pathways for cross-presentation of IEC-derived antigens *in vivo*.

3.2 Results

3.2.1 IECs undergo pyroptosis prior to expulsion following NAIP–NLRC4 activation

Previous work established that NAIP–NLRC4 activation in IECs drives the expulsion of these cells upon *Salmonella* infection (Sellin et al., 2014), so we were interested in building a better understanding of the expulsion process. To do so, we first used a

murine intestinal organoid model. Intestinal organoids are three-dimensional cultures of primary cells derived from stem cells that reside in the small intestinal crypts (Gomez and Boudreau, 2021; Miyoshi and Stappenbeck, 2013). NAIP–NLRC4 can be specifically activated in these cells with the extracellular addition of FlaTox—a protein fusion of *Legionella pneumophila* flagellin (FlaA), which binds and activates NAIP5, and *Bacillus anthracis* lethal factor (LFn), which allows the FlaTox complex to enter the cytosol (von Moltke et al., 2012). Prior to the addition of FlaTox, organoid cultures were treated with the membrane insoluble dye propidium iodide (PI), so we could monitor pyroptosis over time using live microscopy.

We predicted that if IECs underwent pyroptosis following NAIP–NLRC4 activation, it would occur after expulsion to protect membrane barrier integrity. However, we were surprised to see that that individual IECs became PI^+ prior to expulsion, indicating that these cells undergo NAIP–NLRC4 mediated pyroptosis before they become expulsed (Figure 3.1). We confirmed these findings *in vivo* through immunofluorescence staining of the small intestines of mice following intravenous injection of FlaTox and PI (Figure 3.2).

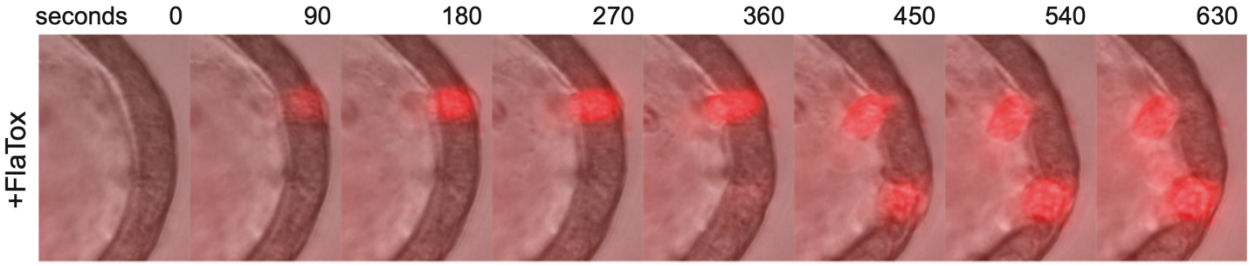

Figure 3.1. NAIP–NLRC4 activation in organoid IECs leads to pyroptosis and then expulsion. Live microscopy time course showing individual IECs becoming PI^+ (red) prior to expulsion following FlaTox treatment.

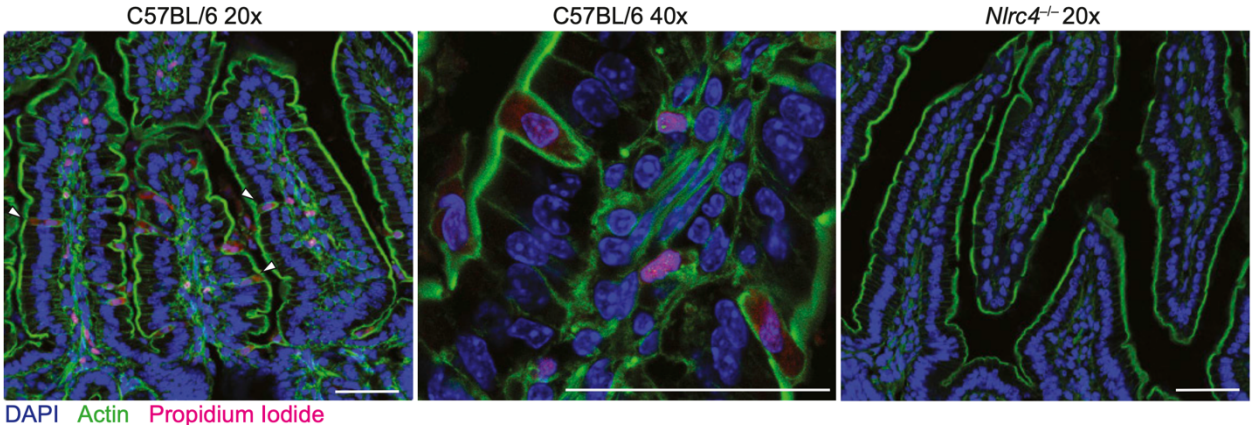

Figure 3.2. NAIP–NLRC4 activation in small intestinal IECs leads to pyroptosis prior to expulsion. Representative immunofluorescence images of the small intestines of mice following intravenous injection of PI and FlaTox. Mice were euthanized at 60 minutes post injection. Arrows indicate expulsing cells, and scale bars represent 40mm.

3.2.2 Genetic system for NAIP–NLRC4 activation in IECs

Because pyroptosis of IECs while they are still in the epithelial monolayer seems as though it may compromise the barrier integrity, we wondered whether this pyroptosis might serve a purpose for the overall immune response. One hypothesis is that permeability of infected IECs might provide an opportunity for that cell to release microbial antigens, along with inflammatory signals, that could help drive an adaptive immune response. To create a genetic system for inducible NAIP–NLRC4 activation in IECs, we crossed the OvaFla mice to Villin-Cre-ER^{T2} mice (el Marjou et al., 2004), which harbor a tamoxifen-inducible Cre recombinase driven by the *Villin* promoter (Figure 3.3A). The resulting OvaFla Villin-Cre-ER^{T2} (hereafter shortened to "OvaFla") mice respond to tamoxifen administration by expressing Cre, and subsequently the OvaFla protein, specifically in IECs. To study the influence of NAIP–NLRC4 activation, pyroptosis, and cytokine production on CD8$^+$ T cell activation, we generated *Nlrc4*$^{-/-}$, *Gsdmd*$^{-/-}$, and *Pycard*$^{-/-}$ OvaFla lines.

After a single day on the tamoxifen diet (as described in Chapter Two), WT OvaFla and *Gsdmd*$^{-/-}$ OvaFla mice lost a significant amount of weight, and by day two of the tamoxifen diet, these mice exceeded the humane weight loss endpoint on our animal protocol and were euthanized (Figure 3.3B, top). In contrast, the *Nlrc4*$^{-/-}$ OvaFla mice, as well as the OvaFla-only and Cre-only littermate control mice, maintained a consistent body weight and appeared healthy over the two-day time course. Although not statistically significant, the WT OvaFla and *Gsdmd*$^{-/-}$ OvaFla mice also exhibited decreases in core body temperature by day two relative to the *Nlrc4*$^{-/-}$ OvaFla mice (Figure 3.3B, bottom), consistent with previous analyses using recombinant flagellin protein (FlaTox) to induce acute NAIP–NLRC4 activation (Rauch et al., 2017; von Moltke et al., 2012).

Serum was collected from OvaFla mice at day two of the tamoxifen diet and assayed for IL-18, which is released from IECs following NAIP–NLRC4 activation (Rauch et al., 2017). The serum of WT OvaFla mice contained approximately 60 times more IL-18 than the serum of *Gsdmd*$^{-/-}$ OvaFla mice, demonstrating that gasdermin D is required for IL-18 release from IECs following NAIP–NLRC4 activation (Figure 3.3C). IL-18 was not detected in the *Nlrc4*$^{-/-}$ mice or in the OvaFla-only or Cre-only littermate controls. Taken together, these data show that the OvaFla system results in robust NAIP–NLRC4 activation in IECs following tamoxifen administration.

To limit confounding effects of morbidity in the NAIP–NLRC4 sufficient strains, we shortened the administration of tamoxifen chow to a single day pulse. We again monitored weight and rectal temperature each day. We found that while the WT, *Pycard*$^{-/-}$, and *Gsdmd*$^{-/-}$ OvaFla mice initially lost weight, weight loss was reversed by day three post tamoxifen chow start (Figure 3.3D, top). No significant difference in core body temperature was found between strains over the five-day experiment (Figure 3.3D, bottom).

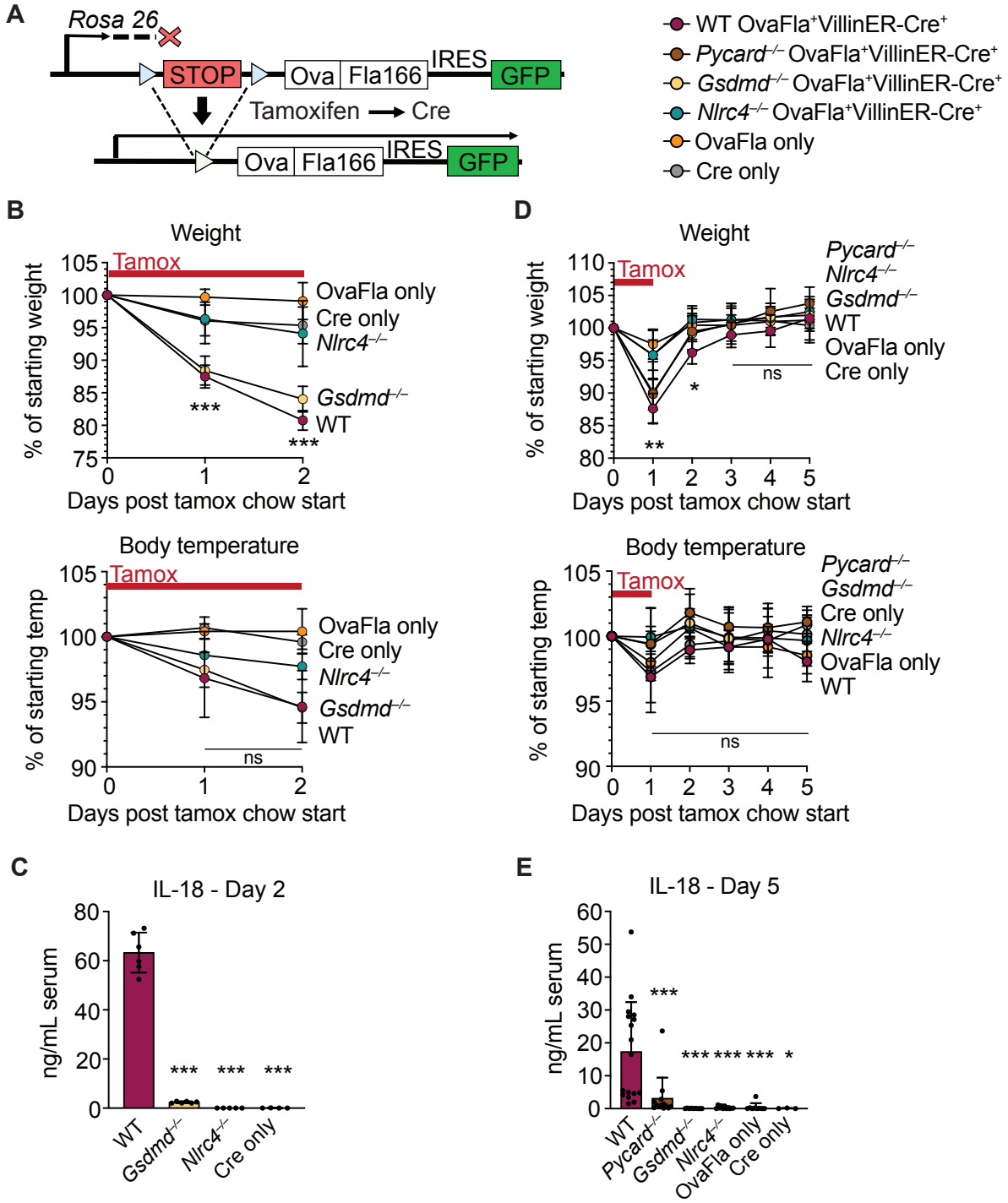
A
Rosa 26
STOP
Ova
Fla166
IRES
GFP
Tamoxifen → Cre
WT OvaFla+VillinER-Cre+
Pycard−/− OvaFla+VillinER-Cre+
Gsdmd−/− OvaFla+VillinER-Cre+
Nlrc4−/− OvaFla+VillinER-Cre+
OvaFla only
Cre only
B
Weight
% of starting weight
Tamox
OvaFla only
Cre only
Nlrc4−/−
Gsdmd−/−
WT
***
***
Days post tamox chow start
Body temperature
% of starting temp
Tamox
OvaFla only
Cre only
Nlrc4−/−
Gsdmd−/−
WT
ns
Days post tamox chow start
D
Weight
% of starting weight
Tamox
Pycard−/−
Nlrc4−/−
Gsdmd−/−
WT
OvaFla only
Cre only
**
*
ns
Days post tamox chow start
Body temperature
% of starting temp
Tamox
Pycard−/−
Gsdmd−/−
Cre only
Nlrc4−/−
OvaFla only
WT
ns
Days post tamox chow start
C
IL-18 - Day 2
ng/mL serum
***
***
***
WT
Gsdmd−/−
Nlrc4−/−
Cre only
E
IL-18 - Day 5
ng/mL serum
***
*** *** *** *
WT
Pycard−/−
Gsdmd−/−
Nlrc4−/−
OvaFla only
Cre only

Figure 3.3. Genetic OvaFla VillinCre-ERT2^{T2} system results in NAIP–NLRC4 activation in IECs of mice upon tamoxifen chow administration. **A.** Schematic of the OvaFla gene cassette on the *Rosa 26* locus. The cassette contains full-length ovalbumin, flagellin with a C-terminal truncation at amino acid 166, and an IRES-GFP. When OvaFla mice are crossed to mice containing the tamoxifen-inducible VillinCre-ERT2^{T2}, tamoxifen administration results in Cre-controlled excision of the stop cassette and expression of the OvaFla fusion protein and GFP within IECs. **B.** Daily weight (top) and rectal temperature (bottom) measurements of OvaFla mice during a two-day course of tamoxifen chow (depicted as red bar). **C.** Quantification of IL-18 ELISA performed on serum from the mice shown in panel B at day 2 post tamoxifen chow start. Each dot represents an individual mouse. **D.** Daily weight (top) and rectal temperature (bottom) measurements of OvaFla mice following a single day pulse of tamoxifen chow (depicted as red bar). **E.** Quantification of IL-18 ELISA performed on serum from the mice shown in panel D at day 5 post tamoxifen chow start. B-E, data shown as mean ± SD and are from a single representative experiment. Each dot represents an individual mouse. Significance calculated using one-way ANOVA and Tukey's multiple comparisons test (*$p < 0.05$, **$p < 0.01$, ***$p < 0.001$).

Serum was collected at day five post start of the tamoxifen chow diet and again assayed for IL-18 through ELISA. Similar to the two-day tamoxifen pulse, a single day of tamoxifen chow resulted in significant IL-18 production in the WT OvaFla mice but minimal to no detectable IL-18 in the other OvaFla strains (Figure 3.3E). The WT mice exhibited heterogeneity in the IL-18 response with the single day chow pulse, which may be related to some mice being averse to consuming the tamoxifen chow (Chiang et al., 2010) or heterogeneity in the kinetics of the response.

In a separate experiment, feces were also collected prior to tamoxifen start, and on days two, four, and five. The feces were homogenized in PBS in a bead beater, and the supernatant was used in a lipocalin 2 ELISA to assay for intestinal inflammation (Chassaing et al., 2012). The WT OvaFla mice had significantly more lipocalin 2 than the OvaFla only control at day two (Figure 3.4). However, because there is a large data spread with this assay, further investigation is required to understand whether NAIP–NLRC4 activation in IECs results in fecal shedding of lipocalin 2.

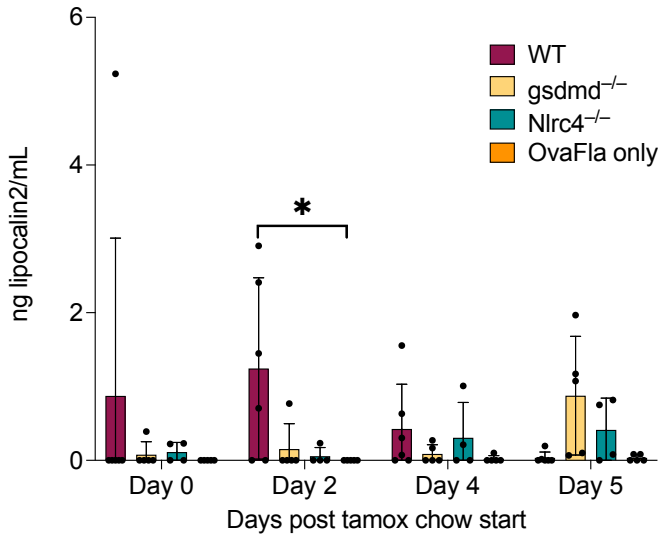

Figure 2.4. NAIP–NLRC4 activation in IECs may result in fecal shedding of lipocalin 2**.** ELISA quantification of lipocalin 2 levels in the feces collected from the indicated mice. Data shown as mean ± SD and are from a single representative experiment. Each dot represents an individual mouse. Significance calculated using two-way ANOVA and Tukey's multiple comparisons test (*$p < 0.05$).

We also performed immunofluorescence imaging of the small intestines of mice from each of the OvaFla lines after a single day pulse of tamoxifen chow. The presence of an IRES-GFP downstream of the OvaFla gene allows us to track the expression of the transgene. While approximately 30% of the IECs were GFP$^+$ in *Nlrc4*$^{-/-}$ OvaFla mice, only about 2% of the IECs were GFP$^+$ in the WT, *Pycard*$^{-/-}$, or *Gsdmd*$^{-/-}$ OvaFla mice at that time point (Figure 3.5B). Additionally, of those GFP$^+$ cells, IECs in the *Nlrc4*$^{-/-}$ OvaFla mice contained significantly more GFP signal when compared with the other OvaFla lines, whereas transgene expression was indistinguishable among WT, *Pycard*$^{-/-}$, and *Gsdmd*$^{-/-}$ mice (Figure 3.5C). Low transgene expression in genotypes other than *Nlrc4*$^{-/-}$ was anticipated because previous work (Rauch et al., 2017; Sellin et al., 2014) found that IECs are rapidly expelled from the epithelium upon NAIP–NLRC4 activation. Given that we observe robust IL-18 levels in the serum of WT mice (Figure 3.3C, E), we believe the transgene is expressed in WT (and *Pycard*$^{-/-}$ and *Gsdmd*$^{-/-}$) mice, but NLRC4$^+$ cells that express high levels of the transgene will be expelled, limiting our ability to detect them. Although pyroptosis of IECs requires Gasdermin D, NAIP–NLRC4-induced IEC expulsion was previously found to be independent of Gasdermin D, likely due to the existence of an NLRC4-Caspase-8-dependent apoptosis pathway that also leads to IEC expulsion (Man et al., 2013; Rauch et al., 2017).

Taken together, these data show that OvaFla production under control of the tamoxifen-inducible Villin-Cre-ER^{T2} system results in robust NAIP–NLRC4 activation in the IECs of mice. A single day pulse of tamoxifen chow leads to significant IL-18 production without gross morbidity or mortality in the NAIP–NLRC4 sufficient strains. Additionally, OvaFla likely accumulates in the IECs of the *Nlrc4*$^{-/-}$ OvaFla mice, as these cells do not undergo NAIP–NLRC4-driven cell expulsion.

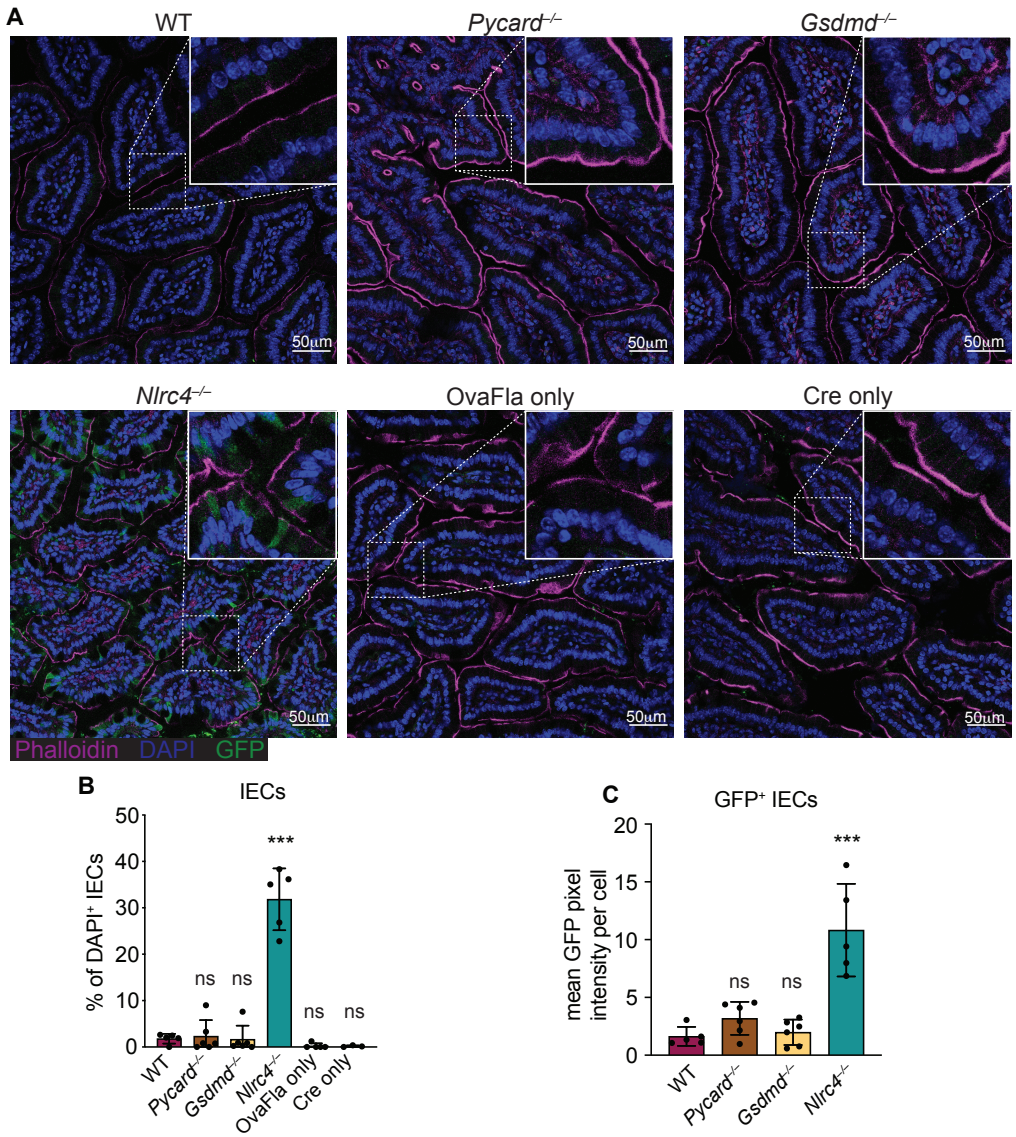

Figure 3.5. GFP⁺ cells accumulate in *Nlrc4*$^{-/-}$ mice following tamoxifen administration. **A**. Representative immunofluorescence images of the small intestines of indicated OvaFla mice on day 2 following a single day pulse of tamoxifen chow. **B.** Quantification of DAPI⁺ IECs that are also GFP⁺ for each OvaFla line. Approximately 100 cells from least 15 separate villi across 4-5 images were counted per mouse **C.** Quantification of mean GFP pixel intensity for GFP⁺ IECs in each OvaFla line. Data represent an averaged value from 12-20 cells per image across 4-5 images per mouse. B-C, data are pooled from two biological replicates, and each dot represents an individual mouse. Data shown as mean ± SD. Significance calculated using one-way ANOVA and Tukey's multiple comparisons test (*$p < 0.05$, **$p < 0.01$, ***$p < 0.001$). Only p values between WT and other experimental groups are shown.

3.2.3 CD8$^+$ T cell activation by epithelial antigens

To understand how NAIP–NLRC4 activation influences IEC-derived antigen release and presentation, we followed the response of Ova-specific TCR transgenic OT-I CD8$^+$ T cells following OvaFla induction in each of our mouse lines. Congenically marked (CD45.1$^+$ or CD45.1$^+$ CD45.2$^+$) OT-I T cells were harvested from the spleens and mesenteric lymph nodes of OT-I *Rag2*$^{-/-}$ mice, labeled with CellTrace Violet proliferation dye, and intravenously transferred into the OvaFla mice (2×10^4 cells per mouse) (Figure 3.6A). Immediately following adoptive transfer, the mice were placed on tamoxifen chow for a single day. At day five post adoptive transfer, the mice were euthanized, and their mesenteric lymph nodes, which drain immune cells from the intestines (Esterhazy et al., 2019), and spleens were analyzed for OT-I T cell proliferation and activation.

A dividing OT-I population was identified by flow cytometry in each Cre$^+$ OvaFla line (Figure 3.7A, 1B), indicating that antigens expressed in IECs can be processed and presented to activate CD8$^+$ T cells *in vivo*. Surprisingly, however, there was minimal difference in the relative percent (Figure 3.6B), absolute number (Figure 3.6C), or activation status (defined as CD62L$^-$CD44$^+$) (Figure 3.6D, Figure 3.7C, D) of OT-I T cells between the WT and *Nlrc4*$^{-/-}$ OvaFla mice in either the spleen or mesenteric lymph node. In fact, relative to the WT OvaFla mice, a higher percent of the OT-I T cells in the *Nlrc4*$^{-/-}$ OvaFla mice produced IFNγ and TNFα following *ex vivo* stimulation with PMA and ionomycin (Figure 3.7E). These data indicate OT-I T cells respond to IEC-expressed Ova in a manner that is independent of NAIP–NLRC4 activation. However, the specific lack of IEC expulsion and the resulting higher accumulation of antigen in IECs in *Nlrc4*$^{-/-}$ mice (Figure 3.4) means that the WT and *Nlrc4*$^{-/-}$ mice are not truly comparable.

In contrast to *Nlrc4*$^{-/-}$ IECs, both *Pycard*$^{-/-}$ and *Gsdmd*$^{-/-}$ IECs are expelled after inflammasome activation and thus exhibit indistinguishably low OvaFla-IRES-GFP transgene expression in IECs as compared to WT mice (Figure 3.4). Both strains are also defective for IL-18 release (Figures 3.3C, E). The major difference between the two strains is that *Pycard*$^{-/-}$ cells can still undergo *Gsdmd*-dependent pyroptosis, whereas *Gsdmd*$^{-/-}$ cells do not undergo lytic pyroptosis but are nevertheless expelled from the epithelium as intact apoptotic cells, likely via a Caspase-1 and/or -8 pathway (Man et al., 2013; Rauch et al., 2017). There was little difference in OT-I numbers (Figures 3.6B, right, 3.6C, right) or activation (Figure 3.6D, right, Figure 3.7C, D, right), as well as no difference in OT-I IFNγ and TNFα production (Figure 3.7E), in the mesenteric lymph nodes of the WT versus *Pycard*$^{-/-}$ OvaFla mice. However, there were significantly more activated OT-Is in the spleens of the *Pycard*$^{-/-}$ OvaFla mice (Figures 3.6C, right, D, right). These data suggest there may be some suppressive role for ASC in NAIP–NLRC4-dependent activation of CD8$^+$ T cells in circulation, though future characterization of these findings is needed. In contrast to the *Pycard*$^{-/-}$ OvaFla mice, the *Gsdmd*$^{-/-}$ OvaFla mice had a significantly lower number of activated cells relative to the WT OvaFla mice, but this difference was only found in the mesenteric lymph nodes (Figures 3.6C, D, Figure 3.7D). Taken together, these results suggest inflammasome activation in IECs is not essential for OT-I CD8$^+$ T cell activation, yet Gasdermin D-mediated pyroptosis of IECs may play a partial role (see Discussion).

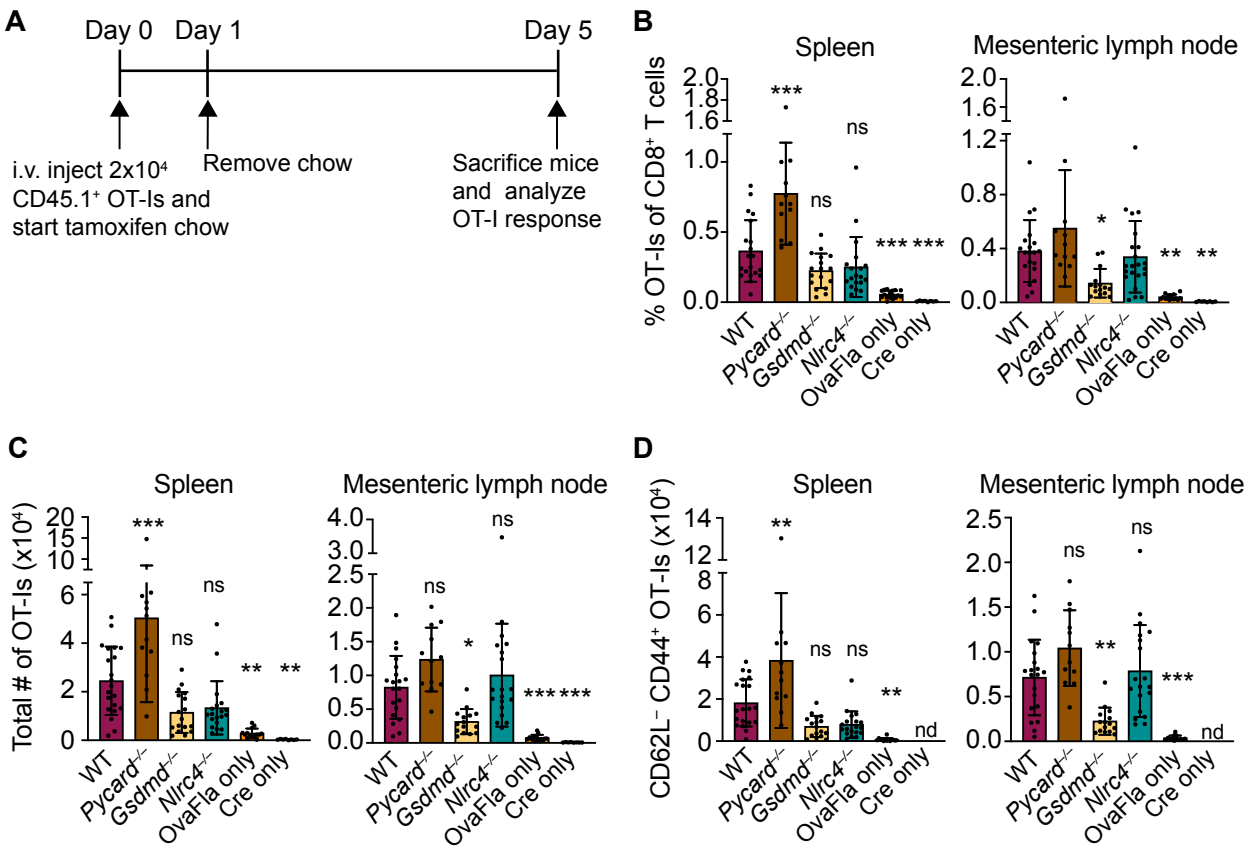

Figure 3.6. OvaFla expression in IECs results in OT-I proliferation and activation that is independent of ASC and NLRC4 but partially dependent on gasdermin D. **A.** Overview of experimental setup for analyzing OT-I responses to OvaFla production in IECs. **B.** Quantification of OT-Is as a percent of total $CD8^+$ T cells per spleen (left) and mesenteric lymph node (right) **C.** Total number of OT-Is per spleen (left) and mesenteric lymph node (right). **D.** Total number of $CD62L^-CD44^+$ OT-Is per spleen (left) and mesenteric lymph node (right). Samples with fewer than 20 OT-Is were excluded from CD62L, CD44 calculations. Tissues were harvested and analyzed at day 5 post tamoxifen chow start. Data are pooled from three biological replicates, and each dot represents an individual mouse. Data shown as mean ± SD. Significance calculated using one-way ANOVA and Tukey's multiple comparisons test (*$p < 0.05$, **$p < 0.01$, ***$p < 0.001$). Only p values between WT and other experimental groups are shown.

Another interesting finding from these experiments was that a small percent of OT-Is in the OvaFla only mice appear to be activated (Figure 3.7D, E). Since these mice are lacking Cre recombinase, we suspect there may be a very low level of Cre-independent expression of the OvaFla transgene. This chronic OvaFla expression is likely to result in exhaustion and/or deletion of any endogenous Ova-specific effector T cells (Kurachi, 2019). Indeed, we were unable to identify any SIINFEKL-specific endogenous $CD8^+$ T cells via tetramer staining or ELISpot assays. Furthermore, tamoxifen-induced estrogen receptor signaling in the Villin-Cre-ER^{T2} mice is known to occur in crypt stem cells, which leads to tamoxifen-independent Cre expression in the IEC progeny (el Marjou et al., 2004). Tamoxifen-independent Cre expression in the OvaFla mice could cause OvaFla to become a chronic stimulus, again likely leading to $CD8^+$ T cell exhaustion. To determine if our OT-I CD8+ T cells become exhausted at later time points, we followed transferred OT-I $CD8^+$ T cells in the OvaFla mice at 11- and 14-days post tamoxifen pulse and looked for expression of PD-1, an inhibitory receptor that becomes upregulated on T cells following chronic stimulation (Jubel et al., 2020). We found that *Nlrc4*$^{-/-}$OvaFla mice retained significantly more OT-Is in their mesenteric lymph nodes and spleen at day 11 relative to the other mouse lines (Figure 3.8A). Additionally, OT-Is in many of the WT, *Gsdmd*$^{-/-}$, and *Nlrc4*$^{-/-}$ OvaFla mice, as well as the OvaFla only mice, expressed high levels of PD-1 (Figure 3.8B), suggesting that these cells are being chronically stimulated. Because of these potentially complicating factors, we believe our OvaFla system is best suited to follow the immediate fate of IEC-derived antigen using the OT-I transgenic system.

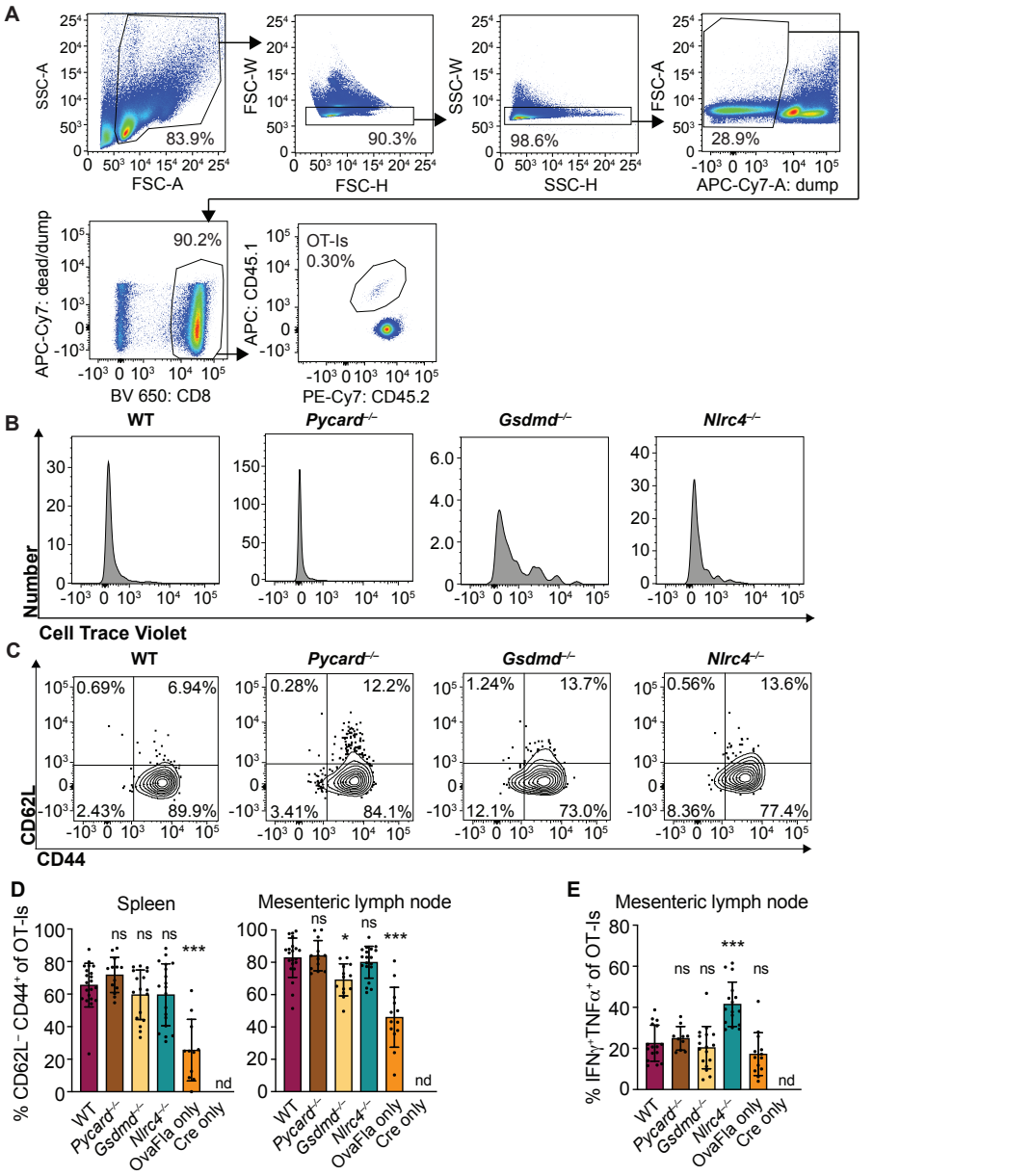

Figure 3.7. OvaFla expression in IECs results in OT-I proliferation and activation that is independent of ASC and NLRC4 but partially dependent on gasdermin D. **A.** Gating strategy for identifying OT-I T cells. **B.** Representative histograms of CellTrace Violet dilution for each OvaFla mouse line. **C.** Representative dot plots of each OvaFla mouse line showing the gating strategy for identifying $CD62L^{-}CD44^{+}$ OT-Is. **D.** Percent of OT-Is that are $CD62L^{-}CD44^{+}$ per spleen (left) and mesenteric lymph node (right). **E.** Percent of OT-Is from the mesenteric lymph node that are $IFN\gamma^{+}TNF\alpha^{+}$ following a 5-hour *ex vivo* stimulation with PMA (1μg/mL) and ionomycin (1μg/mL). D-E, data are from three independent experiments, and each dot represents an individual mouse. Tissues were harvested and analyzed at day 5 post tamoxifen chow start. Samples with fewer than 20 OT-Is were excluded from CD62L, CD44, and cytokine calculations. Data shown as mean ± SD. Significance calculated using one-way ANOVA and Tukey's multiple comparisons test (*$p < 0.05$, **$p < 0.01$, ***$p < 0.001$).

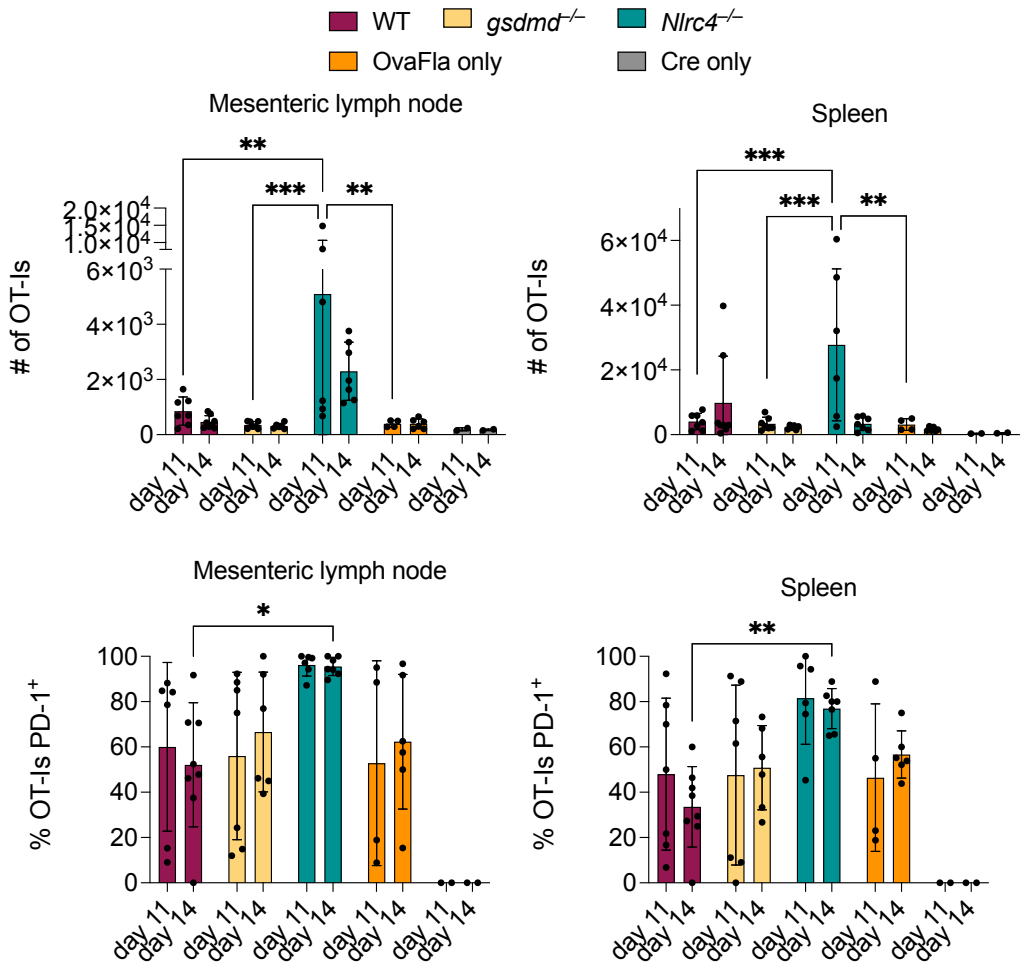

Figure 3.8. OT-Is express PD-1 at later time points post tamoxifen pulse. **A.** Total numbers of OT-Is in the mesenteric lymph nodes (left) and spleen (right) of indicated OvaFla mice at 11- and 14-days post tamoxifen pulse. **B.** Relative percent of OT-Is that express PD-1 in the indicated OvaFla mice at 11- and 14-days post tamoxifen pulse. Data are pooled from two biological replicates, and each dot represents an individual mouse. Data shown as mean ± SD. Significance calculated using two-way ANOVA and Tukey's multiple comparisons test (*$p < 0.05$, **$p < 0.01$, ***$p < 0.001$).

3.2.4 Cross-presentation of IEC antigens

IECs express MHC class I on their surface and are capable of directly presenting antigen to $CD8^+$ T cells (Christ and Blumberg, 1997; Nakazawa et al., 2004). It is therefore possible that the OT-I activation seen in the OvaFla mice is a result of direct presentation of Ova peptide by the IECs expressing OvaFla. However, it is also possible that the OT-I T cells are being cross-primed by cDC1s that engulf and "cross present" the IEC-derived Ova (Cerovic et al., 2015; Liu and Lefrancois, 2004). The fate of IEC-derived antigens and the role of antigen-presentation pathways leading to $CD8^+$ T cell activation has not previously been addressed with a completely *in vivo* system that can genetically distinguish cross from direct presentation of IEC antigens.

To determine whether the OT-Is are being activated through cross presentation or direct presentation of Ova peptide, we used the same H-$2K^{bm1}$ mouse model described in Chapter Two (Schulze et al., 1983). We crossed the various OvaFla Villin-Cre-ER^{T2} mouse lines onto the H-$2K^{bm1}$ background to create mice whose IECs would, upon tamoxifen administration, make OvaFla but be unable to present the SIINFEKL peptide to OT-I $CD8^+$ T cells. We then lethally irradiated these mice and gave them bone marrow from mice with H-$2K^b$ (B6 CD45.1) (Figure 3.9A, left). The donor-derived hematopoietic cells, including cross-presenting cDC1s, do not contain the OvaFla gene cassette but are able to cross-present the SIINFEKL peptide if they acquire it from IECs (Figure 3.9A, right). Therefore, in the $bm1^+$ OvaFla chimeras, OT-I proliferation and activation will only be observed if the SIINFEKL peptide is cross-presented.

Eight to ten weeks after lethal irradiation and reconstitution, $bm1^+$ OvaFla mice received 2×10^4 $CD45.1^+$ $CD45.2^+$ CellTrace Violet labeled OT-I T cells intravenously and were given a one-day pulse of tamoxifen chow (Figure 3.9A, left). The mice were euthanized at day five post OT-I transfer, and their spleens and mesenteric lymph nodes were analyzed for OT-I proliferation and activation. Serum was also collected for IL-18 ELISA to confirm NAIP–NLRC4-dependent IL-18 release following OvaFla induction (Figure 3.10). As in the non-chimera experiments, an obvious, dividing and activated OT-I population was observed by flow cytometry in each of the OvaFla mouse lines (Figures 3.9B, C, Figure 3.10B, C). This population was absent in mice given H-$2K^{bm1}$ bone marrow (Figure 3.11), confirming the requirement for APCs to express K^b to activate OT-I T cells. These data provide formal genetic evidence that IEC-derived antigens can be cross-presented to activate $CD8^+$ T cells *in vivo*.

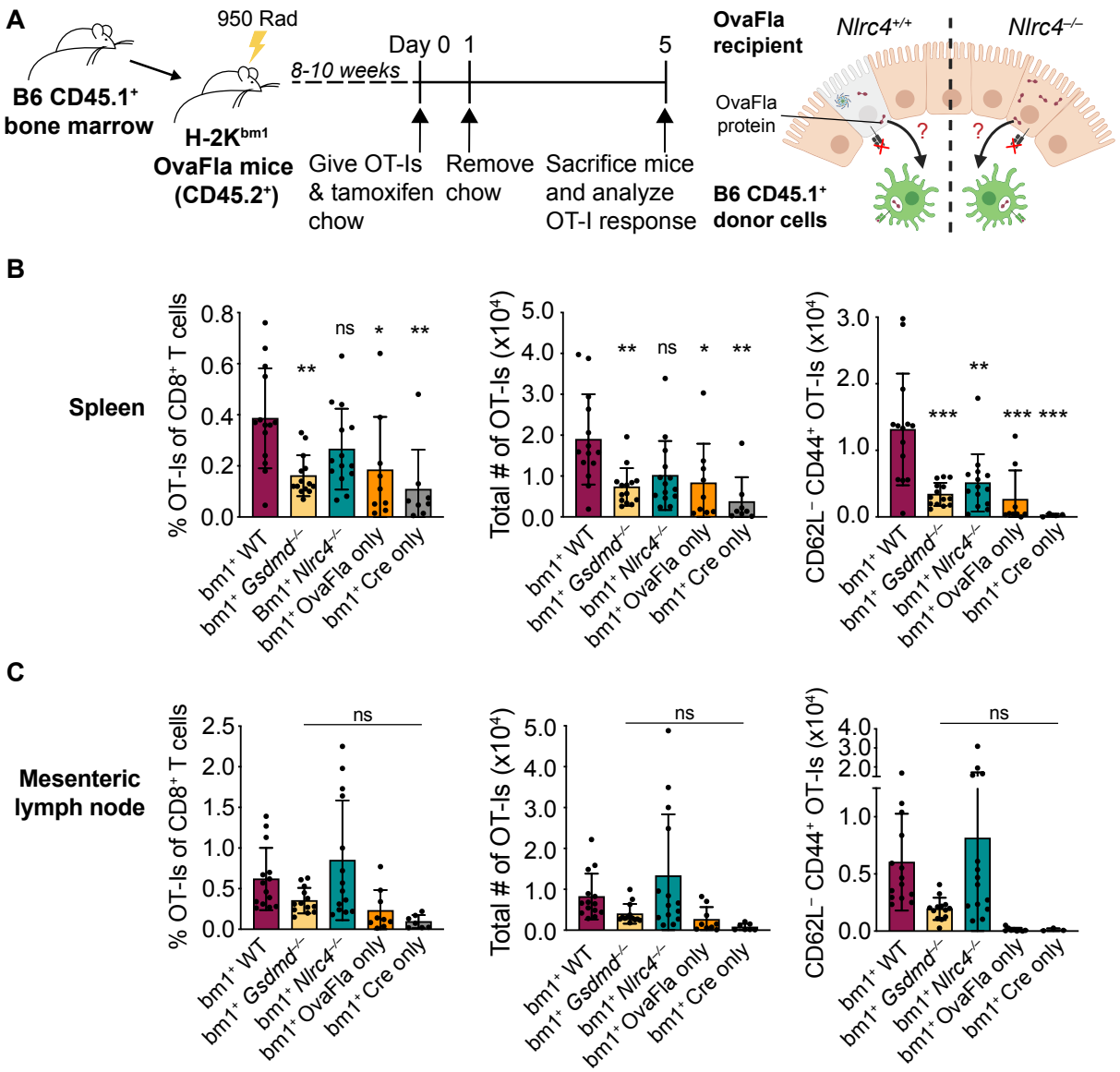

Figure 3.9. OvaFla expression in IECs results in OT-I cross-priming that is independent of NLRC4 but partially dependent on gasdermin D. **A.** Schematic depicting the production and analysis workflow of chimeric bm1^{+}OvaFla mice (left). At the right, an illustration of either WT OvaFla mice (left of the dashed line) or *Nlrc4*$^{-/-}$ OvaFla mice (right of the dashed line) following lethal irradiation and reconstitution with bone marrow from B6.SJL mice. **B.** OT-Is as a percent of total CD8^{+} T cells (left), the total number of OT-Is (middle), and the total number of CD64L^{-}CD44^{+} OT-Is (right) in the spleen. **C.** OT-Is as a percent of total CD8^{+} T cells (left), total number of OT-Is (middle), and total number of CD64L^{-}CD44^{+} OT-Is (right) in the mesenteric lymph nodes. Tissues were harvested and analyzed at day 5 post tamoxifen chow start. B-C, data pooled from three biological replicates, and each dot represents an individual mouse. Data shown as mean ± SD. Significance calculated using one-way ANOVA and Tukey's multiple comparisons test (*p < 0.05, **p < 0.01, ***p < 0.001). Only p values between WT and other experimental groups are shown.

In the spleen, the bm1$^+$ WT and bm1$^+$ *Nlrc4*$^{-/-}$ OvaFla mice harbored significantly more OT-I T cells than the bm1$^+$ *Gsdmd*$^{-/-}$ OvaFla mice, or the bm1$^+$ OvaFla-only and bm1$^+$ Cre-only littermate controls, by both percent (Figure 3.9B, left) and total number (Figure 3.9B, middle). There were also significantly more activated (CD62L$^-$CD44$^+$) OT-I T cells in the spleens of bm1$^+$ WT mice as compared to bm1$^+$ *Gsdmd*$^{-/-}$ mice (Figure 3.9B, left, Figure 3.10C). In the mesenteric lymph nodes, no significant differences were found across any of the OvaFla mouse lines (Figure 3.9C, 3.10C-D). The reason for the weak responses in the mesenteric lymph nodes is unclear, but others have previously noted negative impacts in irradiation chimeras on the expansion of adoptively transferred OT-I T cells (Kurts et al., 1997).

Taken together, these data provide genetic evidence that OT-I T cells are cross-primed from IEC-derived antigen following OvaFla induction. This cross-priming does not strictly require NAIP–NLRC4 activation but Gasdermin D-induced pyroptosis can promote CD8$^+$ T cell responses, at least for splenic OT-I T cells.

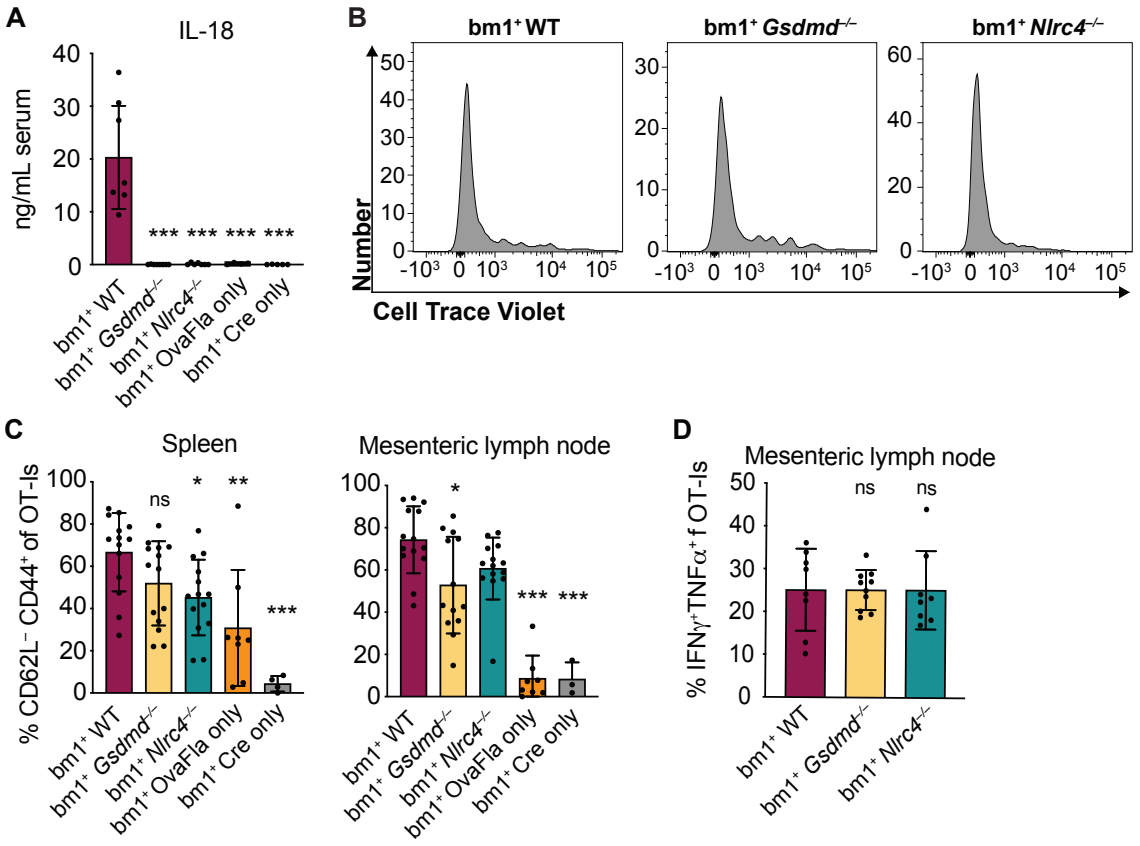

Figure 3.10. OvaFla expression in IECs of bm1^{+}OvaFla mice results in NAIP–NLRC4 expression and OT-I cross-priming that is independent of NLRC4 but partially dependent on gasdermin D **A.** IL-18 ELISA in the serum of the mice shown in Figure 2.9 at day 5 post tamoxifen chow start. **B.** Representative histograms of CellTrace Violet dilution for the indicated OvaFla mouse lines. **C.** OT-Is that are CD62L^{-}CD44^{+} in the spleen (left) and mesenteric lymph nodes (right) of the mice shown in Figure 4. **D.** OT-Is from the mice in Figure 2.9 that are IFNγ^{+}TNFα^{+} following a 5-hour *ex vivo* stimulation with PMA (1μg/mL) and ionomycin (1μg/mL). Samples with fewer than 20 OT-Is were excluded from CD62L, CD44, and cytokine calculations. A, data are pooled from two biological replicates. C, data are pooled from three biological replicates. Each dot represents an individual mouse. Data shown as mean ± SD. Significance calculated using one-way ANOVA and Tukey's multiple comparisons test (*p < 0.05, **p < 0.01, ***p < 0.001). Only p values between WT and other experimental groups are shown.

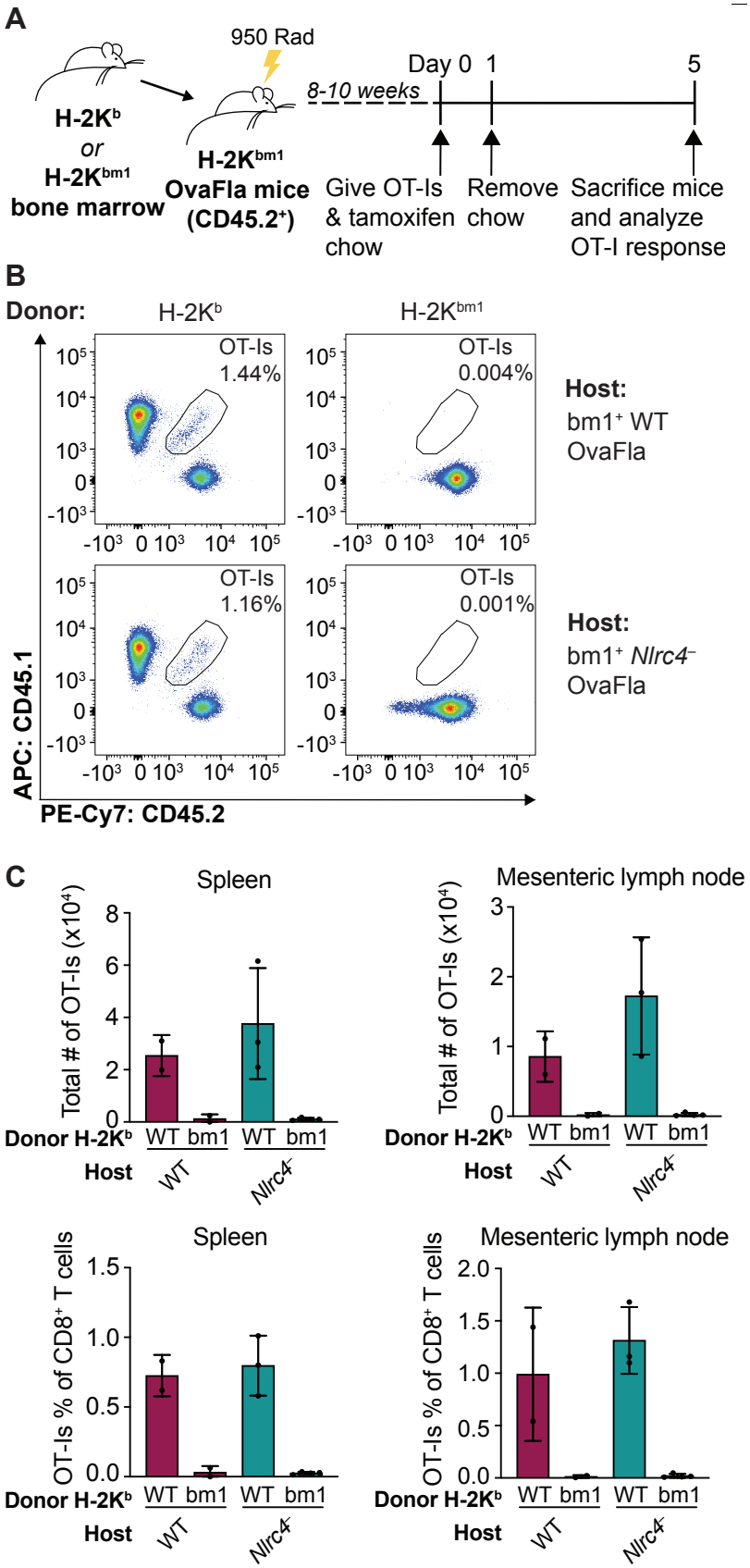

Figure 3.11. K^b donor bone marrow is required for OT-I proliferation and activation in $bm1^+$ OvaFla bone marrow chimeras. **A.** Schematic depicting the production and analysis workflow of chimeric $bm1^+$OvaFla mice that were given either B6 H-2K^b or H-2K^{bm1} bone marrow. **B.** Representative flow plots demonstrating the absence of OT-Is in the mice given H-2K^{bm1} bone marrow, as depicted in A. **C.** Quantification of the total number of OT-Is (top) and the OT-Is as a percent of total $CD8^+$ T cells (bottom) in the spleen (left) and mesenteric lymph nodes (right) of $bm1^+$ WT and $bm1^+$ *Nlrc4*$^-$ OvaFla mice as depicted in A. Data are from a single experiment, and each dot represents an individual mouse. Data shown in C as mean ± SD.

3.2.5 NAIP–NLRC4 activation drives *Batf3*$^{+}$ cDC1-independent cross presentation

Previous work shows that *ex vivo* cDC1s can cross-prime CD8^{+} T cells with IEC-derived antigen (Cerovic et al., 2015). To investigate the role of cDC1s, we first compared the relative number (Figure 3.12B left) and maturation state (MHC II^{high} CD86^{+}) (Figure 3.12B right) of cDC1s in the mesenteric lymph nodes and spleen across the WT, *Pycard*$^{-/-}$, *Gsdmd*$^{-/-}$, and *Nlrc4*$^{-/-}$ OvaFla mice after two days of tamoxifen chow. Although there was a modest reduction in the relative number of cDC1s in the spleens of *Pycard*$^{-/-}$ OvaFla mice relative to the WT OvaFla mice, there was otherwise no clear difference in the presence or maturation state of cDC1s across the various OvaFla lines. These data suggest that NAIP–NLRC4 activation in IECs does not have a broad impact on cDC1s.

However, it is possible that a relatively small number of cDC1s are receiving antigen and maturation signals in our OvaFla model, so we assessed whether cDC1s are required for cross priming OT-Is by genetically eliminating cDC1s. To do so, we used mice deficient for *Batf3*, a gene encoding a transcription factor required for development of XCR1^{+} cross-presenting cDC1s (Hildner et al., 2008; Lukowski et al., 2021). We took advantage of our H-2K^{bm1} bone marrow chimera system and compared bm1^{+} OvaFla recipients that received either B6 CD45.1 bone marrow or bone marrow from *Batf3*$^{-/-}$ mice.

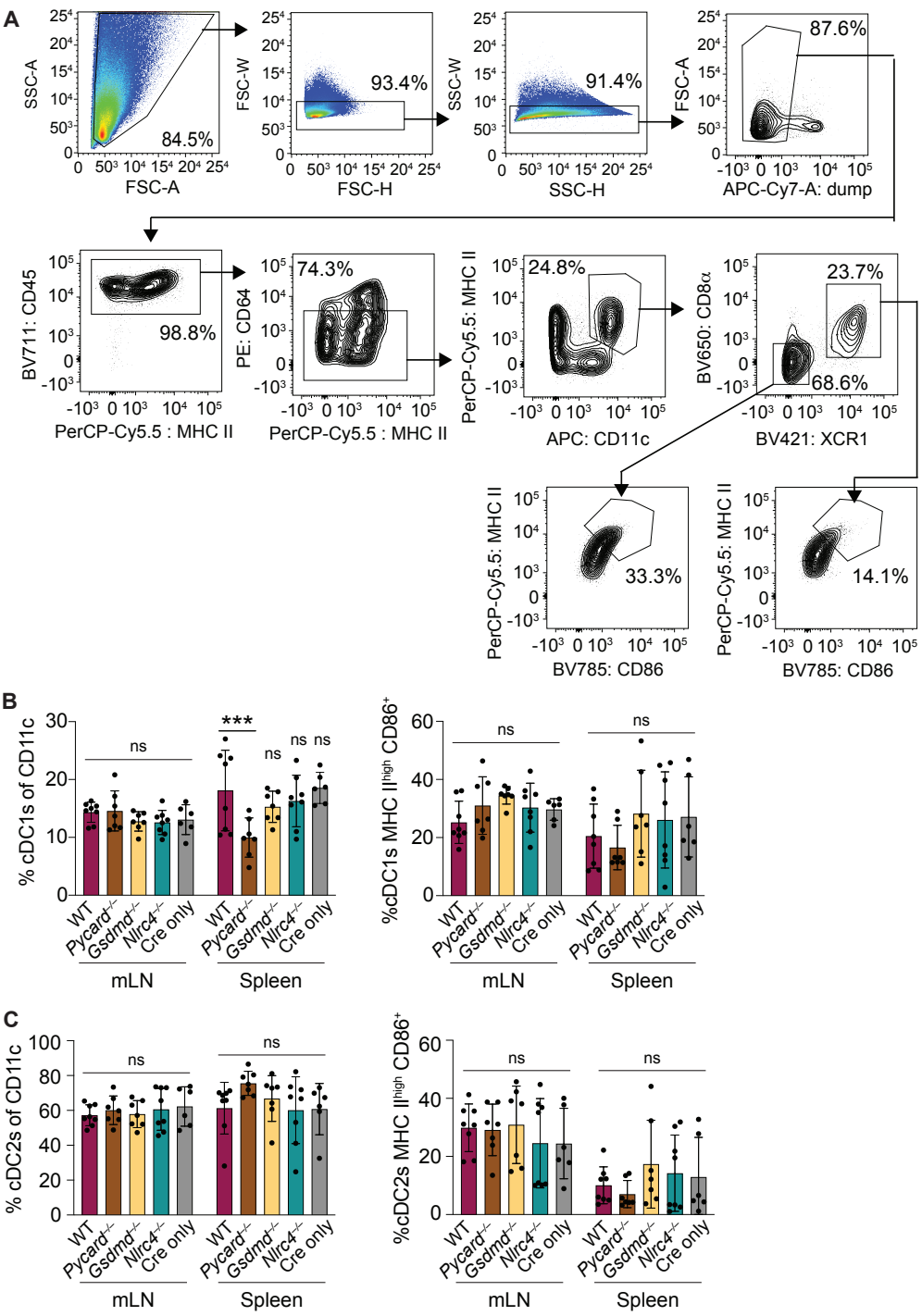

Figure 3.12. NAIP–NLRC4 activation in IECs does not lead to an increase in relative numbers of cDCs or an increase in their maturation state in the mesenteric lymph nodes or spleen. **A.** Flow cytometry gating strategy for identifying cDC1s and cDC2s. **B.** Relative numbers (left) and percent of MHC II^{high} CD86^{+} (right) cDC1s in the mesenteric lymph nodes and spleen three days post the start of tamoxifen chow. **C.** Relative numbers (left) and percent of MHC II^{high} CD86^{+} (right) cDC2s in the mesenteric lymph nodes and spleen three days post the start of tamoxifen chow.

As with the above experiments, bone marrow chimeras were made by lethally irradiating bm1$^+$ OvaFla mice and transferring donor bone marrow from either B6 CD45.1 or *Batf3*$^{-/-}$ donors. Eight to ten weeks post irradiation, 2×10^4 CD45.1$^+$ CD45.2$^+$ CellTrace Violet labeled OT-I T cells were adoptively transferred intravenously, and the mice were given a one-day pulse of tamoxifen chow (as in Figure 3.9A, left). The mice were sacrificed five days later, and their spleens and mesenteric lymph nodes were analyzed for OT-I proliferation and activation. We confirmed an absence of cDC1 cells in the OvaFla mice that received *Batf3*$^{-/-}$ donor bone marrow (Figure 3.13A, Figure 3.14).

To our surprise, there was no difference in the relative (Figures 3.13B-C, top) or total (Figures 3.13B-C, middle) number of OT-I T cells between bm1$^+$ WT OvaFla mice that received B6 CD45.1 or *Batf3*$^{-/-}$ bone marrow in either the spleen or mesenteric lymph node. OT-I T cells in these two mouse groups also appeared to proliferate similarly (Figure 3.13D, Figure 3.15). Additionally, there was no difference in the percent (Figure 3.16) or total number (Figures 3.13B-C, bottom) of CD44$^+$ CD62L$^-$ OT-I T cells. These data suggest a *Batf3*-independent population of DCs are responsible for cross-presentation of IEC-derived antigen following NAIP–NLRC4 activation.

The above findings with WT OvaFla mice are in stark contrast to the *Nlrc4*$^{-/-}$ OvaFla mice, which exhibit a significant decrease in the relative (Figures 3.13B-C, top) and total (Figures 3.13B-C, middle) number of OT-I T cells in the spleens and mesenteric lymph nodes of mice that received *Batf3*$^{-/-}$ donor cells compared to the mice that received B6 CD45.1 donor cells. Correspondingly, there was a significant decrease in the total number of CD44$^+$ CD62L$^-$ OT-I T cells (Figures 3.13B-C, bottom). The difference in OT-I numbers between these two groups of mice may be related to a relative decrease in proliferation of the OT-I T cells in the mice receiving *Batf3*$^{-/-}$ bone marrow, as evidenced by less dilution of the CellTrace Violet dye (Figure 3.13D, Figure 3.14). These data indicate that in the absence of NAIP–NLRC4 inflammasome activation, efficient cross-presentation of IEC-derived antigen *in vivo* requires XCR1$^+$ cDC1s, but that this requirement is circumvented when the inflammasome is activated.

NAIP–NLRC4 activation might promote alternative (cDC1-independent) cross-presentation pathways by the pyroptotic release of antigen and/or inflammatory cytokines. To test whether Gasdermin D is required for cDC1-independent cross-priming, we examined bm1$^+$*Gsdmd*$^{-/-}$ chimeras reconstituted with *Batf3*$^+$ or *Batf3*$^{-/-}$ bone marrow. The bm1$^+$ *Gsdmd*$^{-/-}$ OvaFla mice exhibit a phenotype that falls between the bm1$^+$ WT and bm1$^+$ *Nlrc4*$^{-/-}$ OvaFla mice, with the only significant differences between WT and *Batf3*$^{-/-}$ bone marrow recipients in the division of OT-I T cells (Figure 3.13D, Figure 3.11) and relative percent of OT-I T cells in the spleen (Figure 3.13B, top). These data suggest that the role for NAIP–NLRC4 activation in promoting *Batf3*-independent cross presentation is minimally driven by IEC pyroptosis.

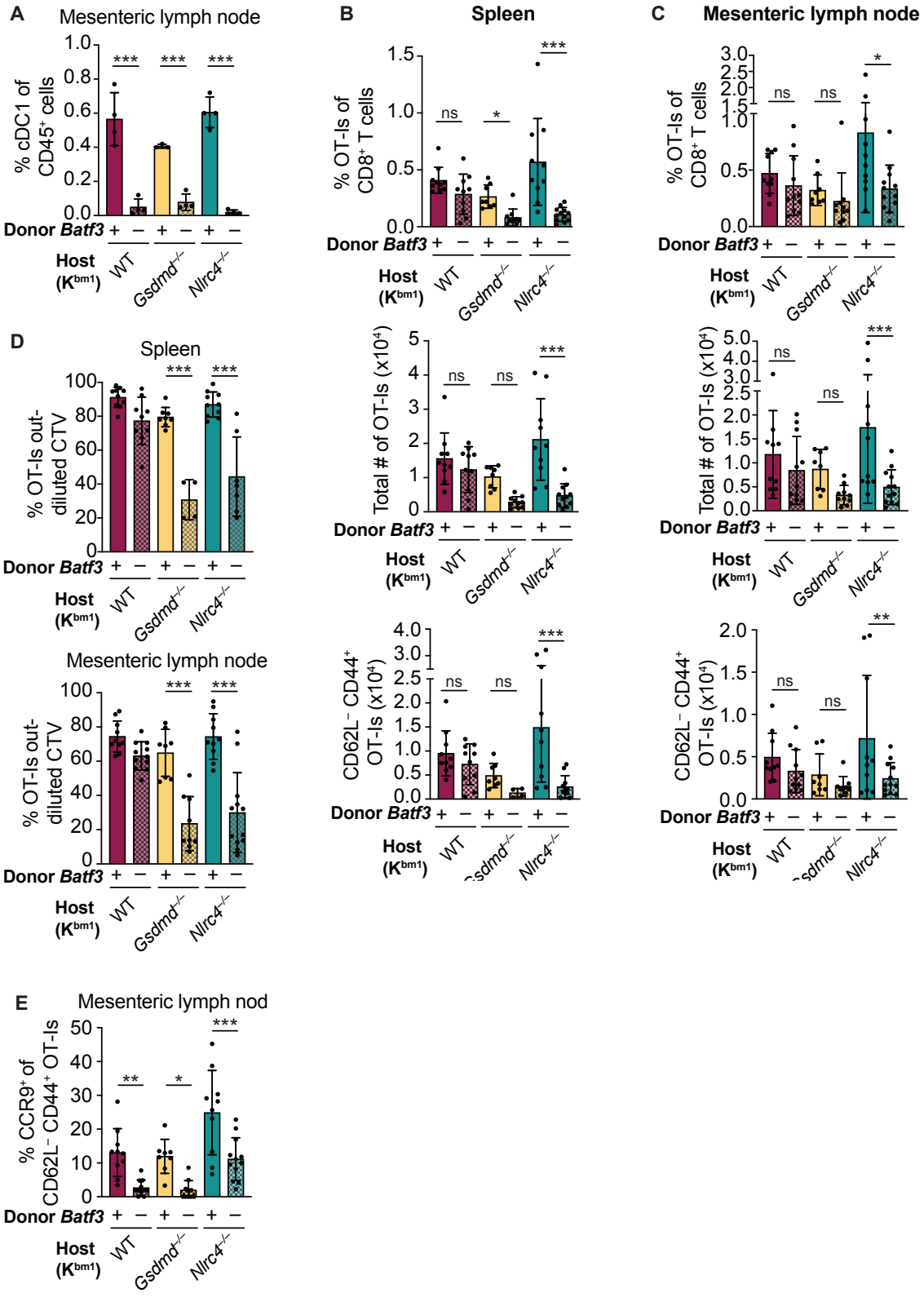
A
Mesenteric lymph node
% cDC1 of CD45+ cells
B
Spleen
% OT-Is of CD8+ T cells
C
Mesenteric lymph node
% OT-Is of CD8+ T cells
D
Spleen
% OT-Is out-diluted CTV
Mesenteric lymph node
% OT-Is out-diluted CTV
Total # of OT-Is (x10^4)
CD62L- CD44+ OT-Is (x10^4)
E
Mesenteric lymph nod
% CCR9+ of CD62L- CD44+ OT-Is
Donor Batf3 + - + - + -
Host (Kbm1) WT Gsdmd-/- Nlrc4-/-
ns
*
**
***

Figure 3.13. Cross-priming of OT-Is is independent of *Batf3*$^{+}$ cDC1s following NAIP–NLRC4 activation in IECs. **A.** Percent of CD45^{+} cells that are cDC1s in bm1 chimera mice that received either *Batf3*$^{+}$ or *Batf3*$^{–}$ donor bone marrow. **B.** Quantification of OT-Is as a percent of total CD8^{+} T cells (top), the total number of OT-Is (middle), and the total number of CD64L$^{–}$CD44^{+} OT-Is (bottom) in the spleen. **C.** Quantification of OT-Is as a percent of total CD8^{+} T cells (top), the total number of OT-Is (middle), and the total number of CD64L$^{–}$CD44^{+} OT-Is (bottom) in the mesenteric lymph nodes. **D.** Quantification of OT-Is that have out-diluted the CellTrace Violet dye in the spleen (top) and mesenteric lymph nodes (bottom). **E.** Percent of CD64L$^{–}$CD44^{+} OT-Is in the mesenteric lymph node that are CCR9^{+}. Tissues were harvested and analyzed at day 5 post tamoxifen chow start. Samples with fewer than 20 OT-Is were excluded from CD62L, CD44, and CCR9 calculations. A, data are from a single experiment. B-D, data are pooled from three biological replicates. E, data are pooled from two biological replicates. Each dot represents an individual mouse. Data shown as mean ± SD. Significance calculated using one-way ANOVA and Šídák's multiple comparisons test (*$p < 0.05$, **$p < 0.01$, ***$p < 0.001$).

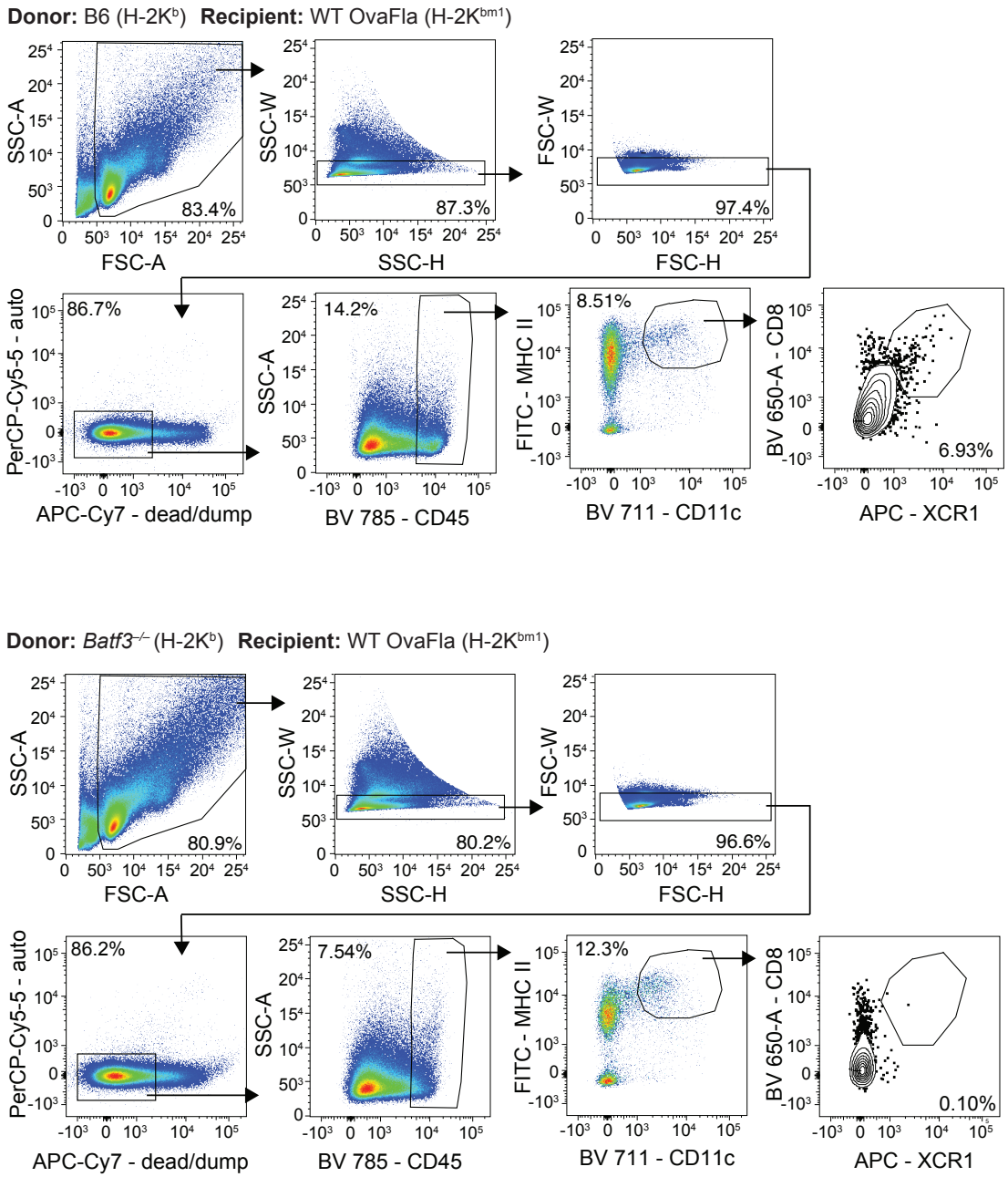

Figure 3.14. Gating demonstration for Figure 5A. Representative dot plots from one bm1^{+} WT OvaFla mouse that received B6 bone marrow (top) and one bm1^{+} WT OvaFla mouse that received *batf3*$^{-/-}$ bone marrow (bottom).

Regardless of the bone marrow donor, OT-I T cells in the bm1^{+} WT, bm1^{+} *Gsdmd*$^{-/-}$, and bm1^{+} *Nlrc4*$^{-/-}$ OvaFla mice all showed similar levels of IFNγ and TNFα production following *ex vivo* stimulation with PMA and ionomycin (Figure 3.14B). However, when we looked at CCR9 expression as a readout of whether the OT-I T cells were homing to the intestine (Svensson et al., 2002), we found a significant decrease in the number of cells expressing CCR9 in the *Batf3*$^{-/-}$ recipients relative to the B6 CD45.1 recipients across all three mouse lines (Figure 3.13E). These data align with previous findings that show that cDC1s play a key role in driving CCR9 expression on CD8^{+} T cells (Joeris et al., 2021). In summary, our data indicate the existence of two potential pathways by which IEC-derived antigens are cross-presented to CD8^{+} T cells: a constitutive pathway that operates in the absence of inflammasome activation that requires *Batf3*$^{+}$ cDC1s, and a pathway that operates in the presence of inflammasome activation that does not require *Batf3*$^{+}$ cDC1s. Interestingly, the *Batf3*$^{+}$ cDC1s appear necessary for instructing antigen specific CD8^{+} T cells back to the intestine.

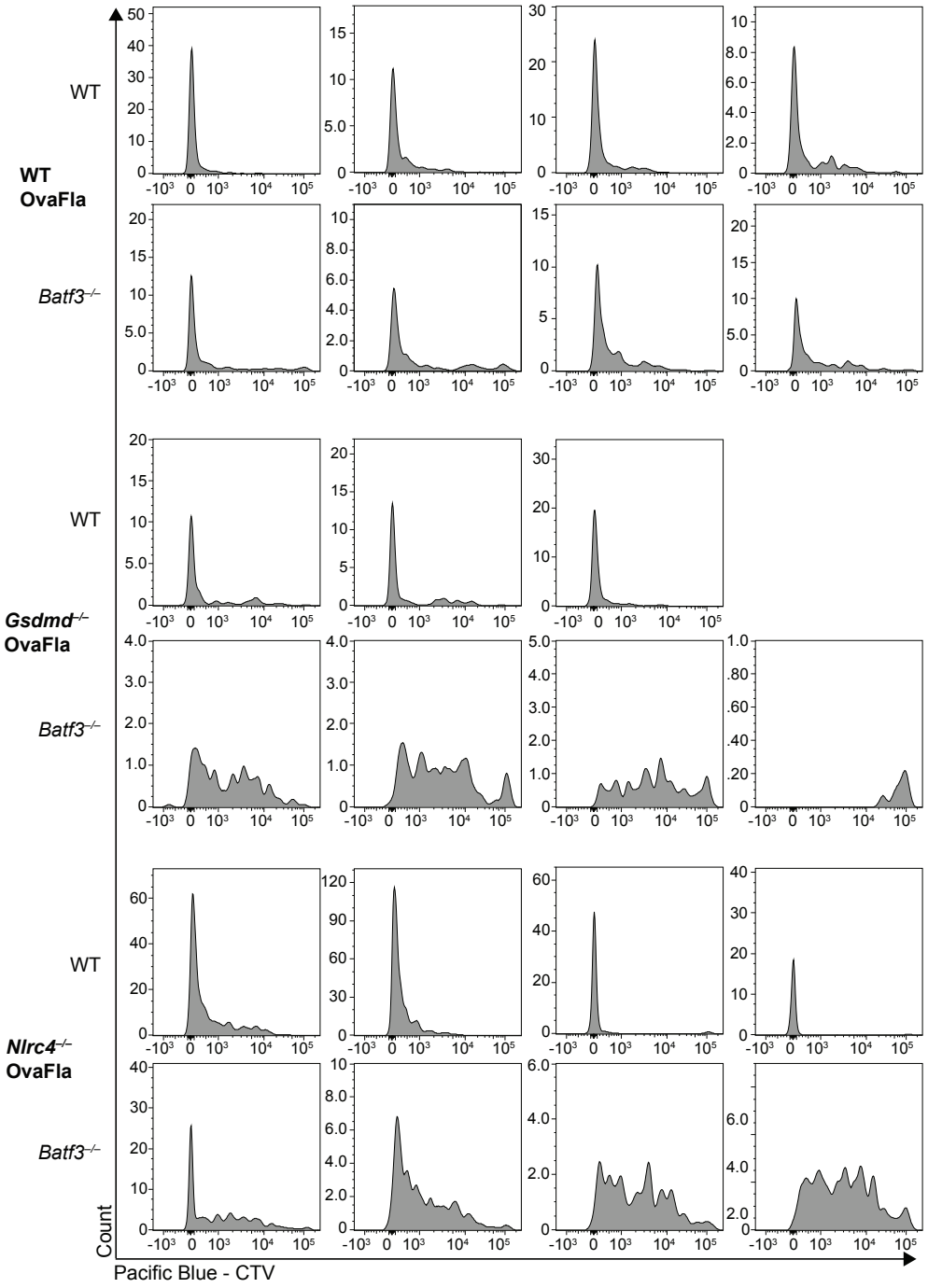

Figure 3.15. Representative histograms demonstrating the dilution of CellTrace Violet dye of OT-Is from individual mice shown in figure 3.13D. OT-Is are gated per Figure 3.12.

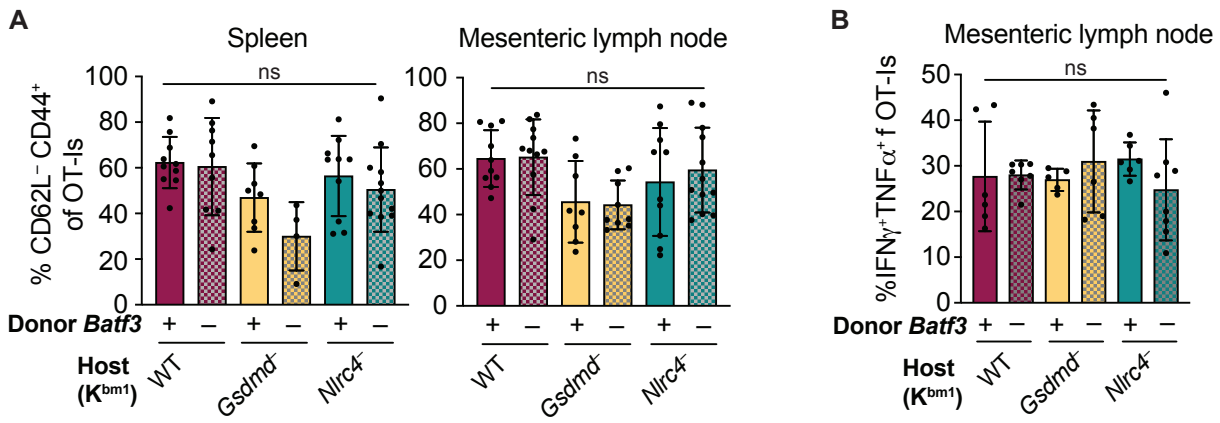

Figure 3.16. No difference in the percent of CD62L⁻CD444⁺ OT-I T cells or in the TNFα and IFNγ production between genotypes of bm1⁺ OvaFla mice. **A.** Percent of OT-Is that are CD62L⁻ CD44⁺ in the spleen (left) and mesenteric lymph nodes (right). **B.** Percent of OT-Is from the mesenteric lymph node that are IFNγ⁺TNFα⁺ following a 5-hour *ex vivo* stimulation with PMA (1μg/mL) and ionomycin (1μg/mL). Tissues were harvested and analyzed at day 5 post tamoxifen chow start. Samples with fewer than 20 OT-Is were excluded from CD62L, CD44, and cytokine calculations. A, data are pooled from three biological replicates. B, data are pooled from two biological replicates. Each dot represents an individual mouse. Data shown as mean ± SD. Significance calculated using one-way ANOVA and Šídák's multiple comparisons test (*$p < 0.05$, **$p < 0.01$, ***$p < 0.001$).

3.2.6 cDCs are required for cross-presentation of IEC derived antigen

Although XCR1-expressing cDC1s are the dominant cross-presenting cell type (Bachem et al., 2012; Dorner et al., 2009), other APCs are reportedly capable of cross-priming CD8⁺ T cells as well. These APCs include monocyte derived DCs (moDCs) (Briseno et al., 2016) and red pulp macrophages (Enders et al., 2020). Additionally, cDC2s have been show to acquire characteristics of cDC1s under inflammatory conditions (Bosteels et al., 2020) or in the absence of *Batf3* (Lukowski et al., 2021), though it remains uncertain if these cells are able to cross prime CD8⁺ T cells or provide T cells with the appropriate homing signals.

To determine whether our *Batf3*-independent cross-presenting population was another cDC population (presumably cDC2s) or a macrophage or moDC population, we conducted a modified version of the above chimera experiments in which we compared OvaFla mice that received bone marrow from either B6 CD45.1 mice or *Zbtb46*-DTR (diphtheria toxin receptor) mice (Meredith et al., 2012). *Zbtb46* is a transcription factor that drives development of cDCs but not moDCs, macrophages or any other myeloid cell populations (Meredith et al., 2012; Satpathy et al., 2012). Insertion of the DTR gene into the 3' untranslated region of *Zbtb46* allows for targeted ablation of these cells in bone marrow chimeras following diphtheria toxin (DT) treatment (Meredith et al., 2012). Eight weeks post bone marrow reconstitution, all mice were given DT one day prior to OT-I transfer and tamoxifen chow pulse and again three days later. As before, spleens

and mesenteric lymph nodes were collected at day five post tamoxifen treatment and analyzed for evidence of cross-primed OT-I CD8$^+$ T cells.

When we compared the *Zbtb46*$^+$ (B6) bone marrow recipients with the *Zbtb46*-DTR bone marrow recipients, we found a significant reduction of cDC1s and cDC2s in the mesenteric lymph nodes (Figure 3.17, 3.18). Furthermore, both the relative (Figure 3.19 B-C, top) and total (Figure 3.19 B-C, bottom) numbers of OT-Is were significantly reduced in the mice that received *Zbtb46*-DTR bone marrow across all WT, *Gsdmd*$^{-/-}$, and *Nlrc4*$^{-/-}$ OvaFla mice. These data clearly demonstrate that the *Batf3*-independent population of cross presenting cells seen in the WT OvaFla mice in Figure 3.13 are dependent on *Zbtb46* and thus are likely due to a non-cDC1 subset (presumably cDC2s).

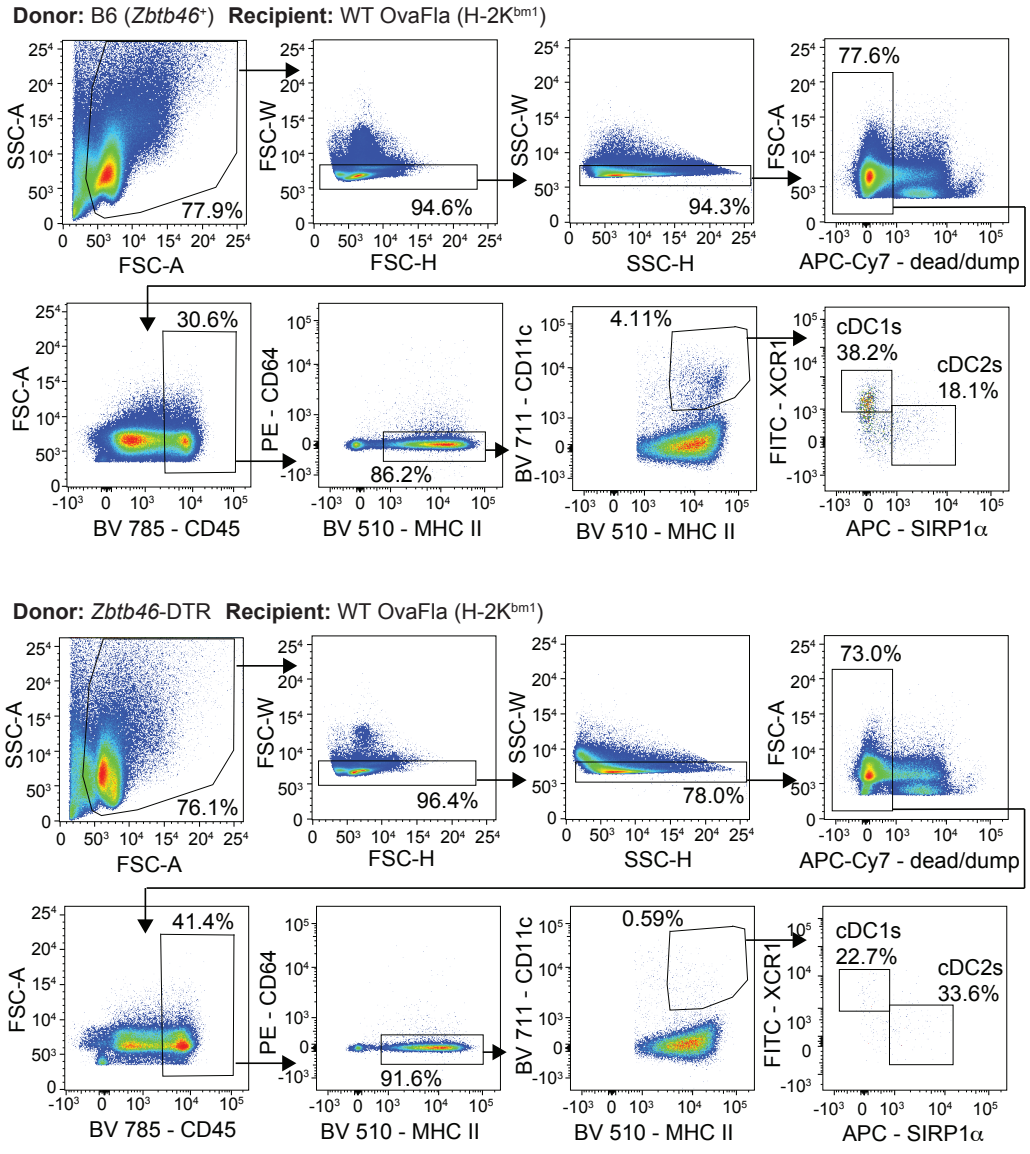

Figure 3.17. Gating strategy to identify cDC1s and cDC2s in chimeric bm1$^+$ OvaFla mice that received bone marrow from either B6 mice (top) or Zbtb46–DTR mice (bottom).

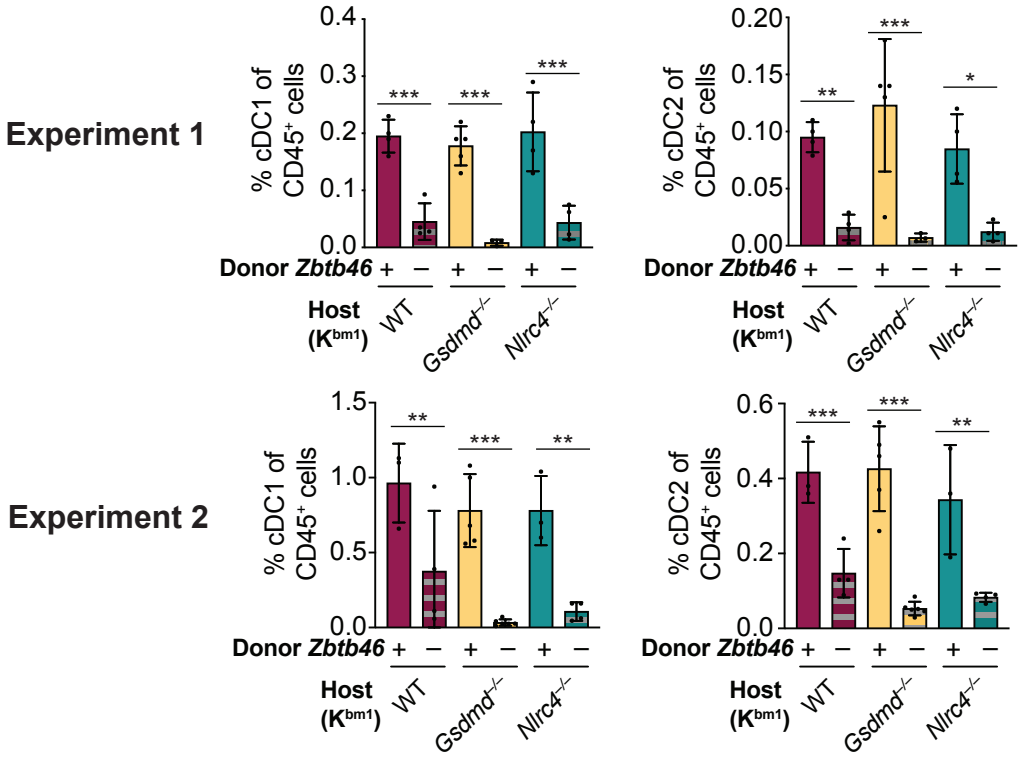

Figure 3.18. Injection of DT results in the depletion of cDC1s and cDC2s from chimeric bm1^{+} OvaFla mice given *Zbtb46*–DTR bone marrow. Percent of CD45^{+} cells in the mesenteric lymph node that are cDC1 (left) or cDC2 (right) from two separate experiments.

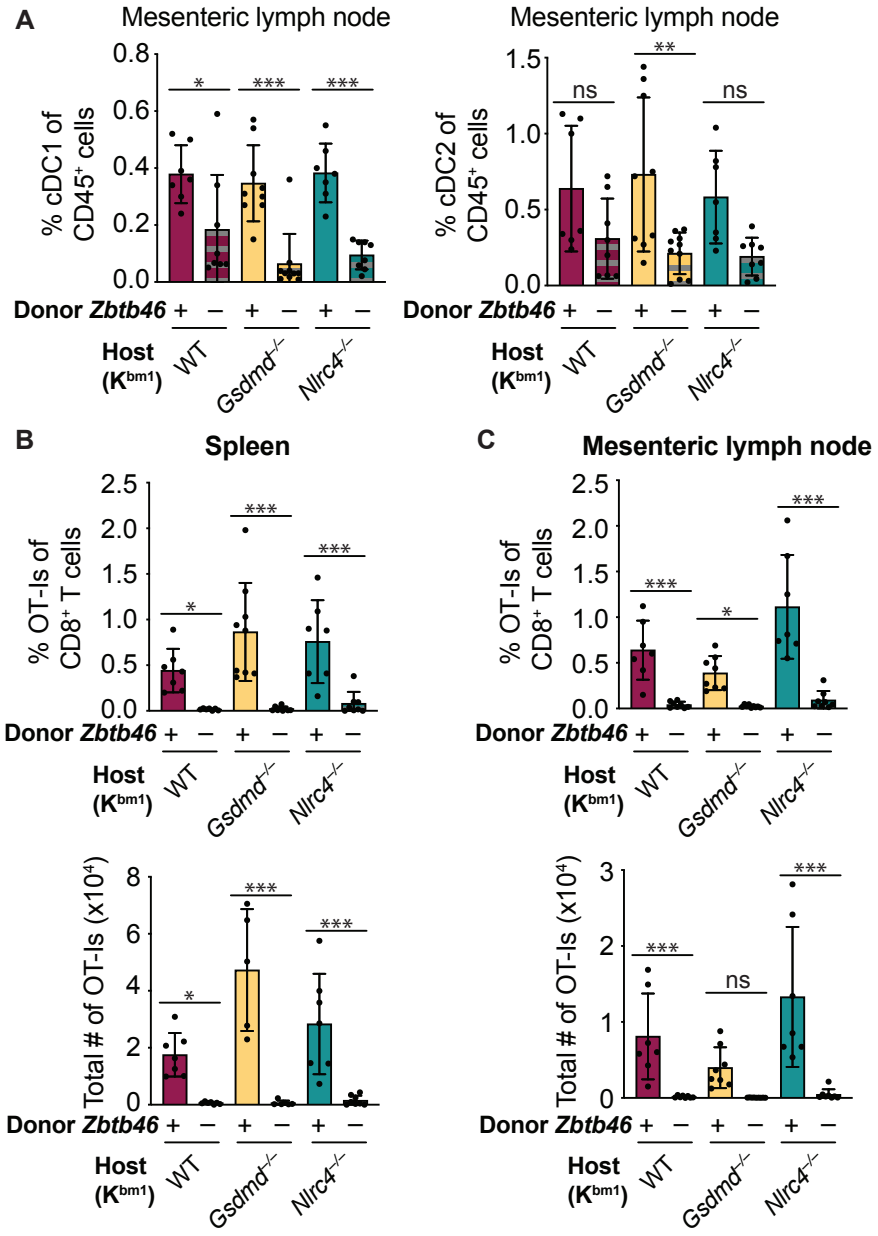

Figure 3.19. No difference in the percent of CD62L⁻CD444⁺ OT-I T cells or in the TNFα and IFNγ production between genotypes of bm1⁺ OvaFla mice. **A.** Percent of OT-Is that are CD62L⁻ CD44⁺ in the spleen (left) and mesenteric lymph nodes (right). **B.** Percent of OT-Is from the mesenteric lymph node that are IFNγ⁺TNFα⁺ following a 5-hour *ex vivo* stimulation with PMA (1μg/mL) and ionomycin (1μg/mL). Tissues were harvested and analyzed at day 5 post tamoxifen chow start. Samples with fewer than 20 OT-Is were excluded from CD62L, CD44, and cytokine calculations. A, data are pooled from three biological replicates. B, data are pooled from two biological replicates. Each dot represents an individual mouse. Data shown as mean ± SD. Significance calculated using one-way ANOVA and Šídák's multiple comparisons test (*$p < 0.05$, **$p < 0.01$, ***$p < 0.001$).

3.3 Discussion

Intestinal epithelial cells (IECs) represent an important barrier surface that protects against enteric pathogens. At the same time, IECs also represent a potential replicative niche for pathogens. As such, the immune system must survey IECs for foreign antigens and present those antigens to activate protective adaptive immune responses. In general, it remains poorly understood whether and how IEC-derived antigens are presented to activate T cell responses. In particular, the relative contributions of direct versus cross-presentation of IEC antigens to $CD8^+$ T cells has not been thoroughly investigated. Here we employed a genetic system that inducibly expresses a model antigen (ovalbumin) fused to a NAIP–NLRC4 agonist (flagellin) within the cytosol of cells (Nichols et al., 2017). We crossed these "OvaFla" mice to Villin-Cre-ER^{T2} mice, allowing for tamoxifen-inducible expression specifically in IECs. By additionally crossing to an H-$2K^{bm1}$ background (Nikolic-Zugic and Bevan, 1990; Schulze et al., 1983), and using the resulting mice as irradiated recipients for wild-type K^b hematopoietic donor cells, we engineered a system in which an IEC-derived ovalbumin antigen (SIINFEKL) cannot be directly presented to OT-I T cells but can still be acquired by hematopoietic cells and cross-presented. Using this system, we established *in vivo* that there is an antigen-presentation pathway in which IEC-derived antigens are cross-presented to activate $CD8^+$ T cells. This finding extends previous work indicating that *ex vivo* isolated DCs can cross present IEC-derived antigens to $CD8^+$ T cells (Cerovic et al., 2015; Cummings et al., 2016). We show these antigens can activate antigen specific $CD8^+$ T cells *in vivo*, and that this activation can occur even when direct presentation is genetically eliminated. We suggest that the cross-presentation pathway revealed by our analyses could be of importance during infection with pathogens that replicate in IECs, though future studies will be required to evaluate this.

Our genetic system also allowed us to assess the contribution of IEC inflammasome activation to the adaptive immune response. Inflammasomes are a critical component of the innate immune response to many pathogens, and their activation is known to influence adaptive immunity (Deets and Vance, 2021). However, in previous studies, it has been difficult to isolate the specific effects of inflammasome activation on adaptive immunity because microbial pathogens activate numerous innate immune signaling pathways over the course of an infection. By providing a genetically encoded antigen and inflammasome stimulus, we were able to overcome this issue and specifically address the role of inflammasomes in adaptive $CD8^+$ T cell responses *in vivo*. We crossed our OvaFla Villin-Cre-ER^{T2} mice to mice deficient in key inflammasome components. Consistent with previous work, we found that *Nlrc4*$^{-/-}$ mice entirely lack the inflammasome response to cytosolic flagellin, whereas *Pycard*$^{-/-}$ mice are defective for IL-18 release but not pyroptotic cell death or IEC expulsion (Rauch et al., 2017) (Figures 3.3C, E). We also crossed OvaFla Villin-Cre-ER^{T2} mice to pyroptosis-deficient *Gsdmd*$^{-/-}$ mice and found that they were defective for IL-18 release *in vivo* (Figures 3.3C, E).

Because *Nlrc4*$^{-/-}$ IECs fail to undergo pyroptosis or IEC expulsion (Rauch et al., 2017), we noted that cells expressing the OvaFla transgene accumulate to much higher levels in the *Nlrc4*$^{-/-}$ mice than in WT, *Pycard*$^{-/-}$, or *Gsdmd*$^{-/-}$ mice, in which IEC expulsion still occurs (Figure 3.5). Higher levels of Ova antigen in IECs has previously found to correlate with higher levels of OT-I expansion in the spleen and mesenteric

lymph nodes of mice (Vezys et al., 2000). Because of the differences in antigen burden, comparisons of *Nlrc4*$^{-/-}$ mice to the other genotypes must be made with caution. Nevertheless, we found that OT-I T cells in the *Nlrc4*$^{-/-}$ OvaFla mice divide and are activated at similar levels to the WT OvaFla mice following tamoxifen administration (Figure 3.6B-D). This activation occurred even when direct presentation of the OT-I peptide by IECs was eliminated on the K^{bm1} background (Figure 3.9B-C). These results are surprising for two reasons. First, it is not clear how IEC-derived antigens would be delivered to APCs in the absence of inflammasome-induced cell death. Other studies have suggested that IEC apoptosis, which may occur during homeostatic IEC turnover (Bullen et al., 2006; Hall et al., 1994; Marshman et al., 2001; Shibahara et al., 1995; Watson et al., 2005), can be a source of antigen for T cell activation (Cummings et al., 2016; Huang et al., 2000). However, apoptotic IECs are expelled apically into the intestinal lumen (Bullen et al., 2006; Hall et al., 1994; Marshman et al., 2001; Shibahara et al., 1995; Watson et al., 2005), and so the exact mechanism of basolateral antigen delivery remains unclear—though it may involve luminal sampling by intestinal phagocytes (Farache et al., 2013) and/or the transfer of plasma membrane components (trogocytosis) (Dance, 2019). Cummings *et al* suggested that IECs can be engulfed by APCs, resulting in antigen presentation on MHC class II to induce $CD4^+$ T regulatory cells, but this work did not examine antigen-specific responses or MHC class I presentation to $CD8^+$ T cells. Additionally, Joeris *et al* recently showed that cDC1s can present IEC-derived antigen to drive cross-tolerant OT-I T cells (Joeris et al., 2021). Further work is therefore needed to understand mechanisms of IEC-derived antigen presentation in the absence of inflammatory cell death. The second reason we were surprised to see $CD8^+$ T cell activation in *Nlrc4*$^{-/-}$ OvaFla mice is that these mice are presumably unable to produce inflammatory signals necessary to induce APC activation. However, previous studies have shown that OT-I T cells can be activated from constitutively expressed Ova in the absence of inflammation. In this scenario, the $CD8^+$ T cells go on to become anergic and are likely eventually deleted from the periphery (Kurts et al., 1996; Kurts et al., 1997; Liu et al., 2007; Vezys et al., 2000).

Since WT, *Pycard*$^{-/-}$, and *Gsdmd*$^{-/-}$ IECs all undergo cell death and IEC expulsion in response to NLRC4 activation, these mice exhibit similar levels of OvaFla transgene expression in IECs, allowing for comparisons between these mouse strains (Figure 3.5 C). We found that OvaFla production leads to $CD8^+$ T cell expansion and activation in all these strains. The expansion is at least partially dependent on gasdermin D, as *Gsdmd*$^{-/-}$ OvaFla mice have significantly fewer OT-I T cells than their WT counterparts (Figure 3.6B, C). Interestingly, ASC-deficient OvaFla mice—in which IECs still undergo pyroptosis following NAIP–NLRC4 activation (Rauch et al., 2016)—show similar, or even increased, OT-I numbers in their tissues relative to WT OvaFla mice (Figure 3.6B, C). These data, combined with the fact that *Gsdmd*$^{-/-}$ and *Pycard*$^{-/-}$ OvaFla mice have little to no detectable IL-18 in their serum (Figures 3.4C, E), suggest that the difference in OT-I T cell proliferation between these strains is in some way related to pyroptotic antigen release. One hypothesis is that the gasdermin D pore, which has been shown to provide a lysis-independent portal for IL-1β, IL-18, and other small proteins (DiPeso et al., 2017; Evavold et al., 2018; Heilig et al., 2018), may act as a channel for small antigens to escape IECs prior to cell expulsion.

Because *Gsdmd*-deficiency only modestly affected OT-I responses, our data additionally suggest that there may both GSDMD-dependent and GSDMD-independent pathways by which IEC antigens can be cross presented to $CD8^+$ T cells. Because *Batf3*$^{-/-}$-dependent cDC1s have a known role in cross-presenting IEC-derived antigen (Cerovic et al., 2015), we sought to determine if the cross presentation occurring in the OvaFla mice similarly relied on these cells. We compared $bm1^+$ OvaFla mice that received B6 CD45.1 bone marrow with those that received bone marrow from *Batf3*-deficient mice (Figure 3.13A). To our surprise, we found OT-I T cells were cross-primed in the $bm1^+$ WT OvaFla mice, even in the recipients that lacked cDC1s (Figure 3.13A-D). Interestingly, these data contrast with the $bm1^+$ *Nlrc4*$^{-/-}$ OvaFla mice, where the recipients given *Batf3*-deficient bone marrow had significantly fewer activated OT-I T cells than their counterparts given *Batf3*-sufficient bone marrow. OT-I T cell activation in the $bm1^+$ *Gsdmd*$^{-/-}$ OvaFla mice partially relied on *Batf3*$^+$ DCs. Furthermore, CellTrace Violet data show the OT-I T cells in the $bm1^+$ *Nlrc4*$^{-/-}$ and $bm1^+$ *Gsdmd*$^{-/-}$ OvaFla mice undergo fewer rounds of division in the absence of *Batf3* cDC1s (Figure 3.13D). These data suggest there may be two possible cross presentation pathways for IEC-derived antigen: one that occurs in the presence, and one in the absence, of inflammasome-derived inflammatory signals. We found that *Zbtb26*$^+$ bone-marrow derived cells were required for both pathways, indicating that cross presentation seen under inflammatory conditions occurs through a *Batf3*-independent but *Zbtb26*-dependent cDC population. We hypothesize that these cells are cDC2s, as recent work shows that cDC2s can take on characteristics of cDC1s under inflammatory conditions (Bosteels et al., 2020) or in the absence of *Batf3* (Lukowski et al., 2021).

Our work raises several interesting questions for future study, including the mechanism of cDC maturation. The traditional model of DC maturation involves TLR signaling on the DC (Dalod et al., 2014). IL-1R (Pang et al., 2013) or IL-18R (Li et al., 2004) on these cells might also trigger maturation, though further investigation is needed to understand how IL-1β, IL-18, or other inflammatory signals, such as eicosanoids (McDougal et al., 2021; Oyesola et al., 2021; Rauch et al., 2017), downstream of inflammasome activation might drive maturation of DCs that have acquired IEC-derived antigen.

Overall, our studies show that show that IEC-derived antigens are cross-presented both following NAIP–NLRC4 activation and under apparent homeostatic conditions in the absence of NAIP–NLRC4 induced inflammation (Figure 3.20). In the context of NAIP–NLRC4 activation, cross-priming of $CD8^+$ T cells is partially dependent on gasdermin D-mediated pyroptosis and requires a *Batf3*-independent cDC population. These data add insights to the complex interactions between innate and adaptive immune responses occurring in the intestine.

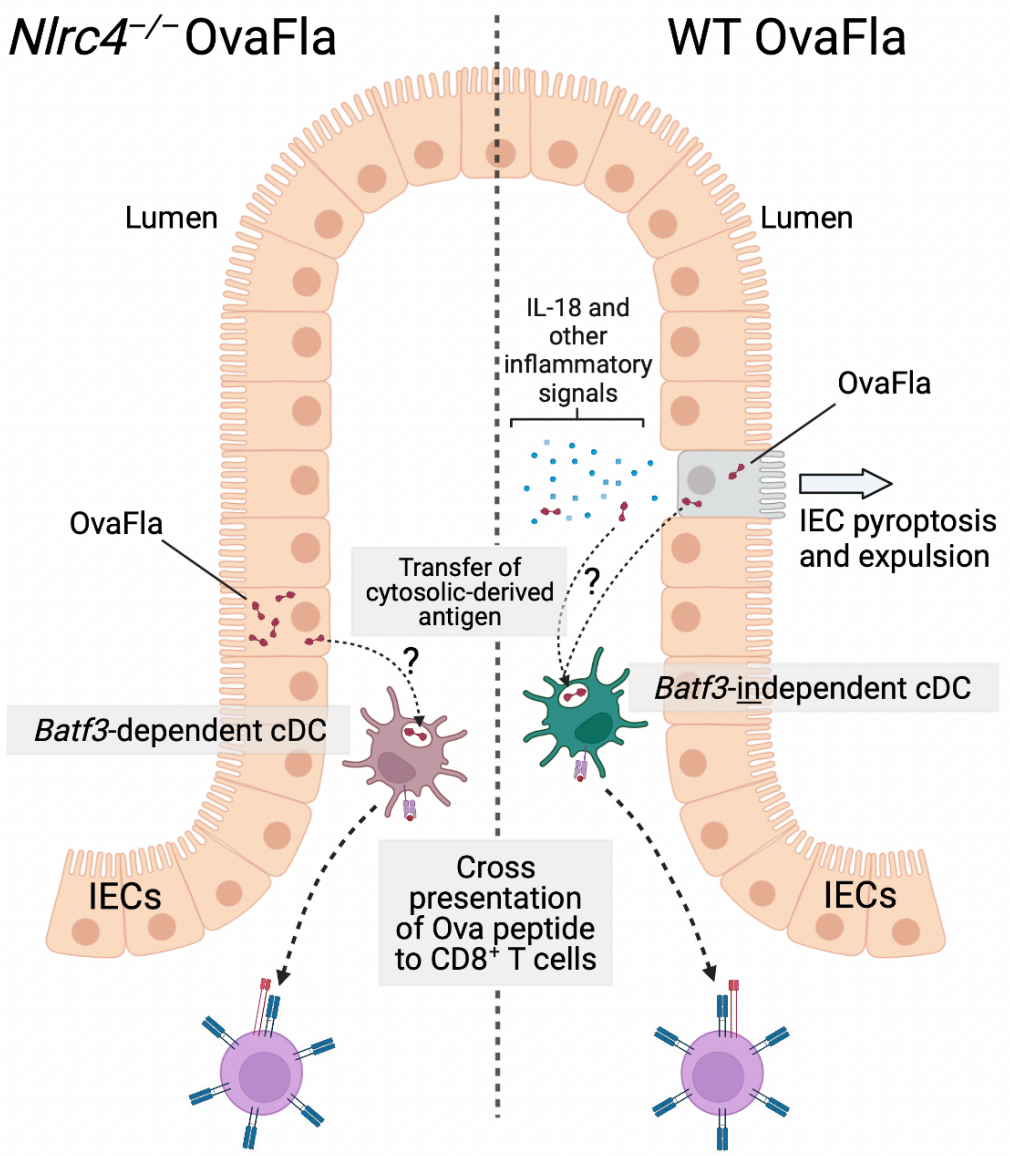

Figure 3.20. Model depicting cross presentation of IEC-derived antigens in *Nlrc4*$^{-/-}$ (left of the dashed line) and WT (right of the dashed line) OvaFla mice following tamoxifen administration. In *Nlrc4*$^{-/-}$ mice, OvaFla accumulates in IECs. *Batf3*-dependent cDCs acquire the Ova antigen through a currently unknown mechanism and cross present Ova peptide to CD8^{+} T cells—likely in the mesenteric lymph nodes. In the WT mice, OvaFla production triggers NAIP–NLRC4 activation, which leads to pyroptosis and expulsion of the IEC. *Batf3*-independent cDCs acquire the Ova antigen through a currently unknown mechanism and cross present Ova peptide to CD8^{+} T cells—likely in the mesenteric lymph nodes.

Chapter Four: Remaining questions and final thoughts

During my dissertation work, I have used a genetic mouse model to better understand how inflammasome activation influences the development of adaptive immunity. I have shown that IEC-derived antigen can be cross presented through two distinct pathways: one that occurs in steady-state and is dependent on *Batf3*$^{+}$ cDC1s and one that occurs following NAIP–NLRC4 activation and is *Zbtb46* (cDC)-dependent yet *Batf3*-independent. These findings, coupled with previously published data, have opened several new questions, which I will discuss below.

4.1 What are the NAIP–NLRC4-dependent signals that drive *Batf3*-independent cross priming of IEC antigens?

As discussed in Chapter 1 and Chapter 2, there is an incomplete understanding of which inflammatory signals are necessary or sufficient to drive the functional DC maturation required to promote activation of naïve T cells. TLR signaling has been long-know to promote DC maturation, but other immune receptors, such as IL-1R (Pang et al., 2013) and IL-18R (Li et al., 2004) have been implicated as well. The experiment presented in Figure 3.8 suggests no role for the IL-18R in the systemic OvaFla system. Additionally, experiments with *Pycard*$^{-/-}$ mice—which do not have detectable levels of IL-18 in their serum despite their IECs still undergoing pyroptosis (Figure 3.3)—show no defects in cross presentation (Figure 3.6). Of course, there are several other potential receptors that could drive cDC maturation. Signaling through Clec9A on cDCs, for example, has been shown to enhance antibody production *in vivo* (Caminschi et al., 2008). Clec9A is particularly interesting because it plays a role in cDC1 sensing of dead cells (Sancho et al., 2009)—perhaps the act of IEC pyroptosis itself could drive functional DC maturation.

One of the major benefits of the bm1^{+} OvaFla Villin-Cre-ER^{T2} system is that we can easily create chimeric mice that are lacking various receptors or components associated with cDCs and cross presentation. Even if a genetic knockout mouse is not available, there are now ways to use the CRISPR/Cas9 gene editing system to knock out specific genes in donor bone marrow donor cells (Sano et al., 2019). A series of CRISPR/Cas9-based chimeric experiments could be used to screen for TLR-independent functional DC maturation signals in the OvaFla mice.

4.2 How are antigens from steady-state IECs acquired by *Batf3*-dependent cDC1s? How are antigens from pyroptotic IECs acquired by *Batf3*-independent cDCs?

It was exciting to find that two separate cDC populations cross present IEC-derived antigen in the presence or absence of NAIP–NLRC4 activation. However, we have yet to uncover exactly how these either of these cell groups are able to acquire the antigen from the IECs.

Cummings *et al.* showed that CD103-expressing cDCs, which can be classified as either migratory DCs from the mLN or lamina propria resident DCs (Sun et al., 2020), acquire antigen by sampling apoptotic IECs (Cummings et al., 2016). Likewise, an older paper from Huang *et al.* showed that rat intestinal DCs acquire and transport apoptotic IEC antigen to the mLN (Huang et al., 2000). Apoptosis is thought to occur regularly at

the tips of the intestinal villi (Negroni et al., 2015), so it is possible that OvaFla-filled IECs in the *Nlrc4*$^{-/-}$ OvaFla mice provide antigen through a mechanism similar to that presented by these papers. Because IECs have a high rate of cellular turnover, and apoptosis is required to maintain intestinal homeostasis, it is difficult to directly test the hypothesis that apoptosis is driving cross-presentation in the *Nlrc4*$^{-/-}$ OvaFla mice. However, further investigation into the cross-presenting cells involved in this inflammasome-independent pathway (as discussed in 4.1 above) might provide insight into the cellular requirements for obtaining and presenting antigens under steady state conditions.

There are relatively few papers that examine cross presentation of IEC-derived antigen under inflammatory conditions. Cerovic *et al*. found that CD103^{+} cDC1s cross present IEC antigen under both homeostatic and TLR7 agonist-treated conditions (Cerovic et al., 2015). The authors hypothesize that the R848 is acting to functionally mature the CD103^{+} cDC1s, but they do not propose a mechanism by which the cDC1s gain access to the cell-associated Ova antigen. It is possible that homeostatic IEC apoptosis is making cytosolic antigen accessible for cross-presentation as well.

The IECs of WT OvaFla Villin-Cre-ER^{T2} mice express very low levels of GFP when compared to the *Nlrc4*$^{-/-}$ OvaFla Villin-Cre-ER^{T2} mice (Figure 3.5), which leads us to believe that WT IECs undergo rapid pyroptosis and expulsion following OvaFla production. Because of this rapid expulsion, it seems unlikely that the cross-presenting cDCs in these mice are acquiring the Ova antigen from apoptotic cells. We originally hypothesized that pyroptosis of IECs might serve to release cytosolic antigen to the underlying tissue; however, experiments using bm1^{+} *Gsdmd*$^{-/-}$mice in Chapter 3 reveal that Gasdermin D-mediated pyroptosis is only partially responsible for OT-I T cell cross priming (Figure 3.9). Work from Rauch *et al.* shows that Gasdermin D-deficient IECs maintain cell membrane integrity during the NAIP–NLRC4-driven expulsion process (Rauch et al., 2017), so it is unlikely, though not impossible, that antigen is leaking from these cells in a Gasdermin D-independent manner.

One possible mechanism of antigen acquisition in the WT OvaFla mice is that intestinal cDCs are able to “reach” across the epithelium to acquire antigen from the rapidly expulsed IECs. Several studies have reported the presence of transepithelial dendrites (e.g., (Vallon-Eberhard et al., 2006) (Chieppa et al., 2006) (Rescigno et al., 2001)), which are mediated by the CX_3CR1 chemokine receptor (Niess et al., 2005). This hypothesis could be tested by generating bm1^{+} OvaFla chimeras with CX_3CR1-deficient donor cells.

4.3 Are the cross-primed OT-I T cells activated in the presence and absence of NAIP–NLRC4 activation functionally similar? Are they able to protect from future challenge with SIINFEKL-expressing pathogens?

The true effector functionality of the activated OT-I T cells in the OvaFla mice remains an important question in our work. As discussed briefly in Chapter 2, we believe that the potential “leakiness” of the OvaFla transgene, coupled with the fact that the Villin-Cre-ER^{T2} promoter can result in Cre recombination in the intestinal crypt stem cells, makes it difficult to assess either endogenous or long-term adaptive immune responses to Ova peptide. We attempted to study the endogenous SIINFEKL-specific CD8^{+} T cell response in the OvaFla mice through use of both tetramer staining and ELISpot assays,

but neither yielded any positive cells. We also attempted to re-challenge tamoxifen-pulsed OvaFla mice that had been given OT-Is with SIINFEKL-expressing *Listeria*, but we were again unable to find any responsive T cells.

Nevertheless, we hypothesize that the active OT-I T cells found in the *Nlrc4*$^{-/-}$ OvaFla mice might become anergic, since the Ova peptide should be seen as a self-antigen in the absence of other inflammatory signals (Figure 1.2, Figure 3.8). This hypothesis is partially supported by the finding from Cerovic *et al.* that OT-Is activated by IEC-derived Ova still proliferate in the absence of TLR7 agonist R848 (Cerovic et al., 2015) yet are unable to produce IFNγ. We did see IFNγ production in the OT-Is from both the WT and *Nlrc4*$^{-/-}$ mice, but other functional readouts remain unchecked. For example, the cytotoxicity of these cells could be tested in an *ex vivo* killing assay, where the OT-I T cells are mixed with labeled APCs that are presenting the cognate T cell antigen. Effector CD8$^+$ T cells will be able to kill these APCs, whereas anergic or tolerized CD8$^+$ T cells will not.

To compare the long-term protection capabilities of OT-Is in the WT versus *Nlrc4*$^{-/-}$ OvaFla mice, it be possible to transfer activated OT-Is from these mice into naïve B6 mice, which would avoid any issues of chronic OvaFla expression. These mice could then be challenged with an Ova-expressing pathogen. This experiment is technically tricky, as activated T cells have a significantly lower survival rate when compared to naïve T cells following adoptive transfer. We have tried this experiment twice without success, but further optimization might make it possible.

4.4 Final thoughts

Although the OvaFla system bears little resemblance to an actual infection model, I hope that my findings with the Villin-Cre-ER^{T2} mice will help progress the field of intestinal immunology toward a better understanding of the complex mechanisms at play between innate and adaptive immunity.

Materials and Methods

Animals

All mice were maintained under specific pathogen-free conditions and, unless otherwise indicated, fed a standard chow diet (Harlan irradiated laboratory animal diet) *ad libitum*. OvaFla mice were generated as previously described (Nichols et al., 2017) and crossed to Villin-Cre-ER^{T2}, which we obtained from Avril Ma (UCSF, San Francisco, CA) (el Marjou et al., 2004) or Cre-ER^{T2} (Jax strain 008463). OvaFla Villin-Cre-ER^{T2} mice were additionally bred to *Gsdmd*$^{-/-}$, *Pycard*$^{-/-}$ and *Nlrc4*$^{-/-}$ mice. *Nlrc4*$^{-/-}$ and *Pycard*$^{-/-}$ mice were from V. Dixit (Mariathasan et al., 2004) (Genentech, South San Francisco, CA). *Gsdmd*$^{-/-}$ mice were previously described (Rauch et al., 2017). OT-I *Rag2*$^{-/-}$ mice (from E. Robey, Berkeley, CA) were used as a source of OT-Is for all adoptive transfer experiments.

For chimera experiments, the above OvaFla lines were crossed to B6.C-*H-2K*^{bm1}/ByJ mice (Schulze et al., 1983) (Jax strain 001060). For the bone marrow donors, B6.CD45.1 (Jax strain 002014), *Batf3*$^{-/-}$ (Jax strain 013755), *Zbtb46*–DTR (Jax strain 019506), and IL-18R$^{-/-}$ (Jax strain 004130) mice were used.

Mice used for non-chimera experiments were 8-12 weeks old upon tissue harvest, and mice used as chimeras were 16-20 weeks old upon tissue harvest. Female mice were cohoused, and all experimental mice were age- and sex-matched when possible. OvaFla-only and Cre-only controls were littermates of the experimental mice. All animal experiments and endpoints were approved by and performed in accordance with the regulations of the University of California Berkeley Institutional Animal Care and Use Committee.

Adoptive transfer of OT-I T cells

The spleen and mesenteric lymph nodes were harvested from OT-I *Rag2*$^{-/-}$ mice, mashed between the frosted ends of two glass slides to create a single cell suspension, filtered through 100mm nylon mesh, and pooled into a single tube. Red blood cells were lysed with ACK Lysing Buffer (Gibco; A10492-01). Cells were labeled with CellTrace Violet (ThermoFisher; C34557) following the manufacturers protocol and transferred i.v. to mice anesthetized with isoflurane at 2×10^4 cells per mouse.

Tamoxifen administration

The tamoxifen chow used in these studies was purchased from Envigo (https://www.envigo.com/tamoxifen-custom-diets; 120856). The diet contains 250 mg of tamoxifen per kilogram of chow and was irradiated prior to shipping. Mice were fed *ab libitum* for the number of days indicated in each data figure. Envigo assumes approximately 40 mg of tamoxifen is consumed per kilogram of body weight per day for each mouse, though feed aversion leads to variable and limited initial food intake (Chiang et al., 2010).

Diphtheria Toxin treatment

To deplete cDCs in the *Zbtb46*–DTR → bm1^{+}OvaFla chimeras, all mice were given two doses of diphtheria toxin (DT) (Sigma; D-0564) as described in (Meredith et al., 2012). Each animal was given an initial dose of 20ng DT per gram bodyweight one day prior to

OT-I T cell transfer and tamoxifen chow pulse. The mice were then given a second dose of 4ng DT per gram bodyweight three days after the initial dose.

Flow cytometry

Spleens and mesenteric lymph nodes were harvested from euthanized mice and stored on ice in T cell media: RMPI 1640 (Gibco; 21870092) containing 10% FBS (Gibco, Cat#16140071, Lot#1447825), 1% penicillin-streptomycin, 1% L-glutamine, 1% sodium pyruvate, 0.5% 2-mercaptoethanol, and 25mM HEPES. For lymphocyte staining, tissues were mashed between the frosted ends of glass slides and filtered through 100mm nylon mesh. For myeloid staining, tissues were minced with scissors and forceps and incubated in T cell media containing 1 mg/mL collagenase VIII (Sigma; C2139-1G) or in HBSS (Ca^{2+}, Mg^{2+}) (Gibco; 14025076) containing DNase I (900mg/1mL) (Sigma; DN25-10MG) and Liberase TM (Roche; 5401119001), at 37 °C for 25-45 minutes. The digested tissues were then passed through 70 mm filters and washed with T cell media. For all stains, red blood cells were lysed from a single cell suspension using ACK Lysing Buffer. Cells were counted using a Beckman Vi-CELL XR Cell Viability Analyzer (Beckman Coulter, Brea, CA), and 3×10^6 cells per tissue per mouse were added to individual FACS tubes or wells of a 96-well non tissue culture treated round bottom plate.

For extracellular surface staining, cells were blocked for 20-30 minutes with a 1:1000 dilution of anti-mouse CD16 and CD32 antibodies (eBioscience; 14-0161-85) at 4 °C and then stained with a cocktail of antibodies for extracellular markers (Supplemental Table 1) at RT for 1 hour. All dilutions and washes were done with 1X PBS (Gibco; 10010049) containing 5% FBS/FCS.

For intracellular cytokine analysis, cells were incubated at 1×10^6 cells/mL T cell media plus 1μg/mL phorbol myristate acetate (PMA) (Invivogen; tlrl-pma), 1μg/mL ionomycin (Calbiochem; 407952-1MG), and 1μg/mL GolgiPlug™ (BD Biosciences; 555029) at 37°C for 5 hours. Cells were then washed and blocked for 20-30 minutes with a 1:1000 dilution of anti-mouse CD16 and CD32 antibodies at 4°C, and a surface stain was applied for 1 hour at RT (see Key Reagents table below). Cells were then fixed in 100mL eBioscience™ IC Fixation Buffer (Thermo; 00-8222-49) for 20-60 minutes RT, and then stained with an intracellular staining cocktail (Supplemental Table 1) in 1X eBioscience™ Permeabilization Buffer (Thermo; 00-8333-56) at RT for 1 hour. Cells were washed and resuspended in PBS prior to analysis. The data were collected on a BD Biosciences Fortessa (San Jose, CA) in the UC Berkeley Cancer Research Laboratory Flow Cytometry facility, and analysis was performed using FlowJo 10 Software (BD Biosciences, San Jose, CA).

Generation of bone marrow chimeras

Eight- to twelve-week-old mice were lethally irradiated with a Precision X-Rad320 X-ray irradiator (North Branford, CT) using a split dose of 500 rads and then 450 rads, approximately 15 hours apart. Bone marrow was harvested from the long bones of the indicated donor strains, red blood cells were lysed using ACK Lysing Buffer, and $CD3^+$ cells were depleted from the donor cells using a biotinylated anti-mouse CD3e mAb (BioLegend; 100304) and the Miltenyi MACS® MicroBead (Miltenyi; 130-105-637) magnetic depletion protocol with LD columns (Miltenyi; 130-042-901) to reduce graft vs

host reactions (Selvaggi et al., 1996). Recipient mice were anesthetized with isoflurane, and approximately 5×10^6 donor cells were injected retro-orbitally. Females from the different strains were co-housed, and at least eight weeks passed between reconstitution and the start of any experiment.

Immunofluorescence

Mice were fed a single day pulse of tamoxifen chow and euthanized two days from start of the chow feeding. Approximately 2.5 cm pieces were taken from the proximal and distal ends of the small intestine. These pieces were flushed and fixed in PLP buffer (0.05 M phosphate buffer containing 0.1 M L-lysine [pH 7.4], 2 mg/mL $NaIO_4$, and 1% PFA) overnight at 4 °C. The following day, tissues were washed 2x in phosphate buffer and placed in 30% sucrose overnight at 4 °C. Tissue was frozen in Tissue-Tek® OCT (VWR; 25608-930), cut on a Leica cryostat, and sections were placed on Fisherbrand™ Tissue Path Superfrost™ Plus Gold Slides (Fisher Scientific; 15-188-48).

For staining, slides were allowed to warm to room temperature, traced with an ImmEdge Hydrophobic Barrier Pen (Vector Labs; H-4000), washed 3× in 1× PBS with 0.5% Tween-20, and blocked with 10% normal donkey serum (Sigma; D9663) in 0.5% Tween-20, 100 mM TrisHCl [pH 7.5], 150 mM NaCl, 0.5% blocking reagent (Perkin Elmer; FP1020) for 30 minutes. Tissues were then stained with 1:300 GFP polyclonal antibody (Invitrogen; A-6455) overnight at 4 °C. Slides were washed 3X and stained with donkey anti-rabbit Alexa Fluor 488 (Jackson Immunoresearch; 711-545-152) for 60 minutes at RT, followed by 150 nM Acti-stain™ 555 phalloidin (Cytoskeleton, Inc; PHDH1-A) and 100 mM DAPI (D1306) for 30 minutes at RT. Slides were then washed 2X in H_20 and sealed under glass coverslips prior to imaging. All antibody dilutions were done in 100 mM TrisHCl [pH 7.5], 150 mM NaCl, 0.5% blocking reagent; all washes were done in 1X PBS with 0.5% Tween-20.

Slides were imaged on a Zeiss LSM710 at the CNR Biological Imaging Facility at the University of California, Berkeley. Images were blinded and manually quantified for GFP^+ IECs. For quantification of GFP^+ cells, $DAPI^+$ IECs were counted in at least 15 villi per mouse—$DAPI^+$ cells were counted prior to revealing the GFP^+ cells in the 488 channel. For quantification of amount GFP levels per IEC, ImageJ (National Institutes of Health) was used to trace and measure the mean pixel intensity in the GFP channel for individual GFP^+ cells, with 12-20 cells per image. ImageJ was used to visualize images and globally adjust contrast and brightness for print quality following quantification.

Serum IL-18 measurement

Thermo Scientific Immuno MaxiSorp ELISA plates (Thermo Fisher; 439454) were coated with 1µg/mL anti-mouse IL-18 mAb (MBL; D048-6) overnight at 4°C, and blocked with 1× PBS containing 1% BSA for 2-4 hours at RT. Serum was diluted 1:5 in PBS with 1% BSA, added to the plate with a purified IL-18 standard, and incubated overnight at 4°C. A biotinylated anti-mouse IL-18 sandwich mAb (BioXcell; BE0237) was added at 1:2000 in PBS with 1% BSA and incubated for 1-2 hours at RT. BD Pharmingen™ Streptavidin HRP (BD Biosciences; 554066) was added at 1:1000 in PBS with 1% BSA. Following a final 5× wash, plates were developed with 1 mg/mL OPD (Sigma; P3804-100TAB) in citrate buffer (PBS with 0.05 M NaH2PO4 and 0.02 M Citric acid) plus 9.8M H_2O_2. The reaction was stopped with a 3 M HCl acid stop after

approximately 10 minutes. Absorbance at 490 nm was measured on a Tecan Spark® multimode microplate reader (Tecan Trading AG, Switzerland).

Lipocalin 2 measurement

The R&D Systems Mouse Lipocalin-2/NGAL DuoSet ELISA kit (cat# DY1857) was used to measure lipocalin-2 levels in the feces. The assay was conducted with Thermo Scientific Immuno MaxiSorp ELISA plates (Thermo Fisher; 439454).

Feces were collected at the indicated times and stored at –20C prior to processing. For processing, feces samples were weighed and resuspended at 50mg per mL in PBS. They were then homogenized with a BioSpec Mini-Beadbeater at max speed for 30 seconds. Afterwards, the solid contents were pelleted at 10,000*g* for 5 minutes, and the supernatants were collected in clean tubes and stored at –20C. Samples were diluted 1:40 in PBS for the ELISA.

Generation of BMDCs

For the bone marrow harvest, marrow was flushed from the femurs and tibias of donor mice using a 23-gauge needle and syringe filled with complete RPMI (RMPI 1640 (Gibco; 21870092) containing 10% FBS (Gibco, Cat#16140071, Lot#1447825), 1% penicillin-streptomycin, 1% L-glutamine, 1% sodium pyruvate, 0.5% 2-mercaptoethanol, and 25mM HEPES) under sterile conditions. The marrow was broken into a single cell suspension by pipetting up and down with a P1000 pipet, pelleted, and then resuspended in cRPMI. The cells were split into 6-8 150mm petri dishes, and additional media containing 10ng/mL GMCSF (PeproTech; 315-03) was added. At day four of culture, the cells were fed with cRPMI containing 10ng/mL GMCSF. At seven days of culture, the cells were harvested, and 5×10^6 cells were injected subcutaneously into the scruff of each mouse.

B3Z assay

B3Z assays were performed as described in (Shastri and Gonzalez, 1993). Briefly, 1×10^5 primary BMDCs were mixed with 1×10^5 B3Z hybridomas (Nilabh Shastri, Berkeley, CA) in a 96-well plate and incubated overnight at 37°C with 5% CO_2. A titration of SIINFEKL peptide was used for the standard curve. The following day, the plates were spun at 800*g* for 2 minutes, and the supernatant was removed. CPRG reagent (Sigma; 10884308001) was used to detect the presence of β-galactosidase, and the plates were read on a SpectraMax M2 at an absorbance of 595nm.

Statistical analysis

For all bar graphs, data are shown as mean ± SD. See figure legends for specific statistical tests used for each analysis. For all data, $*p < 0.05$, $**p < 0.01$, $***p < 0.001$. Tests were run using GraphPad Prism (San Diego, CA).

The sample size for each experiment ranged from three to five mice per genotype, and two to three biological replicates (independent experiments) were performed per experiment, as indicated in figure legends. Sample size was chosen to provide the highest number of data points within the technical limitations of the tissue processing during the experiment.

Key Resources table

Reagent type (species) or resource	Designation	Source or reference	Identifiers	Additional information
Gene (*Mus musculus*)	*Nlrc4*	GenBank	Gene ID: 268973	
Gene (*Mus musculus*)	*Gsdmd*	GenBank	Gene ID: 69146	
Gene (*Mus musculus*)	*Pycard–*	GenBank	Gene ID: 66824	
Gene (*Mus musculus*)	*Batf3*	GenBank	Gene ID: 55509	
Gene (*Mus musculus*)	*Zbtb46*	GenBank	Gene ID: 72147	
strain, strain background (*Mus musculus*)	*Nlrc4*$^{-/-}$	PMID: 15190255	RRID:MGI:3047280	Vishva Dixit, Genentech, South San Francisco, CA
strain, strain background (*Mus musculus*)	*Gsdmd*$^{-/-}$	PMID: 28410991	RRID:IMSR_JAX:032663	Generated via CRISPR/Cas9 from UC Berkeley Gene Targeting Facility
strain, strain background (*Mus musculus*)	*Pycard*$^{-/-}$	PMID: 15190255	RRID:MGI:3047277	Vishva Dixit, Genentech, South San Francisco, CA
strain, strain background (*Mus musculus*)	*Batf3*$^{-/-}$	Jackson Laboratory	RRID:IMSR_JAX:013755	C57BL/6J background
strain, strain background (*Mus musculus*)	*Zbtb46*$^{-/-}$	Jackson Laboratory	RRID:IMSR_JAX:019506	

strain, strain background (*Mus musculus*)	Villin-Cre-ER^{T2}	Jackson Laboratory	RRID:IMSR_JAX:020282	C57BL/6NJ background
strain, strain background (*Mus musculus*)	OT-I *Rag2*$^{-/-}$	Jackson Laboratory	RRID:IMSR_JAX:003831	C57BL/6 background
genetic reagent (*Mus musculus*)	*OvaFla*	PMID: 29263322	MGI:6196853	
Antibody	CD16/CD32 Purified (rat monoclonal)	eBioscience	Clone: 93; Cat#: 14-0161-85	FC(1:1000)
Antibody	anti-mouse CD45.1 APC (mouse monoclonal)	eBioscience	Clone: A20; Cat#: 17-0453-81	FC(1:300)
Antibody	anti-mouse CD45 APC (rat monoclonal)	Biolegend	Clone: 30-F11; Cat#: 103111	FC(1:300)
Antibody	anti-mouse CD45.2 PE/Cy7 (mouse monoclonal)	BioLegend	Clone: 104; Cat#: 109830	FC(1:300)
Antibody	anti-mouse CD8a Brilliant Violet 650™ (rat monoclonal)	BioLegend	Clone: 53-6.7; Cat#: 100742	FC(1:300)
Antibody	anti-Mouse CD44 BB515 (rat monoclonal)	BD	Clone: IM9; Cat#: 564587	FC(1:300)
Antibody	anti-mouse CD62L Brilliant Violet 711™ (rat monoclonal)	BioLegend	Clone: MEL-14; Cat#: 104445	FC(1:300)
Antibody	anti-mouse CD199 (CCR9) PE (rat monoclonal)	BioLegend	Clone: 9B1; Cat#: 129707	FC(1:100)
Antibody	anti-mouse TNFa FITC (mouse monoclonal)	eBioscience	Clone: MP6-XT22; Cat#: 11-7321-82	FC(1:100)
Antibody	anti-mouse CD11c PE (arm hamster monoclonal)	eBioscience	Clone: 418; Cat#: 12-0114-81	FC(1:300)
Antibody	anti-mouse MHC Class II (I-A/I-E) APC-eFluor 780 (rat monoclonal)	BioLegend	Clone: M5/114.15.2; Cat#: 107628	FC(1:300)

Antibody	anto-mouse CD4 APC/Fire™ 750 (rat monoclonal)	BioLegend	Clone: GK1.5; Cat#: 100460	FC(1:300)
Antibody	anti-Mouse CD11b PE-Cyanine7 (rat monoclonal)	eBioscience	Clone: M1/70; Cat#: 25-0112-81	FC(1:300)
Antibody	anti-mouse CD11c Brilliant Violet 711™ (arm hamster monoclonal)	Biolegend	Clone: N418; Cat#: 117349	FC(1:300)
Antibody	anti-mouse CD45 Brilliant Violet 785™(rat monoclonal)	Biolegend	Clone: 30-F11; Cat#: 103149	FC(1:300)
Antibody	anti-mouse MHC II I-A/I-E FITC (rat monoclonal)	Biolegend	Clone: M5/114.15.2; Cat#: 107605	FC(1:400)
Antibody	anti-mouse/rat XCR1 APC (mouse monoclonal)	Biolegend	Clone: ZET; Cat#: 148206	FC(1:300)
Antibody	anti-mouse CD90.2 (Thy-1.2) APC/Fire™ 750 (rat monoclonal)	Biolegend	Clone: 53-2.1; Cat#: 140326	FC(1:300)
Antibody	anti-mouse Ly-6G/Ly-6C (Gr-1) APC/Cyanine7 (rat monoclonal)	Biolegend	Clone: Gr1; Cat#: 108424	FC(1:300)
Antibody	anti-mouse CD64 (FcγRI) APC (mouse monoclonal)	Biolegend	Clone: X54-5/7.1; Cat#: 139306	FC(1:100)
Antibody	anti-mouse CD45.2 PerCP-Cyanine5.5 (mouse monoclonal)	eBio	Clone: 45-0454-82; Cat#: 17-0454-82	FC(1:100)
Antibody	anti-mouse MHC Class II (I-A/I-E) FITC (rat monoclonal)	Fisher	Clone: M5/114.15.2; Cat#: 11-5321-82	FC(1:300)
Antibody	anti-mouse CD64 PE (mouse monoclonal)	Fisher	Clone: X54-5/7.1; Cat#: 12-0641-82	FC(1:200)
Antibody	anti-mouse CD45.2 PE (mouse monoclonal)	Fisher	Clonne: 104; Cat#: 12-0454-82	FC(1:300)

Antibody	anti-mouse CD11b PE-Cyanine7 (rat monoclonal)	Fisher	Clone: M1/70; Cat#: 25-0112-82	FC(1:300)
Antibody	anti-mouse CD90.2 (Thy-1.2) Pacific Blue™ (rat monoclonal)	BioLegend	Clond: 53-2.1; Cat#: 140306	FC(1:300)
Antibody	anti-mouse CD86 Brilliant Violet 785™ (rat monoclonal)	BioLegend	Clone: GL-1; Cat#: 105043	FC(1:200)
Antibody	anti-mouse CD172a (SIRPα) Brilliant Violet 510™ (rat monoclonal)	BioLegend	Clone: P84; Cat#: 144032	FC(1:200)
Antibody	Ghost Dye Red 780	Tonbo	Cat#: 13-0865-T500	FC(1:1000)
Antibody	anti-rabbit IgG (H+L) AF 488 (donkey polyclonal)	Jackson Immunoresearch	Cat#: 711-545-152	IF(1:500)
Antibody	anti-mouse GFP Polyclonal Antibody (rabbit polyclonal)	Invitrogen	Cat#: A-6455	IF(1:300)
Antibody	anti-mouse IL-18 Biotin (rat monoclonal)	MBL	Clone: 93-10C; Cat#: D048-6	ELISA(1ug/mL)
Antibody	anti-mouse IL-18 (rat monoclonal)	BioXcell	Clone: YIGIF74-1G7; Cat#: BE0237	ELISA(1:2000)
Antibody	anti-mouse CD3 biotin (arm ham monoclonal)	BioLegend	Clone: 145-2C11; Cat#: 100304	For depletion, 10uL/10^7 cells
Antibody	BD Pharmingen™ Streptavidin HRP	BD Biosciences	RRID: AB_2868972; Cat#: 554066	ELISA(1:1000)
Commercial assay, kit	CellTrace™ Violet Cell Proliferation Kit	ThermoFisher	Cat#: C34557	See Methods section; 1uL/10^6 cells
Commercial assay, kit	Anti-Biotin MicroBeads	Miltenyi	Cat#: 130-105-637	For depletion, 20uL/10^7 cells

Commercial assay, kit	LD Columns	Miltenyi	Cat#: 130-042-901	See Methods section
Chemical compound, drug	DAPI	invitrogen	Cat#: D1306	IF(10nM)
Chemical compound, drug	BD GolgiPlugTM	BD Biosciences	Cat#: 555029	FC(1:1000)
Chemical compound, drug	Phorbol myristate acetate (PMA)	Invivogen	Cat#: tlrl-pma	FC(1ug/mL)
Chemical compound, drug	Ionomycin	Calbiochem	Cat#: 407952-1MG	FC(1ug/mL)
Chemical compound, drug	o-Phenylenediamine dihydrochloride	Sigma	Cat#: P3804-100TAB	ELISA(1 tab/ 5mL)
Chemical compound, drug	tamoxifen chow	envigo	Cat#: 130856	See Methods section
Chemical compound, drug	Diphtheria Toxin from Corynebacterium diphtheriae	Sigma	Cat#: D0564-1MG	See Methods section
Software, algorithm	ImageJ	NIH	RRID:SCR_003070	
Software, algorithm	FlowJo	BD	RRID:SCR_008520	
Software, algorithm	Prism	GraphPad	RRID:SCR_002798	

References

Aachoui, Y., Leaf, I.A., Hagar, J.A., Fontana, M.F., Campos, C.G., Zak, D.E., Tan, M.H., Cotter, P.A., Vance, R.E., Aderem, A.*, et al.* (2013). Caspase-11 protects against bacteria that escape the vacuole. Science *339*, 975-978.

Adams, A.B., Ford, M.L., and Larsen, C.P. (2016). Costimulation Blockade in Autoimmunity and Transplantation: The CD28 Pathway. J Immunol *197*, 2045-2050.

Ahmadi, M., Emery, D.C., and Morgan, D.J. (2008). Prevention of both direct and cross-priming of antitumor CD8+ T-cell responses following overproduction of prostaglandin E2 by tumor cells in vivo. Cancer Res *68*, 7520-7529.

Ahmed, M., Puckett, S., Arimilli, S., Braxton, C.L., Mizel, S.B., and Lyles, D.S. (2010). Stimulation of human dendritic cells by wild-type and M protein mutant vesicular stomatitis viruses engineered to express bacterial flagellin. J Virol *84*, 12093-12098.

Ahrens, S., Zelenay, S., Sancho, D., Hanc, P., Kjaer, S., Feest, C., Fletcher, G., Durkin, C., Postigo, A., Skehel, M.*, et al.* (2012). F-actin is an evolutionarily conserved damage-associated molecular pattern recognized by DNGR-1, a receptor for dead cells. Immunity *36*, 635-645.

Alhallaf, R., Agha, Z., Miller, C.M., Robertson, A.A.B., Sotillo, J., Croese, J., Cooper, M.A., Masters, S.L., Kupz, A., Smith, N.C.*, et al.* (2018). The NLRP3 Inflammasome Suppresses Protective Immunity to Gastrointestinal Helminth Infection. Cell Rep *23*, 1085-1098.

Allen, I.C., Scull, M.A., Moore, C.B., Holl, E.K., McElvania-TeKippe, E., Taxman, D.J., Guthrie, E.H., Pickles, R.J., and Ting, J.P. (2009). The NLRP3 inflammasome mediates in vivo innate immunity to influenza A virus through recognition of viral RNA. Immunity *30*, 556-565.

Antonopoulos, C., Russo, H.M., El Sanadi, C., Martin, B.N., Li, X., Kaiser, W.J., Mocarski, E.S., and Dubyak, G.R. (2015). Caspase-8 as an Effector and Regulator of NLRP3 Inflammasome Signaling. J Biol Chem *290*, 20167-20184.

Bachem, A., Hartung, E., Guttler, S., Mora, A., Zhou, X., Hegemann, A., Plantinga, M., Mazzini, E., Stoitzner, P., Gurka, S.*, et al.* (2012). Expression of XCR1 Characterizes the Batf3-Dependent Lineage of Dendritic Cells Capable of Antigen Cross-Presentation. Front Immunol *3*, 214.

Barclay, W., and Shinohara, M.L. (2017). Inflammasome activation in multiple sclerosis and experimental autoimmune encephalomyelitis (EAE). Brain Pathol *27*, 213-219.

Beachboard, D.C., and Horner, S.M. (2016). Innate immune evasion strategies of DNA and RNA viruses. Curr Opin Microbiol *32*, 113-119.

Ben-Sasson, S.Z., Hogg, A., Hu-Li, J., Wingfield, P., Chen, X., Crank, M., Caucheteux, S., Ratner-Hurevich, M., Berzofsky, J.A., Nir-Paz, R.*, et al.* (2013a). IL-1 enhances expansion, effector function, tissue localization, and memory response of antigen-specific CD8 T cells. J Exp Med *210*, 491-502.

Ben-Sasson, S.Z., Wang, K., Cohen, J., and Paul, W.E. (2013b). IL-1beta strikingly enhances antigen-driven CD4 and CD8 T-cell responses. Cold Spring Harb Symp Quant Biol *78*, 117-124.

Bernhard, C.A., Ried, C., Kochanek, S., and Brocker, T. (2015). CD169+ macrophages are sufficient for priming of CTLs with specificities left out by cross-priming dendritic cells. Proc Natl Acad Sci U S A *112*, 5461-5466.

Bevan, M.J. (1976). Cross-priming for a secondary cytotoxic response to minor H antigens with H-2 congenic cells which do not cross-react in the cytotoxic assay. J Exp Med *143*, 1283-1288.

Bhattacharyya, N.D., and Feng, C.G. (2020). Regulation of T Helper Cell Fate by TCR Signal Strength. Front Immunol *11*, 624.

Bibo-Verdugo, B., Snipas, S.J., Kolt, S., Poreba, M., and Salvesen, G.S. (2020). Extended subsite profiling of the pyroptosis effector protein gasdermin D reveals a region recognized by inflammatory caspase-11. J Biol Chem *295*, 11292-11302.

Bluestone, J.A., and Anderson, M. (2020). Tolerance in the Age of Immunotherapy. N Engl J Med *383*, 1156-1166.

Blum, J.S., Wearsch, P.A., and Cresswell, P. (2013). Pathways of antigen processing. Annu Rev Immunol *31*, 443-473.

Boada-Romero, E., Martinez, J., Heckmann, B.L., and Green, D.R. (2020). The clearance of dead cells by efferocytosis. Nat Rev Mol Cell Biol *21*, 398-414.

Bosteels, C., Neyt, K., Vanheerswynghels, M., van Helden, M.J., Sichien, D., Debeuf, N., De Prijck, S., Bosteels, V., Vandamme, N., Martens, L.*, et al.* (2020). Inflammatory Type 2 cDCs Acquire Features of cDC1s and Macrophages to Orchestrate Immunity to Respiratory Virus Infection. Immunity *52*, 1039-1056 e1039.

Braga, T.T., Brandao, W.N., Azevedo, H., Terra, F.F., Melo, A.C.L., Pereira, F.V., Andrade-Oliveira, V., Hiyane, M.I., Peron, J.P.S., and Camara, N.O.S. (2019). NLRP3 gain-of-function in CD4(+) T lymphocytes ameliorates experimental autoimmune encephalomyelitis. Clin Sci (Lond) *133*, 1901-1916.

Briseno, C.G., Haldar, M., Kretzer, N.M., Wu, X., Theisen, D.J., Kc, W., Durai, V., Grajales-Reyes, G.E., Iwata, A., Bagadia, P.*, et al.* (2016). Distinct Transcriptional Programs Control Cross-Priming in Classical and Monocyte-Derived Dendritic Cells. Cell Rep *15*, 2462-2474.

Broz, P., and Dixit, V.M. (2016). Inflammasomes: mechanism of assembly, regulation and signalling. Nat Rev Immunol *16*, 407-420.

Broz, P., Newton, K., Lamkanfi, M., Mariathasan, S., Dixit, V.M., and Monack, D.M. (2010a). Redundant roles for inflammasome receptors NLRP3 and NLRC4 in host defense against Salmonella. J Exp Med *207*, 1745-1755.

Broz, P., von Moltke, J., Jones, J.W., Vance, R.E., and Monack, D.M. (2010b). Differential requirement for Caspase-1 autoproteolysis in pathogen-induced cell death and cytokine processing. Cell Host Microbe *8*, 471-483.

Brubaker, S.W., Bonham, K.S., Zanoni, I., and Kagan, J.C. (2015). Innate immune pattern recognition: a cell biological perspective. Annu Rev Immunol *33*, 257-290.

Brydges, S.D., Mueller, J.L., McGeough, M.D., Pena, C.A., Misaghi, A., Gandhi, C., Putnam, C.D., Boyle, D.L., Firestein, G.S., Horner, A.A.*, et al.* (2009). Inflammasome-mediated disease animal models reveal roles for innate but not adaptive immunity. Immunity *30*, 875-887.

Bullen, T.F., Forrest, S., Campbell, F., Dodson, A.R., Hershman, M.J., Pritchard, D.M., Turner, J.R., Montrose, M.H., and Watson, A.J. (2006). Characterization of epithelial cell shedding from human small intestine. Lab Invest *86*, 1052-1063.

Caminschi, I., Proietto, A.I., Ahmet, F., Kitsoulis, S., Shin Teh, J., Lo, J.C., Rizzitelli, A., Wu, L., Vremec, D., van Dommelen, S.L.*, et al.* (2008). The dendritic cell subtype-restricted C-type lectin Clec9A is a target for vaccine enhancement. Blood *112*, 3264-3273.

Cantrell, D. (2015). Signaling in lymphocyte activation. Cold Spring Harb Perspect Biol *7*.

Carlos, D., Costa, F.R., Pereira, C.A., Rocha, F.A., Yaochite, J.N., Oliveira, G.G., Carneiro, F.S., Tostes, R.C., Ramos, S.G., Zamboni, D.S.*, et al.* (2017). Mitochondrial DNA Activates the NLRP3 Inflammasome and Predisposes to Type 1 Diabetes in Murine Model. Front Immunol *8*, 164.

Cerovic, V., Houston, S.A., Westlund, J., Utriainen, L., Davison, E.S., Scott, C.L., Bain, C.C., Joeris, T., Agace, W.W., Kroczek, R.A.*, et al.* (2015). Lymph-borne CD8alpha+ dendritic cells are uniquely able to cross-prime CD8+ T cells with antigen acquired from intestinal epithelial cells. Mucosal Immunol *8*, 38-48.

Chang, M.K., Binder, C.J., Miller, Y.I., Subbanagounder, G., Silverman, G.J., Berliner, J.A., and Witztum, J.L. (2004). Apoptotic cells with oxidation-specific epitopes are immunogenic and proinflammatory. J Exp Med *200*, 1359-1370.

Chassaing, B., Srinivasan, G., Delgado, M.A., Young, A.N., Gewirtz, A.T., and Vijay-Kumar, M. (2012). Fecal lipocalin 2, a sensitive and broadly dynamic non-invasive biomarker for intestinal inflammation. PLoS One *7*, e44328.

Chen, K.W., Demarco, B., Heilig, R., Shkarina, K., Boettcher, A., Farady, C.J., Pelczar, P., and Broz, P. (2019). Extrinsic and intrinsic apoptosis activate pannexin-1 to drive NLRP3 inflammasome assembly. EMBO J *38*.

Chen, K.W., Gross, C.J., Sotomayor, F.V., Stacey, K.J., Tschopp, J., Sweet, M.J., and Schroder, K. (2014). The neutrophil NLRC4 inflammasome selectively promotes IL-1beta maturation without pyroptosis during acute Salmonella challenge. Cell Rep *8*, 570-582.

Chiang, P.M., Ling, J., Jeong, Y.H., Price, D.L., Aja, S.M., and Wong, P.C. (2010). Deletion of TDP-43 down-regulates Tbc1d1, a gene linked to obesity, and alters body fat metabolism. Proc Natl Acad Sci U S A *107*, 16320-16324.

Chieppa, M., Rescigno, M., Huang, A.Y., and Germain, R.N. (2006). Dynamic imaging of dendritic cell extension into the small bowel lumen in response to epithelial cell TLR engagement. J Exp Med *203*, 2841-2852.

Choy, M.C., Visvanathan, K., and De Cruz, P. (2017). An Overview of the Innate and Adaptive Immune System in Inflammatory Bowel Disease. Inflamm Bowel Dis *23*, 2-13.

Christ, A.D., and Blumberg, R.S. (1997). The intestinal epithelial cell: immunological aspects. Springer Semin Immunopathol *18*, 449-461.

Chu, L.H., Indramohan, M., Ratsimandresey, R.A., Gangopadhyay, A., Morris, E.P., Monack, D.M., Dorfleutner, A., and Stehlik, C. (2018). The oxidized phospholipid oxPAPC protects from septic shock by targeting the non-canonical inflammasome in macrophages. Nat Commun *9*, 996.

Chudnovskiy, A., Mortha, A., Kana, V., Kennard, A., Ramirez, J.D., Rahman, A., Remark, R., Mogno, I., Ng, R., Gnjatic, S*., et al.* (2016). Host-Protozoan Interactions Protect from Mucosal Infections through Activation of the Inflammasome. Cell *167*, 444-456 e414.

Chudnovskiy, A., Pasqual, G., and Victora, G.D. (2019). Studying interactions between dendritic cells and T cells in vivo. Curr Opin Immunol *58*, 24-30.

Chulkina, M., Beswick, E.J., and Pinchuk, I.V. (2020). Role of PD-L1 in Gut Mucosa Tolerance and Chronic Inflammation. Int J Mol Sci *21*.

Chung, Y., Chang, S.H., Martinez, G.J., Yang, X.O., Nurieva, R., Kang, H.S., Ma, L., Watowich, S.S., Jetten, A.M., Tian, Q*., et al.* (2009). Critical regulation of early Th17 cell differentiation by interleukin-1 signaling. Immunity *30*, 576-587.

Churchill, M.J., Mitchell, P.S., and Rauch, I. (2021). Epithelial pyroptosis in host defense. J Mol Biol, 167278.

Coates, M., Lee, M.J., Norton, D., and MacLeod, A.S. (2019). The Skin and Intestinal Microbiota and Their Specific Innate Immune Systems. Front Immunol *10*, 2950.

Conley, J.M., Gallagher, M.P., and Berg, L.J. (2016). T Cells and Gene Regulation: The Switching On and Turning Up of Genes after T Cell Receptor Stimulation in CD8 T Cells. Front Immunol *7*, 76.

Constant, D.A., Nice, T.J., and Rauch, I. (2021). Innate immune sensing by epithelial barriers. Curr Opin Immunol *73*, 1-8.

Cox, M.A., Kahan, S.M., and Zajac, A.J. (2013). Anti-viral CD8 T cells and the cytokines that they love. Virology *435*, 157-169.

Cruz, F.M., Colbert, J.D., Merino, E., Kriegsman, B.A., and Rock, K.L. (2017). The Biology and Underlying Mechanisms of Cross-Presentation of Exogenous Antigens on MHC-I Molecules. Annu Rev Immunol *35*, 149-176.

Cueto, F.J., Del Fresno, C., and Sancho, D. (2019). DNGR-1, a Dendritic Cell-Specific Sensor of Tissue Damage That Dually Modulates Immunity and Inflammation. Front Immunol *10*, 3146.

Cui, B., Liu, X., Fang, Y., Zhou, P., Zhang, Y., and Wang, Y. (2018). Flagellin as a vaccine adjuvant. Expert Rev Vaccines *17*, 335-349.

Cummings, R.J., Barbet, G., Bongers, G., Hartmann, B.M., Gettler, K., Muniz, L., Furtado, G.C., Cho, J., Lira, S.A., and Blander, J.M. (2016). Different tissue phagocytes sample apoptotic cells to direct distinct homeostasis programs. Nature *539*, 565-569.

Curtsinger, J.M., and Mescher, M.F. (2010). Inflammatory cytokines as a third signal for T cell activation. Curr Opin Immunol *22*, 333-340.

Cyster, J.G., and Allen, C.D.C. (2019). B Cell Responses: Cell Interaction Dynamics and Decisions. Cell *177*, 524-540.

Daley, D., Mani, V.R., Mohan, N., Akkad, N., Pandian, G., Savadkar, S., Lee, K.B., Torres-Hernandez, A., Aykut, B., Diskin, B.*, et al.* (2017). NLRP3 signaling drives macrophage-induced adaptive immune suppression in pancreatic carcinoma. J Exp Med *214*, 1711-1724.

Dalod, M., Chelbi, R., Malissen, B., and Lawrence, T. (2014). Dendritic cell maturation: functional specialization through signaling specificity and transcriptional programming. EMBO J *33*, 1104-1116.

Dance, A. (2019). Core Concept: Cells nibble one another via the under-appreciated process of trogocytosis. Proc Natl Acad Sci U S A *116*, 17608-17610.

Das, S., Shapiro, B., Vucic, E.A., Vogt, S., and Bar-Sagi, D. (2020). Tumor Cell-Derived IL1beta Promotes Desmoplasia and Immune Suppression in Pancreatic Cancer. Cancer Res *80*, 1088-1101.

Davis, M.A., Fairgrieve, M.R., Den Hartigh, A., Yakovenko, O., Duvvuri, B., Lood, C., Thomas, W.E., Fink, S.L., and Gale, M., Jr. (2019). Calpain drives pyroptotic vimentin cleavage, intermediate filament loss, and cell rupture that mediates immunostimulation. Proc Natl Acad Sci U S A *116*, 5061-5070.

de Vasconcelos, N.M., and Lamkanfi, M. (2020). Recent Insights on Inflammasomes, Gasdermin Pores, and Pyroptosis. Cold Spring Harb Perspect Biol *12*, a036392.

de Vasconcelos, N.M., Van Opdenbosch, N., Van Gorp, H., Parthoens, E., and Lamkanfi, M. (2019). Single-cell analysis of pyroptosis dynamics reveals conserved GSDMD-mediated subcellular events that precede plasma membrane rupture. Cell Death Differ *26*, 146-161.

Deets, K.A., and Vance, R.E. (2021). Inflammasomes and adaptive immune responses. Nat Immunol *22*, 412-422.

Deng, J., Yu, X.Q., and Wang, P.H. (2019). Inflammasome activation and Th17 responses. Mol Immunol *107*, 142-164.

DiPeso, L., Ji, D.X., Vance, R.E., and Price, J.V. (2017). Cell death and cell lysis are separable events during pyroptosis. Cell Death Discov *3*, 17070.

Doitsh, G., Cavrois, M., Lassen, K.G., Zepeda, O., Yang, Z., Santiago, M.L., Hebbeler, A.M., and Greene, W.C. (2010). Abortive HIV infection mediates CD4 T cell depletion and inflammation in human lymphoid tissue. Cell *143*, 789-801.

Dorner, B.G., Dorner, M.B., Zhou, X., Opitz, C., Mora, A., Guttler, S., Hutloff, A., Mages, H.W., Ranke, K., Schaefer, M.*, et al.* (2009). Selective expression of the chemokine receptor XCR1 on cross-presenting dendritic cells determines cooperation with CD8+ T cells. Immunity *31*, 823-833.

Dostert, C., Ludigs, K., and Guarda, G. (2013). Innate and adaptive effects of inflammasomes on T cell responses. Curr Opin Immunol *25*, 359-365.

Dupaul-Chicoine, J., Arabzadeh, A., Dagenais, M., Douglas, T., Champagne, C., Morizot, A., Rodrigue-Gervais, I.G., Breton, V., Colpitts, S.L., Beauchemin, N.*, et al.* (2015). The Nlrp3 Inflammasome Suppresses Colorectal Cancer Metastatic Growth in the Liver by Promoting Natural Killer Cell Tumoricidal Activity. Immunity *43*, 751-763.

Durkin, E.T., Jones, K.A., Rajesh, D., and Shaaban, A.F. (2008). Early chimerism threshold predicts sustained engraftment and NK-cell tolerance in prenatal allogeneic chimeras. Blood *112*, 5245-5253.

Eisenbarth, S.C., Colegio, O.R., O'Connor, W., Sutterwala, F.S., and Flavell, R.A. (2008). Crucial role for the Nalp3 inflammasome in the immunostimulatory properties of aluminium adjuvants. Nature *453*, 1122-1126.

el Marjou, F., Janssen, K.P., Chang, B.H., Li, M., Hindie, V., Chan, L., Louvard, D., Chambon, P., Metzger, D., and Robine, S. (2004). Tissue-specific and inducible Cre-mediated recombination in the gut epithelium. Genesis *39*, 186-193.

ElTanbouly, M.A., and Noelle, R.J. (2021). Rethinking peripheral T cell tolerance: checkpoints across a T cell's journey. Nat Rev Immunol *21*, 257-267.

Enders, M., Franken, L., Philipp, M.S., Kessler, N., Baumgart, A.K., Eichler, M., Wiertz, E.J.H., Garbi, N., and Kurts, C. (2020). Splenic Red Pulp Macrophages Cross-Prime Early Effector CTL That Provide Rapid Defense against Viral Infections. J Immunol *204*, 87-100.

Engwerda, C.R., Ng, S.S., and Bunn, P.T. (2014). The Regulation of CD4(+) T Cell Responses during Protozoan Infections. Front Immunol *5*, 498.

Erlich, Z., Shlomovitz, I., Edry-Botzer, L., Cohen, H., Frank, D., Wang, H., Lew, A.M., Lawlor, K.E., Zhan, Y., Vince, J.E.*, et al.* (2019). Macrophages, rather than DCs, are responsible for inflammasome activity in the GM-CSF BMDC model. Nat Immunol *20*, 397-406.

Esterhazy, D., Canesso, M.C.C., Mesin, L., Muller, P.A., de Castro, T.B.R., Lockhart, A., ElJalby, M., Faria, A.M.C., and Mucida, D. (2019). Compartmentalized gut lymph node drainage dictates adaptive immune responses. Nature *569*, 126-130.

Evavold, C.L., and Kagan, J.C. (2018). How Inflammasomes Inform Adaptive Immunity. J Mol Biol *430*, 217-237.

Evavold, C.L., Ruan, J., Tan, Y., Xia, S., Wu, H., and Kagan, J.C. (2018). The Pore-Forming Protein Gasdermin D Regulates Interleukin-1 Secretion from Living Macrophages. Immunity *48*, 35-44 e36.

Farache, J., Koren, I., Milo, I., Gurevich, I., Kim, K.W., Zigmond, E., Furtado, G.C., Lira, S.A., and Shakhar, G. (2013). Luminal bacteria recruit CD103+ dendritic cells into the intestinal epithelium to sample bacterial antigens for presentation. Immunity *38*, 581-595.

Fattinger, S.A., Geiser, P., Samperio Ventayol, P., Di Martino, M.L., Furter, M., Felmy, B., Bakkeren, E., Hausmann, A., Barthel-Scherrer, M., Gul, E.*, et al.* (2021). Epithelium-autonomous NAIP/NLRC4 prevents TNF-driven inflammatory destruction of the gut epithelial barrier in Salmonella-infected mice. Mucosal Immunol *14*, 615-629.

Feriotti, C., de Araujo, E.F., Loures, F.V., da Costa, T.A., Galdino, N.A.L., Zamboni, D.S., and Calich, V.L.G. (2017). NOD-Like Receptor P3 Inflammasome Controls Protective Th1/Th17 Immunity against Pulmonary Paracoccidioidomycosis. Front Immunol *8*, 786.

Fitzgerald, K.A., and Kagan, J.C. (2020). Toll-like Receptors and the Control of Immunity. Cell *180*, 1044-1066.

Franchi, L., and Nunez, G. (2008). The Nlrp3 inflammasome is critical for aluminium hydroxide-mediated IL-1beta secretion but dispensable for adjuvant activity. Eur J Immunol *38*, 2085-2089.

Fu, C., and Jiang, A. (2018). Dendritic Cells and CD8 T Cell Immunity in Tumor Microenvironment. Front Immunol *9*, 3059.

Gaidt, M.M., Ebert, T.S., Chauhan, D., Schmidt, T., Schmid-Burgk, J.L., Rapino, F., Robertson, A.A., Cooper, M.A., Graf, T., and Hornung, V. (2016). Human Monocytes Engage an Alternative Inflammasome Pathway. Immunity *44*, 833-846.

Gao, Y., Deason, K., Jain, A., Irizarry-Caro, R.A., Dozmorov, I., Coughlin, L.A., Rauch, I., Evers, B.M., Koh, A.Y., Wakeland, E.K.*, et al.* (2020). Transcriptional profiling identifies caspase-1 as a T cell-intrinsic regulator of Th17 differentiation. J Exp Med *217*, e20190476.

Garaude, J., Kent, A., van Rooijen, N., and Blander, J.M. (2012). Simultaneous targeting of toll- and nod-like receptors induces effective tumor-specific immune responses. Sci Transl Med *4*, 120ra116.

Ghiringhelli, F., Apetoh, L., Tesniere, A., Aymeric, L., Ma, Y., Ortiz, C., Vermaelen, K., Panaretakis, T., Mignot, G., Ullrich, E.*, et al.* (2009). Activation of the NLRP3 inflammasome in dendritic cells induces IL-1beta-dependent adaptive immunity against tumors. Nat Med *15*, 1170-1178.

Godfrey, D.I., Uldrich, A.P., McCluskey, J., Rossjohn, J., and Moody, D.B. (2015). The burgeoning family of unconventional T cells. Nat Immunol *16*, 1114-1123.

Gomez, D.P., and Boudreau, F. (2021). Organoids and Their Use in Modeling Gut Epithelial Cell Lineage Differentiation and Barrier Properties During Intestinal Diseases. Front Cell Dev Biol *9*, 732137.

Goncalves, A.V., Margolis, S.R., Quirino, G.F.S., Mascarenhas, D.P.A., Rauch, I., Nichols, R.D., Ansaldo, E., Fontana, M.F., Vance, R.E., and Zamboni, D.S. (2019). Gasdermin-D and Caspase-7 are the key Caspase-1/8 substrates downstream of the NAIP5/NLRC4 inflammasome required for restriction of Legionella pneumophila. PLoS Pathog *15*, e1007886.

Gong, Z., Zhao, S., Zhou, J., Yan, J., Wang, L., Du, X., Li, H., Chen, Y., Cai, W., and Wu, J. (2018). Curcumin alleviates DSS-induced colitis via inhibiting NLRP3 inflammsome activation and IL-1beta production. Mol Immunol *104*, 11-19.

Gordon, S. (2016). Phagocytosis: An Immunobiologic Process. Immunity *44*, 463-475.

Gris, D., Ye, Z., Iocca, H.A., Wen, H., Craven, R.R., Gris, P., Huang, M., Schneider, M., Miller, S.D., and Ting, J.P. (2010). NLRP3 plays a critical role in the development of experimental autoimmune encephalomyelitis by mediating Th1 and Th17 responses. J Immunol *185*, 974-981.

Gros, M., and Amigorena, S. (2019). Regulation of Antigen Export to the Cytosol During Cross-Presentation. Front Immunol *10*, 41.

Guan, Q., Warrington, R., Moreno, S., Qing, G., Weiss, C., and Peng, Z. (2019). Sustained suppression of IL-18 by employing a vaccine ameliorates intestinal inflammation in TNBS-induced murine colitis. Future Sci OA *5*, FSO405.

Gutierrez-Martinez, E., Planes, R., Anselmi, G., Reynolds, M., Menezes, S., Adiko, A.C., Saveanu, L., and Guermonprez, P. (2015). Cross-Presentation of Cell-Associated Antigens by MHC Class I in Dendritic Cell Subsets. Front Immunol *6*, 363.

Hagar, J.A., Powell, D.A., Aachoui, Y., Ernst, R.K., and Miao, E.A. (2013). Cytoplasmic LPS activates caspase-11: implications in TLR4-independent endotoxic shock. Science *341*, 1250-1253.

Hall, P.A., Coates, P.J., Ansari, B., and Hopwood, D. (1994). Regulation of cell number in the mammalian gastrointestinal tract: the importance of apoptosis. J Cell Sci *107 (Pt 12)*, 3569-3577.

Halle, S., Halle, O., and Forster, R. (2017). Mechanisms and Dynamics of T Cell-Mediated Cytotoxicity In Vivo. Trends Immunol *38*, 432-443.

Harapas, C.R., Steiner, A., Davidson, S., and Masters, S.L. (2018). An Update on Autoinflammatory Diseases: Inflammasomopathies. Curr Rheumatol Rep *20*, 40.

Harrison, O.J., Srinivasan, N., Pott, J., Schiering, C., Krausgruber, T., Ilott, N.E., and Maloy, K.J. (2015). Epithelial-derived IL-18 regulates Th17 cell differentiation and Foxp3(+) Treg cell function in the intestine. Mucosal Immunol *8*, 1226-1236.

Hausmann, A., Bock, D., Geiser, P., Berthold, D.L., Fattinger, S.A., Furter, M., Bouman, J.A., Barthel-Scherrer, M., Lang, C.M., Bakkeren, E*., et al.* (2020). Intestinal epithelial NAIP/NLRC4 restricts systemic dissemination of the adapted pathogen Salmonella Typhimurium due to site-specific bacterial PAMP expression. Mucosal Immunol *13*, 530-544.

He, W.T., Wan, H., Hu, L., Chen, P., Wang, X., Huang, Z., Yang, Z.H., Zhong, C.Q., and Han, J. (2015). Gasdermin D is an executor of pyroptosis and required for interleukin-1beta secretion. Cell Res *25*, 1285-1298.

Heilig, R., Dick, M.S., Sborgi, L., Meunier, E., Hiller, S., and Broz, P. (2018). The Gasdermin-D pore acts as a conduit for IL-1beta secretion in mice. Eur J Immunol *48*, 584-592.

Helft, J., Manicassamy, B., Guermonprez, P., Hashimoto, D., Silvin, A., Agudo, J., Brown, B.D., Schmolke, M., Miller, J.C., Leboeuf, M*., et al.* (2012). Cross-presenting CD103+ dendritic cells are protected from influenza virus infection. J Clin Invest *122*, 4037-4047.

Heuberger, C., Pott, J., and Maloy, K.J. (2021). Why do intestinal epithelial cells express MHC class II? Immunology *162*, 357-367.

Hildner, K., Edelson, B.T., Purtha, W.E., Diamond, M., Matsushita, H., Kohyama, M., Calderon, B., Schraml, B.U., Unanue, E.R., Diamond, M.S.*, et al.* (2008). Batf3 deficiency reveals a critical role for CD8alpha+ dendritic cells in cytotoxic T cell immunity. Science *322*, 1097-1100.

Hirano, M., Das, S., Guo, P., and Cooper, M.D. (2011). The evolution of adaptive immunity in vertebrates. Adv Immunol *109*, 125-157.

Hogquist, K.A., Jameson, S.C., Heath, W.R., Howard, J.L., Bevan, M.J., and Carbone, F.R. (1994). T cell receptor antagonist peptides induce positive selection. Cell *76*, 17-27.

Holdsworth, S.R., and Gan, P.Y. (2015). Cytokines: Names and Numbers You Should Care About. Clin J Am Soc Nephrol *10*, 2243-2254.

Holmkvist, P., Pool, L., Hagerbrand, K., Agace, W.W., and Rivollier, A. (2016). IL-18Ralpha-deficient CD4(+) T cells induce intestinal inflammation in the CD45RB(hi) transfer model of colitis despite impaired innate responsiveness. Eur J Immunol *46*, 1371-1382.

Hu, C., Ding, H., Li, Y., Pearson, J.A., Zhang, X., Flavell, R.A., Wong, F.S., and Wen, L. (2015). NLRP3 deficiency protects from type 1 diabetes through the regulation of chemotaxis into the pancreatic islets. Proc Natl Acad Sci U S A *112*, 11318-11323.

Hua, Z., and Hou, B. (2020). The role of B cell antigen presentation in the initiation of CD4+ T cell response. Immunol Rev *296*, 24-35.

Huang, F.P., Platt, N., Wykes, M., Major, J.R., Powell, T.J., Jenkins, C.D., and MacPherson, G.G. (2000). A discrete subpopulation of dendritic cells transports apoptotic intestinal epithelial cells to T cell areas of mesenteric lymph nodes. J Exp Med *191*, 435-444.

Hughes, C.E., and Nibbs, R.J.B. (2018). A guide to chemokines and their receptors. FEBS J *285*, 2944-2971.

Hwang, J.R., Byeon, Y., Kim, D., and Park, S.G. (2020). Recent insights of T cell receptor-mediated signaling pathways for T cell activation and development. Exp Mol Med *52*, 750-761.

Ichinohe, T., Lee, H.K., Ogura, Y., Flavell, R., and Iwasaki, A. (2009). Inflammasome recognition of influenza virus is essential for adaptive immune responses. J Exp Med *206*, 79-87.

Ichinohe, T., Pang, I.K., and Iwasaki, A. (2010). Influenza virus activates inflammasomes via its intracellular M2 ion channel. Nat Immunol *11*, 404-410.

Imai, Y., Kuba, K., Neely, G.G., Yaghubian-Malhami, R., Perkmann, T., van Loo, G., Ermolaeva, M., Veldhuizen, R., Leung, Y.H., Wang, H.*, et al.* (2008). Identification of oxidative stress and Toll-like receptor 4 signaling as a key pathway of acute lung injury. Cell *133*, 235-249.

Inoue, M., Williams, K.L., Gunn, M.D., and Shinohara, M.L. (2012). NLRP3 inflammasome induces chemotactic immune cell migration to the CNS in experimental autoimmune encephalomyelitis. Proc Natl Acad Sci U S A *109*, 10480-10485.

Iwasaki, A., and Medzhitov, R. (2015). Control of adaptive immunity by the innate immune system. Nat Immunol *16*, 343-353.

Jain, A., and Pasare, C. (2017). Innate Control of Adaptive Immunity: Beyond the Three-Signal Paradigm. J Immunol *198*, 3791-3800.

Jain, A., Song, R., Wakeland, E.K., and Pasare, C. (2018). T cell-intrinsic IL-1R signaling licenses effector cytokine production by memory CD4 T cells. Nat Commun *9*, 3185.

Janeway, C.A., Jr. (1989). Approaching the asymptote? Evolution and revolution in immunology. Cold Spring Harb Symp Quant Biol *54 Pt 1*, 1-13.

Joeris, T., Gomez-Casado, C., Holmkvist, P., Tavernier, S.J., Silva-Sanchez, A., Klotz, L., Randall, T.D., Mowat, A.M., Kotarsky, K., Malissen, B.*, et al.* (2021). Intestinal cDC1 drive cross-tolerance to epithelial-derived antigen via induction of FoxP3(+)CD8(+) Tregs. Sci Immunol *6*.

Johnson, D.C., Okondo, M.C., Orth, E.L., Rao, S.D., Huang, H.C., Ball, D.P., and Bachovchin, D.A. (2020). DPP8/9 inhibitors activate the CARD8 inflammasome in resting lymphocytes. Cell Death Dis *11*, 628.

Jorgensen, I., Lopez, J.P., Laufer, S.A., and Miao, E.A. (2016a). IL-1beta, IL-18, and eicosanoids promote neutrophil recruitment to pore-induced intracellular traps following pyroptosis. Eur J Immunol *46*, 2761-2766.

Jorgensen, I., Rayamajhi, M., and Miao, E.A. (2017). Programmed cell death as a defence against infection. Nat Rev Immunol *17*, 151-164.

Jorgensen, I., Zhang, Y., Krantz, B.A., and Miao, E.A. (2016b). Pyroptosis triggers pore-induced intracellular traps (PITs) that capture bacteria and lead to their clearance by efferocytosis. J Exp Med *213*, 2113-2128.

Jubel, J.M., Barbati, Z.R., Burger, C., Wirtz, D.C., and Schildberg, F.A. (2020). The Role of PD-1 in Acute and Chronic Infection. Front Immunol *11*, 487.

Kajiwara, Y., Schiff, T., Voloudakis, G., Gama Sosa, M.A., Elder, G., Bozdagi, O., and Buxbaum, J.D. (2014). A critical role for human caspase-4 in endotoxin sensitivity. J Immunol *193*, 335-343.

Karki, R., Man, S.M., Malireddi, R.K.S., Gurung, P., Vogel, P., Lamkanfi, M., and Kanneganti, T.D. (2015). Concerted activation of the AIM2 and NLRP3 inflammasomes orchestrates host protection against Aspergillus infection. Cell Host Microbe *17*, 357-368.

Karttunen, J., Sanderson, S., and Shastri, N. (1992). Detection of rare antigen-presenting cells by the lacZ T-cell activation assay suggests an expression cloning strategy for T-cell antigens. Proc Natl Acad Sci U S A *89*, 6020-6024.

Kaufmann, S.H., and Schaible, U.E. (2005). Antigen presentation and recognition in bacterial infections. Curr Opin Immunol *17*, 79-87.

Kayagaki, N., Stowe, I.B., Lee, B.L., O'Rourke, K., Anderson, K., Warming, S., Cuellar, T., Haley, B., Roose-Girma, M., Phung, Q.T.*, et al.* (2015). Caspase-11 cleaves gasdermin D for non-canonical inflammasome signalling. Nature *526*, 666-671.

Ketelut-Carneiro, N., Silva, G.K., Rocha, F.A., Milanezi, C.M., Cavalcanti-Neto, F.F., Zamboni, D.S., and Silva, J.S. (2015). IL-18 triggered by the Nlrp3 inflammasome induces host innate resistance in a pulmonary model of fungal infection. J Immunol *194*, 4507-4517.

Ketelut-Carneiro, N., Souza, C.O.S., Benevides, L., Gardinassi, L.G., Silva, M.C., Tavares, L.A., Zamboni, D.S., and Silva, J.S. (2019). Caspase-11-dependent IL-1alpha release boosts Th17 immunity against Paracoccidioides brasiliensis. PLoS Pathog *15*, e1007990.

Knudsen, M.L., Johansson, D.X., Kostic, L., Nordstrom, E.K., Tegerstedt, K., Pasetto, A., Applequist, S.E., Ljungberg, K., Sirard, J.C., and Liljestrom, P. (2013). The adjuvant activity of alphavirus replicons is enhanced by incorporating the microbial molecule flagellin into the replicon. PLoS One *8*, e65964.

Ko, E.J., Lee, Y., Lee, Y.T., Jung, Y.J., Ngo, V.L., Kim, M.C., Kim, K.H., Wang, B.Z., Gewirtz, A.T., and Kang, S.M. (2019). Flagellin-expressing virus-like particles exhibit adjuvant effects on promoting IgG isotype-switched long-lasting antibody induction and protection of influenza vaccines in CD4-deficient mice. Vaccine *37*, 3426-3434.

Kofoed, E.M., and Vance, R.E. (2011). Innate immune recognition of bacterial ligands by NAIPs determines inflammasome specificity. Nature *477*, 592-595.

Kupz, A., Guarda, G., Gebhardt, T., Sander, L.E., Short, K.R., Diavatopoulos, D.A., Wijburg, O.L., Cao, H., Waithman, J.C., Chen, W.*, et al.* (2012). NLRC4 inflammasomes in dendritic cells regulate noncognate effector function by memory CD8(+) T cells. Nat Immunol *13*, 162-169.

Kurachi, M. (2019). CD8(+) T cell exhaustion. Semin Immunopathol *41*, 327-337.

Kurd, N., and Robey, E.A. (2016). T-cell selection in the thymus: a spatial and temporal perspective. Immunol Rev *271*, 114-126.

Kurts, C., Heath, W.R., Carbone, F.R., Allison, J., Miller, J.F., and Kosaka, H. (1996). Constitutive class I-restricted exogenous presentation of self antigens in vivo. J Exp Med *184*, 923-930.

Kurts, C., Kosaka, H., Carbone, F.R., Miller, J.F., and Heath, W.R. (1997). Class I-restricted cross-presentation of exogenous self-antigens leads to deletion of autoreactive CD8(+) T cells. J Exp Med *186*, 239-245.

Lamkanfi, M., and Dixit, V.M. (2014). Mechanisms and functions of inflammasomes. Cell *157*, 1013-1022.

Lamkanfi, M., Sarkar, A., Vande Walle, L., Vitari, A.C., Amer, A.O., Wewers, M.D., Tracey, K.J., Kanneganti, T.D., and Dixit, V.M. (2010). Inflammasome-dependent release of the alarmin HMGB1 in endotoxemia. J Immunol *185*, 4385-4392.

Larsen, S.B., Cowley, C.J., and Fuchs, E. (2020). Epithelial cells: liaisons of immunity. Curr Opin Immunol *62*, 45-53.

Lazzaro, B.P., Zasloff, M., and Rolff, J. (2020). Antimicrobial peptides: Application informed by evolution. Science *368*.

Lebreton, F., Berishvili, E., Parnaud, G., Rouget, C., Bosco, D., Berney, T., and Lavallard, V. (2018). NLRP3 inflammasome is expressed and regulated in human islets. Cell Death Dis *9*, 726.

Lee, P.H., Bird, N., MacKenzie-Kludas, C., Mansell, A., Kedzierska, K., Brown, L., and McAuley, J. (2016). Induction of memory cytotoxic T cells to influenza A virus and subsequent viral clearance is not modulated by PB1-F2-dependent inflammasome activation. Immunol Cell Biol *94*, 439-446.

Lee, P.H., Yamamoto, T.N., Gurusamy, D., Sukumar, M., Yu, Z., Hu-Li, J., Kawabe, T., Gangaplara, A., Kishton, R.J., Henning, A.N.*, et al.* (2019). Host conditioning with IL-1beta improves the antitumor function of adoptively transferred T cells. J Exp Med *216*, 2619-2634.

Lei-Leston, A.C., Murphy, A.G., and Maloy, K.J. (2017). Epithelial Cell Inflammasomes in Intestinal Immunity and Inflammation. Front Immunol *8*, 1168.

Li, C., Jiang, P., Wei, S., Xu, X., and Wang, J. (2020). Regulatory T cells in tumor microenvironment: new mechanisms, potential therapeutic strategies and future prospects. Mol Cancer *19*, 116.

Li, H., Willingham, S.B., Ting, J.P., and Re, F. (2008). Cutting edge: inflammasome activation by alum and alum's adjuvant effect are mediated by NLRP3. J Immunol *181*, 17-21.

Li, J., Mbow, M.L., Sun, L., Li, L., Yang, G., Griswold, D.E., Schantz, A., Shealy, D.J., Goletz, T.J., Wan, J.*, et al.* (2004). Induction of dendritic cell maturation by IL-18. Cell Immunol *227*, 103-108.

Li, S., Wu, Y., Yang, D., Wu, C., Ma, C., Liu, X., Moynagh, P.N., Wang, B., Hu, G., and Yang, S. (2019). Gasdermin D in peripheral myeloid cells drives neuroinflammation in experimental autoimmune encephalomyelitis. J Exp Med *216*, 2562-2581.

Li, W., Yang, J., Zhang, E., Zhong, M., Xiao, Y., Yu, J., Zhou, D., Cao, Y., Yang, Y., Li, Y.*, et al.* (2016). Activation of NLRC4 downregulates TLR5-mediated antibody immune responses against flagellin. Cell Mol Immunol *13*, 514-523.

Lin, K.H., Chang, L.S., Tian, C.Y., Yeh, Y.C., Chen, Y.J., Chuang, T.H., Liu, S.J., and Leng, C.H. (2016). Carboxyl-terminal fusion of E7 into Flagellin shifts TLR5 activation to NLRC4/NAIP5 activation and induces TLR5-independent anti-tumor immunity. Sci Rep *6*, 24199.

Linder, A., Bauernfried, S., Cheng, Y., Albanese, M., Jung, C., Keppler, O.T., and Hornung, V. (2020). CARD8 inflammasome activation triggers pyroptosis in human T cells. EMBO J *39*, e105071.

Liu, H., Xu, R., Kong, Q., Liu, J., Yu, Z., and Zhao, C. (2017). Downregulated NLRP3 and NLRP1 inflammasomes signaling pathways in the development and progression of type 1 diabetes mellitus. Biomed Pharmacother *94*, 619-626.

Liu, J., Zhang, X., Cheng, Y., and Cao, X. (2021). Dendritic cell migration in inflammation and immunity. Cell Mol Immunol.

Liu, W., Evanoff, D.P., Chen, X., and Luo, Y. (2007). Urinary bladder epithelium antigen induces CD8+ T cell tolerance, activation, and autoimmune response. J Immunol *178*, 539-546.

Liu, Z., and Lefrancois, L. (2004). Intestinal epithelial antigen induces mucosal CD8 T cell tolerance, activation, and inflammatory response. J Immunol *173*, 4324-4330.

Lu, A., Li, H., Niu, J., Wu, S., Xue, G., Yao, X., Guo, Q., Wan, N., Abliz, P., Yang, G.*, et al.* (2017). Hyperactivation of the NLRP3 Inflammasome in Myeloid Cells Leads to Severe Organ Damage in Experimental Lupus. J Immunol *198*, 1119-1129.

Lukowski, S.W., Rodahl, I., Kelly, S., Yu, M., Gotley, J., Zhou, C., Millard, S., Andersen, S.B., Christ, A.N., Belz, G.*, et al.* (2021). Absence of Batf3 reveals a new dimension of cell state heterogeneity within conventional dendritic cells. iScience *24*, 102402.

Mak'Anyengo, R., Duewell, P., Reichl, C., Horth, C., Lehr, H.A., Fischer, S., Clavel, T., Denk, G., Hohenester, S., Kobold, S.*, et al.* (2018). Nlrp3-dependent IL-1beta inhibits CD103+ dendritic cell differentiation in the gut. JCI Insight *3*, e96322.

Man, S.M., Tourlomousis, P., Hopkins, L., Monie, T.P., Fitzgerald, K.A., and Bryant, C.E. (2013). Salmonella infection induces recruitment of Caspase-8 to the inflammasome to modulate IL-1beta production. J Immunol *191*, 5239-5246.

Mantovani, A., Dinarello, C.A., Molgora, M., and Garlanda, C. (2019). Interleukin-1 and Related Cytokines in the Regulation of Inflammation and Immunity. Immunity *50*, 778-795.

Mariathasan, S., Newton, K., Monack, D.M., Vucic, D., French, D.M., Lee, W.P., Roose-Girma, M., Erickson, S., and Dixit, V.M. (2004). Differential activation of the inflammasome by caspase-1 adaptors ASC and Ipaf. Nature *430*, 213-218.

Marshman, E., Ottewell, P.D., Potten, C.S., and Watson, A.J. (2001). Caspase activation during spontaneous and radiation-induced apoptosis in the murine intestine. J Pathol *195*, 285-292.

Martin, B.N., Wang, C., Zhang, C.J., Kang, Z., Gulen, M.F., Zepp, J.A., Zhao, J., Bian, G., Do, J.S., Min, B.*, et al.* (2016). T cell-intrinsic ASC critically promotes T(H)17-mediated experimental autoimmune encephalomyelitis. Nat Immunol *17*, 583-592.

Masumoto, J., Dowds, T.A., Schaner, P., Chen, F.F., Ogura, Y., Li, M., Zhu, L., Katsuyama, T., Sagara, J., Taniguchi, S.*, et al.* (2003). ASC is an activating adaptor for NF-kappa B and caspase-8-dependent apoptosis. Biochem Biophys Res Commun *303*, 69-73.

McDaniel, M.M., Kottyan, L.C., Singh, H., and Pasare, C. (2020). Suppression of Inflammasome Activation by IRF8 and IRF4 in cDCs Is Critical for T Cell Priming. Cell Rep *31*, 107604.

McDougal, C.E., Morrow, Z.T., Kim, S., Carter, D., Stevenson, D.M., Amador-Noguez, D., Miller, M.J., and Sauer, J.-D. (2021). Prostaglandin E₂ induction by cytosolic Listeria monocytogenes in phagocytes is necessary for optimal T-cell priming. bioRxiv, 2021.2003.2023.436585.

McKee, A.S., Munks, M.W., MacLeod, M.K., Fleenor, C.J., Van Rooijen, N., Kappler, J.W., and Marrack, P. (2009). Alum induces innate immune responses through macrophage and mast cell sensors, but these sensors are not required for alum to act as an adjuvant for specific immunity. J Immunol *183*, 4403-4414.

McSorley, S.J. (2014). Immunity to intestinal pathogens: lessons learned from Salmonella. Immunol Rev *260*, 168-182.

Meng, G., Zhang, F., Fuss, I., Kitani, A., and Strober, W. (2009). A mutation in the Nlrp3 gene causing inflammasome hyperactivation potentiates Th17 cell-dominant immune responses. Immunity *30*, 860-874.

Meredith, M.M., Liu, K., Darrasse-Jeze, G., Kamphorst, A.O., Schreiber, H.A., Guermonprez, P., Idoyaga, J., Cheong, C., Yao, K.H., Niec, R.E.*, et al.* (2012).

Expression of the zinc finger transcription factor zDC (Zbtb46, Btbd4) defines the classical dendritic cell lineage. J Exp Med *209*, 1153-1165.

Mitchell, P.S., Roncaioli, J.L., Turcotte, E.A., Goers, L., Chavez, R.A., Lee, A.Y., Lesser, C.F., Rauch, I., and Vance, R.E. (2020). NAIP-NLRC4-deficient mice are susceptible to shigellosis. Elife *9*.

Miyoshi, H., and Stappenbeck, T.S. (2013). In vitro expansion and genetic modification of gastrointestinal stem cells in spheroid culture. Nat Protoc *8*, 2471-2482.

Monroe, K.M., Yang, Z., Johnson, J.R., Geng, X., Doitsh, G., Krogan, N.J., and Greene, W.C. (2014). IFI16 DNA sensor is required for death of lymphoid CD4 T cells abortively infected with HIV. Science *343*, 428-432.

Morris, S.C., Lees, A., and Finkelman, F.D. (1994). In vivo activation of naive T cells by antigen-presenting B cells. J Immunol *152*, 3777-3785.

Motta, V.N., Markle, J.G., Gulban, O., Mortin-Toth, S., Liao, K.C., Mogridge, J., Steward, C.A., and Danska, J.S. (2015). Identification of the inflammasome Nlrp1b as the candidate gene conferring diabetes risk at the Idd4.1 locus in the nonobese diabetic mouse. J Immunol *194*, 5663-5673.

Muntjewerff, E.M., Meesters, L.D., and van den Bogaart, G. (2020). Antigen Cross-Presentation by Macrophages. Front Immunol *11*, 1276.

Muri, J., Feng, Q., Wolleb, H., Shamshiev, A., Ebner, C., Tortola, L., Broz, P., Carreira, E.M., and Kopf, M. (2020). Cyclopentenone Prostaglandins and Structurally Related Oxidized Lipid Species Instigate and Share Distinct Pro- and Anti-inflammatory Pathways. Cell Rep *30*, 4399-4417 e4397.

Murphy, T.L., and Murphy, K.M. (2021). Dendritic cells in cancer immunology. Cell Mol Immunol.

Nakazawa, A., Dotan, I., Brimnes, J., Allez, M., Shao, L., Tsushima, F., Azuma, M., and Mayer, L. (2004). The expression and function of costimulatory molecules B7H and B7-H1 on colonic epithelial cells. Gastroenterology *126*, 1347-1357.

Negroni, A., Cucchiara, S., and Stronati, L. (2015). Apoptosis, Necrosis, and Necroptosis in the Gut and Intestinal Homeostasis. Mediators Inflamm *2015*, 250762.

Netea, M.G., van de Veerdonk, F.L., van der Meer, J.W., Dinarello, C.A., and Joosten, L.A. (2015). Inflammasome-independent regulation of IL-1-family cytokines. Annu Rev Immunol *33*, 49-77.

Ng, S.L., Teo, Y.J., Setiagani, Y.A., Karjalainen, K., and Ruedl, C. (2018). Type 1 Conventional CD103(+) Dendritic Cells Control Effector CD8(+) T Cell Migration, Survival, and Memory Responses During Influenza Infection. Front Immunol *9*, 3043.

Nguyen, Q.P., Deng, T.Z., Witherden, D.A., and Goldrath, A.W. (2019). Origins of CD4(+) circulating and tissue-resident memory T-cells. Immunology *157*, 3-12.

Nichols, R.D. (2017). Systemic Effects downstream of NAIP/NLRC4 Inflammasome Activation in vivo. In Molecular & Cell Biology (UC Berkeley), pp. 58.

Nichols, R.D., von Moltke, J., and Vance, R.E. (2017). NAIP/NLRC4 inflammasome activation in MRP8(+) cells is sufficient to cause systemic inflammatory disease. Nat Commun *8*, 2209.

Niess, J.H., Brand, S., Gu, X., Landsman, L., Jung, S., McCormick, B.A., Vyas, J.M., Boes, M., Ploegh, H.L., Fox, J.G.*, et al.* (2005). CX3CR1-mediated dendritic cell access to the intestinal lumen and bacterial clearance. Science *307*, 254-258.

Nikolic-Zugic, J., and Bevan, M.J. (1990). Role of self-peptides in positively selecting the T-cell repertoire. Nature *344*, 65-67.

Nordlander, S., Pott, J., and Maloy, K.J. (2014). NLRC4 expression in intestinal epithelial cells mediates protection against an enteric pathogen. Mucosal Immunol *7*, 775-785.

Noubade, R., Majri-Morrison, S., and Tarbell, K.V. (2019). Beyond cDC1: Emerging Roles of DC Crosstalk in Cancer Immunity. Front Immunol *10*, 1014.

Nystrom, S., Brave, A., Falkeborn, T., Devito, C., Rissiek, B., Johansson, D.X., Schroder, U., Uematsu, S., Akira, S., Hinkula, J.*, et al.* (2013). DNA-Encoded Flagellin Activates Toll-Like Receptor 5 (TLR5), Nod-like Receptor Family CARD Domain-Containing Protein 4 (NRLC4), and Acts as an Epidermal, Systemic, and Mucosal-Adjuvant. Vaccines (Basel) *1*, 415-443.

O'Donnell, H., Pham, O.H., Li, L.X., Atif, S.M., Lee, S.J., Ravesloot, M.M., Stolfi, J.L., Nuccio, S.P., Broz, P., Monack, D.M.*, et al.* (2014). Toll-like receptor and inflammasome signals converge to amplify the innate bactericidal capacity of T helper 1 cells. Immunity *40*, 213-224.

Odendall, C., and Kagan, J.C. (2017). Activation and pathogenic manipulation of the sensors of the innate immune system. Microbes Infect *19*, 229-237.

Orning, P., Weng, D., Starheim, K., Ratner, D., Best, Z., Lee, B., Brooks, A., Xia, S., Wu, H., Kelliher, M.A.*, et al.* (2018). Pathogen blockade of TAK1 triggers caspase-8-dependent cleavage of gasdermin D and cell death. Science *362*, 1064-1069.

Oyesola, O.O., Shanahan, M.T., Kanke, M., Mooney, B.M., Webb, L.M., Smita, S., Matheson, M.K., Campioli, P., Pham, D., Fruh, S.P.*, et al.* (2021). PGD2 and CRTH2 counteract Type 2 cytokine-elicited intestinal epithelial responses during helminth infection. J Exp Med *218*.

Palazon-Riquelme, P., and Lopez-Castejon, G. (2018). The inflammasomes, immune guardians at defence barriers. Immunology *155*, 320-330.

Palm, N.W., de Zoete, M.R., and Flavell, R.A. (2015). Immune-microbiota interactions in health and disease. Clin Immunol *159*, 122-127.

Pang, I.K., Ichinohe, T., and Iwasaki, A. (2013). IL-1R signaling in dendritic cells replaces pattern-recognition receptors in promoting CD8(+) T cell responses to influenza A virus. Nat Immunol *14*, 246-253.

Paroli, A.F., Gonzalez, P.V., Diaz-Lujan, C., Onofrio, L.I., Arocena, A., Cano, R.C., Carrera-Silva, E.A., and Gea, S. (2018). NLRP3 Inflammasome and Caspase-1/11 Pathway Orchestrate Different Outcomes in the Host Protection Against Trypanosoma cruzi Acute Infection. Front Immunol *9*, 913.

Patel, R., and Sad, S. (2016). Transcription factor Batf3 is important for development of CD8+ T-cell response against a phagosomal bacterium regardless of the location of antigen. Immunol Cell Biol *94*, 378-387.

Pedra, J.H., Sutterwala, F.S., Sukumaran, B., Ogura, Y., Qian, F., Montgomery, R.R., Flavell, R.A., and Fikrig, E. (2007). ASC/PYCARD and caspase-1 regulate the IL-18/IFN-gamma axis during Anaplasma phagocytophilum infection. J Immunol *179*, 4783-4791.

Penteado, L.A., Dejani, N.N., Verdan, F.F., Orlando, A.B., Nino, V.E., Dias, F.N., Salina, A.C.G., and Medeiros, A.I. (2017). Distinctive role of efferocytosis in dendritic cell maturation and migration in sterile or infectious conditions. Immunology *151*, 304-313.

Pham, O.H., O'Donnell, H., Al-Shamkhani, A., Kerrinnes, T., Tsolis, R.M., and McSorley, S.J. (2017). T cell expression of IL-18R and DR3 is essential for non-cognate stimulation of Th1 cells and optimal clearance of intracellular bacteria. PLoS Pathog *13*, e1006566.

Pilla, D.M., Hagar, J.A., Haldar, A.K., Mason, A.K., Degrandi, D., Pfeffer, K., Ernst, R.K., Yamamoto, M., Miao, E.A., and Coers, J. (2014). Guanylate binding proteins promote caspase-11-dependent pyroptosis in response to cytoplasmic LPS. Proc Natl Acad Sci U S A *111*, 6046-6051.

Qiu, C.C., Caricchio, R., and Gallucci, S. (2019). Triggers of Autoimmunity: The Role of Bacterial Infections in the Extracellular Exposure of Lupus Nuclear Autoantigens. Front Immunol *10*, 2608.

Radema, S.A., van Deventer, S.J., and Cerami, A. (1991). Interleukin 1 beta is expressed predominantly by enterocytes in experimental colitis. Gastroenterology *100*, 1180-1186.

Ramirez, M.L.G., Poreba, M., Snipas, S.J., Groborz, K., Drag, M., and Salvesen, G.S. (2018). Extensive peptide and natural protein substrate screens reveal that mouse

caspase-11 has much narrower substrate specificity than caspase-1. J Biol Chem *293*, 7058-7067.

Rathinam, V.A., and Fitzgerald, K.A. (2016). Inflammasome Complexes: Emerging Mechanisms and Effector Functions. Cell *165*, 792-800.

Rauch, I., Deets, K.A., Ji, D.X., von Moltke, J., Tenthorey, J.L., Lee, A.Y., Philip, N.H., Ayres, J.S., Brodsky, I.E., Gronert, K.*, et al.* (2017). NAIP-NLRC4 Inflammasomes Coordinate Intestinal Epithelial Cell Expulsion with Eicosanoid and IL-18 Release via Activation of Caspase-1 and -8. Immunity *46*, 649-659.

Rauch, I., Tenthorey, J.L., Nichols, R.D., Al Moussawi, K., Kang, J.J., Kang, C., Kazmierczak, B.I., and Vance, R.E. (2016). NAIP proteins are required for cytosolic detection of specific bacterial ligands in vivo. J Exp Med *213*, 657-665.

Reboldi, A., Dang, E.V., McDonald, J.G., Liang, G., Russell, D.W., and Cyster, J.G. (2014). Inflammation. 25-Hydroxycholesterol suppresses interleukin-1-driven inflammation downstream of type I interferon. Science *345*, 679-684.

Reis, E.S., Mastellos, D.C., Hajishengallis, G., and Lambris, J.D. (2019). New insights into the immune functions of complement. Nat Rev Immunol *19*, 503-516.

Rescigno, M., Urbano, M., Valzasina, B., Francolini, M., Rotta, G., Bonasio, R., Granucci, F., Kraehenbuhl, J.P., and Ricciardi-Castagnoli, P. (2001). Dendritic cells express tight junction proteins and penetrate gut epithelial monolayers to sample bacteria. Nat Immunol *2*, 361-367.

Rostami, A., Riahi, S.M., Haghighi, A., Saber, V., Armon, B., and Seyyedtabaei, S.J. (2017). The role of Blastocystis sp. and Dientamoeba fragilis in irritable bowel syndrome: a systematic review and meta-analysis. Parasitol Res *116*, 2361-2371.

Rubtsov, A.V., Rubtsova, K., Kappler, J.W., Jacobelli, J., Friedman, R.S., and Marrack, P. (2015). CD11c-Expressing B Cells Are Located at the T Cell/B Cell Border in Spleen and Are Potent APCs. J Immunol *195*, 71-79.

Samji, T., and Khanna, K.M. (2017). Understanding memory CD8(+) T cells. Immunol Lett *185*, 32-39.

Sancho, D., Joffre, O.P., Keller, A.M., Rogers, N.C., Martinez, D., Hernanz-Falcon, P., Rosewell, I., and Reis e Sousa, C. (2009). Identification of a dendritic cell receptor that couples sensing of necrosis to immunity. Nature *458*, 899-903.

Sano, S., Wang, Y., Evans, M.A., Yura, Y., Sano, M., Ogawa, H., Horitani, K., Doviak, H., and Walsh, K. (2019). Lentiviral CRISPR/Cas9-Mediated Genome Editing for the Study of Hematopoietic Cells in Disease Models. J Vis Exp.

Sanos, S.L., Kassub, R., Testori, M., Geiger, M., Patzold, J., Giessel, R., Knallinger, J., Bathke, B., Grabnitz, F., Brinkmann, K.*, et al.* (2017). NLRC4 Inflammasome-Driven

Immunogenicity of a Recombinant MVA Mucosal Vaccine Encoding Flagellin. Front Immunol *8*, 1988.

Santos, J.C., Boucher, D., Schneider, L.K., Demarco, B., Dilucca, M., Shkarina, K., Heilig, R., Chen, K.W., Lim, R.Y.H., and Broz, P. (2020). Human GBP1 binds LPS to initiate assembly of a caspase-4 activating platform on cytosolic bacteria. Nat Commun *11*, 3276.

Santos, J.C., Dick, M.S., Lagrange, B., Degrandi, D., Pfeffer, K., Yamamoto, M., Meunier, E., Pelczar, P., Henry, T., and Broz, P. (2018). LPS targets host guanylate-binding proteins to the bacterial outer membrane for non-canonical inflammasome activation. EMBO J *37*, e98089.

Sarhan, J., Liu, B.C., Muendlein, H.I., Li, P., Nilson, R., Tang, A.Y., Rongvaux, A., Bunnell, S.C., Shao, F., Green, D.R.*, et al.* (2018). Caspase-8 induces cleavage of gasdermin D to elicit pyroptosis during Yersinia infection. Proc Natl Acad Sci U S A *115*, E10888-E10897.

Satpathy, A.T., Kc, W., Albring, J.C., Edelson, B.T., Kretzer, N.M., Bhattacharya, D., Murphy, T.L., and Murphy, K.M. (2012). Zbtb46 expression distinguishes classical dendritic cells and their committed progenitors from other immune lineages. J Exp Med *209*, 1135-1152.

Sauer, J.D., Pereyre, S., Archer, K.A., Burke, T.P., Hanson, B., Lauer, P., and Portnoy, D.A. (2011). Listeria monocytogenes engineered to activate the Nlrc4 inflammasome are severely attenuated and are poor inducers of protective immunity. Proc Natl Acad Sci U S A *108*, 12419-12424.

Schneider, K.S., Gross, C.J., Dreier, R.F., Saller, B.S., Mishra, R., Gorka, O., Heilig, R., Meunier, E., Dick, M.S., Cikovic, T.*, et al.* (2017). The Inflammasome Drives GSDMD-Independent Secondary Pyroptosis and IL-1 Release in the Absence of Caspase-1 Protease Activity. Cell Rep *21*, 3846-3859.

Schulz, O., Hanc, P., Bottcher, J.P., Hoogeboom, R., Diebold, S.S., Tolar, P., and Reis e Sousa, C. (2018). Myosin II Synergizes with F-Actin to Promote DNGR-1-Dependent Cross-Presentation of Dead Cell-Associated Antigens. Cell Rep *24*, 419-428.

Schulze, D.H., Pease, L.R., Geier, S.S., Reyes, A.A., Sarmiento, L.A., Wallace, R.B., and Nathenson, S.G. (1983). Comparison of the cloned H-2Kbm1 variant gene with the H-2Kb gene shows a cluster of seven nucleotide differences. Proc Natl Acad Sci U S A *80*, 2007-2011.

Segovia, M., Russo, S., Jeldres, M., Mahmoud, Y.D., Perez, V., Duhalde, M., Charnet, P., Rousset, M., Victoria, S., Veigas, F.*, et al.* (2019). Targeting TMEM176B Enhances Antitumor Immunity and Augments the Efficacy of Immune Checkpoint Blockers by Unleashing Inflammasome Activation. Cancer Cell *35*, 767-781 e766.

Sellin, M.E., Muller, A.A., Felmy, B., Dolowschiak, T., Diard, M., Tardivel, A., Maslowski, K.M., and Hardt, W.D. (2014). Epithelium-intrinsic NAIP/NLRC4 inflammasome drives infected enterocyte expulsion to restrict Salmonella replication in the intestinal mucosa. Cell Host Microbe *16*, 237-248.

Selvaggi, G., Ricordi, C., Podack, E.R., and Inverardi, L. (1996). The role of the perforin and Fas pathways of cytotoxicity in skin graft rejection. Transplantation *62*, 1912-1915.

Seydoux, E., Liang, H., Dubois Cauwelaert, N., Archer, M., Rintala, N.D., Kramer, R., Carter, D., Fox, C.B., and Orr, M.T. (2018). Effective Combination Adjuvants Engage Both TLR and Inflammasome Pathways To Promote Potent Adaptive Immune Responses. J Immunol *201*, 98-112.

Shastri, N., and Gonzalez, F. (1993). Endogenous generation and presentation of the ovalbumin peptide/Kb complex to T cells. J Immunol *150*, 2724-2736.

Shi, J., Zhao, Y., Wang, K., Shi, X., Wang, Y., Huang, H., Zhuang, Y., Cai, T., Wang, F., and Shao, F. (2015). Cleavage of GSDMD by inflammatory caspases determines pyroptotic cell death. Nature *526*, 660-665.

Shi, J., Zhao, Y., Wang, Y., Gao, W., Ding, J., Li, P., Hu, L., and Shao, F. (2014). Inflammatory caspases are innate immune receptors for intracellular LPS. Nature *514*, 187-192.

Shibahara, T., Sato, N., Waguri, S., Iwanaga, T., Nakahara, A., Fukutomi, H., and Uchiyama, Y. (1995). The fate of effete epithelial cells at the villus tips of the human small intestine. Arch Histol Cytol *58*, 205-219.

Shin, M.S., Kang, Y., Lee, N., Wahl, E.R., Kim, S.H., Kang, K.S., Lazova, R., and Kang, I. (2013). Self double-stranded (ds)DNA induces IL-1beta production from human monocytes by activating NLRP3 inflammasome in the presence of anti-dsDNA antibodies. J Immunol *190*, 1407-1415.

Silva, G.K., Costa, R.S., Silveira, T.N., Caetano, B.C., Horta, C.V., Gutierrez, F.R., Guedes, P.M., Andrade, W.A., De Niz, M., Gazzinelli, R.T.*, et al.* (2013). Apoptosis-associated speck-like protein containing a caspase recruitment domain inflammasomes mediate IL-1beta response and host resistance to Trypanosoma cruzi infection. J Immunol *191*, 3373-3383.

Smedberg, J.R., Westcott, M.M., Ahmed, M., and Lyles, D.S. (2014). Signaling pathways in murine dendritic cells that regulate the response to vesicular stomatitis virus vectors that express flagellin. J Virol *88*, 777-785.

Sonnenberg, G.F., and Hepworth, M.R. (2019). Functional interactions between innate lymphoid cells and adaptive immunity. Nat Rev Immunol *19*, 599-613.

Srinivasan, A., Salazar-Gonzalez, R.M., Jarcho, M., Sandau, M.M., Lefrancois, L., and McSorley, S.J. (2007). Innate immune activation of CD4 T cells in salmonella-infected mice is dependent on IL-18. J Immunol *178*, 6342-6349.

Stuart, L.M., Paquette, N., and Boyer, L. (2013). Effector-triggered versus pattern-triggered immunity: how animals sense pathogens. Nat Rev Immunol *13*, 199-206.

Sun, T., Nguyen, A., and Gommerman, J.L. (2020). Dendritic Cell Subsets in Intestinal Immunity and Inflammation. J Immunol *204*, 1075-1083.

Suschak, J.J., Wang, S., Fitzgerald, K.A., and Lu, S. (2015). Identification of Aim2 as a sensor for DNA vaccines. J Immunol *194*, 630-636.

Svensson, M., Marsal, J., Ericsson, A., Carramolino, L., Broden, T., Marquez, G., and Agace, W.W. (2002). CCL25 mediates the localization of recently activated CD8alphabeta(+) lymphocytes to the small-intestinal mucosa. J Clin Invest *110*, 1113-1121.

Takeuchi, M., Nishizaki, Y., Sano, O., Ohta, T., Ikeda, M., and Kurimoto, M. (1997). Immunohistochemical and immuno-electron-microscopic detection of interferon-gamma-inducing factor ("interleukin-18") in mouse intestinal epithelial cells. Cell Tissue Res *289*, 499-503.

Tartey, S., and Kanneganti, T.D. (2020). Inflammasomes in the pathophysiology of autoinflammatory syndromes. J Leukoc Biol *107*, 379-391.

Theisen, E., and Sauer, J.D. (2017). Listeria monocytogenes-Induced Cell Death Inhibits the Generation of Cell-Mediated Immunity. Infect Immun *85*, e00733-00716.

Theivanthiran, B., Evans, K.S., DeVito, N.C., Plebanek, M., Sturdivant, M., Wachsmuth, L.P., Salama, A.K., Kang, Y., Hsu, D., Balko, J.M.*, et al.* (2020). A tumor-intrinsic PD-L1/NLRP3 inflammasome signaling pathway drives resistance to anti-PD-1 immunotherapy. J Clin Invest *130*, 2570-2586.

Thomas, P.G., Dash, P., Aldridge, J.R., Jr., Ellebedy, A.H., Reynolds, C., Funk, A.J., Martin, W.J., Lamkanfi, M., Webby, R.J., Boyd, K.L.*, et al.* (2009). The intracellular sensor NLRP3 mediates key innate and healing responses to influenza A virus via the regulation of caspase-1. Immunity *30*, 566-575.

Torchinsky, M.B., Garaude, J., Martin, A.P., and Blander, J.M. (2009). Innate immune recognition of infected apoptotic cells directs T(H)17 cell differentiation. Nature *458*, 78-82.

Tourlomousis, P., Wright, J.A., Bittante, A.S., Hopkins, L.J., Webster, S.J., Bryant, O.J., Mastroeni, P., Maskell, D.J., and Bryant, C.E. (2020). Modifying bacterial flagellin to evade Nod-like Receptor CARD 4 recognition enhances protective immunity against Salmonella. Nat Microbiol *5*, 1588-1597.

Tran, H.Q., Ley, R.E., Gewirtz, A.T., and Chassaing, B. (2019). Flagellin-elicited adaptive immunity suppresses flagellated microbiota and vaccinates against chronic inflammatory diseases. Nat Commun *10*, 5650.

Trunk, G., and Oxenius, A. (2012). Innate instruction of CD4+ T cell immunity in respiratory bacterial infection. J Immunol *189*, 616-628.

Tye, H., Yu, C.H., Simms, L.A., de Zoete, M.R., Kim, M.L., Zakrzewski, M., Penington, J.S., Harapas, C.R., Souza-Fonseca-Guimaraes, F., Wockner, L.F.*, et al.* (2018). NLRP1 restricts butyrate producing commensals to exacerbate inflammatory bowel disease. Nat Commun *9*, 3728.

Uribe-Querol, E., and Rosales, C. (2020). Phagocytosis: Our Current Understanding of a Universal Biological Process. Front Immunol *11*, 1066.

Vallon-Eberhard, A., Landsman, L., Yogev, N., Verrier, B., and Jung, S. (2006). Transepithelial pathogen uptake into the small intestinal lamina propria. J Immunol *176*, 2465-2469.

van de Veerdonk, F.L., Joosten, L.A., and Netea, M.G. (2015). The interplay between inflammasome activation and antifungal host defense. Immunol Rev *265*, 172-180.

van Deventer, H.W., Burgents, J.E., Wu, Q.P., Woodford, R.M., Brickey, W.J., Allen, I.C., McElvania-Tekippe, E., Serody, J.S., and Ting, J.P. (2010). The inflammasome component NLRP3 impairs antitumor vaccine by enhancing the accumulation of tumor-associated myeloid-derived suppressor cells. Cancer Res *70*, 10161-10169.

Vance, R.E., Isberg, R.R., and Portnoy, D.A. (2009). Patterns of pathogenesis: discrimination of pathogenic and nonpathogenic microbes by the innate immune system. Cell Host Microbe *6*, 10-21.

Ventura, A., Kirsch, D.G., McLaughlin, M.E., Tuveson, D.A., Grimm, J., Lintault, L., Newman, J., Reczek, E.E., Weissleder, R., and Jacks, T. (2007). Restoration of p53 function leads to tumour regression in vivo. Nature *445*, 661-665.

Vezys, V., Olson, S., and Lefrancois, L. (2000). Expression of intestine-specific antigen reveals novel pathways of CD8 T cell tolerance induction. Immunity *12*, 505-514.

Vijay-Kumar, M., Carvalho, F.A., Aitken, J.D., Fifadara, N.H., and Gewirtz, A.T. (2010). TLR5 or NLRC4 is necessary and sufficient for promotion of humoral immunity by flagellin. Eur J Immunol *40*, 3528-3534.

von Moltke, J., Trinidad, N.J., Moayeri, M., Kintzer, A.F., Wang, S.B., van Rooijen, N., Brown, C.R., Krantz, B.A., Leppla, S.H., Gronert, K.*, et al.* (2012). Rapid induction of inflammatory lipid mediators by the inflammasome in vivo. Nature *490*, 107-111.

Wandel, M.P., Kim, B.H., Park, E.S., Boyle, K.B., Nayak, K., Lagrange, B., Herod, A., Henry, T., Zilbauer, M., Rohde, J.*, et al.* (2020). Guanylate-binding proteins convert cytosolic bacteria into caspase-4 signaling platforms. Nat Immunol *21*, 880-891.

Wang, Q., Wang, Y., Ding, J., Wang, C., Zhou, X., Gao, W., Huang, H., Shao, F., and Liu, Z. (2020a). A bioorthogonal system reveals antitumour immune function of pyroptosis. Nature *579*, 421-426.

Wang, Y., Gao, W., Shi, X., Ding, J., Liu, W., He, H., Wang, K., and Shao, F. (2017). Chemotherapy drugs induce pyroptosis through caspase-3 cleavage of a gasdermin. Nature *547*, 99-103.

Wang, Y., Liu, J., Burrows, P.D., and Wang, J.Y. (2020b). B Cell Development and Maturation. Adv Exp Med Biol *1254*, 1-22.

Watson, A.J., Chu, S., Sieck, L., Gerasimenko, O., Bullen, T., Campbell, F., McKenna, M., Rose, T., and Montrose, M.H. (2005). Epithelial barrier function in vivo is sustained despite gaps in epithelial layers. Gastroenterology *129*, 902-912.

Wen, Y., and Shi, Y. (2016). Alum: an old dog with new tricks. Emerg Microbes Infect *5*, e25.

Winsor, N., Krustev, C., Bruce, J., Philpott, D.J., and Girardin, S.E. (2019). Canonical and noncanonical inflammasomes in intestinal epithelial cells. Cell Microbiol *21*, e13079.

Xi, G., Gao, J., Wan, B., Zhan, P., Xu, W., Lv, T., and Song, Y. (2019). GSDMD is required for effector CD8(+) T cell responses to lung cancer cells. Int Immunopharmacol *74*, 105713.

Xia, X., Wang, X., Cheng, Z., Qin, W., Lei, L., Jiang, J., and Hu, J. (2019). The role of pyroptosis in cancer: pro-cancer or pro-"host"? Cell Death Dis *10*, 650.

Yao, X., Zhang, C., Xing, Y., Xue, G., Zhang, Q., Pan, F., Wu, G., Hu, Y., Guo, Q., Lu, A.*, et al.* (2017). Remodelling of the gut microbiota by hyperactive NLRP3 induces regulatory T cells to maintain homeostasis. Nat Commun *8*, 1896.

Yasuda, K., Nakanishi, K., and Tsutsui, H. (2019). Interleukin-18 in Health and Disease. Int J Mol Sci *20*, 649.

Yi, Y.S. (2020). Functional crosstalk between non-canonical caspase-11 and canonical NLRP3 inflammasomes during infection-mediated inflammation. Immunology *159*, 142-155.

Zamboni, D.S., and Lima-Junior, D.S. (2015). Inflammasomes in host response to protozoan parasites. Immunol Rev *265*, 156-171.

Zanoni, I., Tan, Y., Di Gioia, M., Broggi, A., Ruan, J., Shi, J., Donado, C.A., Shao, F., Wu, H., Springstead, J.R.*, et al.* (2016). An endogenous caspase-11 ligand elicits interleukin-1 release from living dendritic cells. Science *352*, 1232-1236.

Zelenay, S., Keller, A.M., Whitney, P.G., Schraml, B.U., Deddouche, S., Rogers, N.C., Schulz, O., Sancho, D., and Reis e Sousa, C. (2012). The dendritic cell receptor DNGR-1 controls endocytic handling of necrotic cell antigens to favor cross-priming of CTLs in virus-infected mice. J Clin Invest *122*, 1615-1627.

Zhang, H., Luo, J., Alcorn, J.F., Chen, K., Fan, S., Pilewski, J., Liu, A., Chen, W., Kolls, J.K., and Wang, J. (2017). AIM2 Inflammasome Is Critical for Influenza-Induced Lung Injury and Mortality. J Immunol *198*, 4383-4393.

Zhang, J.G., Czabotar, P.E., Policheni, A.N., Caminschi, I., Wan, S.S., Kitsoulis, S., Tullett, K.M., Robin, A.Y., Brammananth, R., van Delft, M.F.*, et al.* (2012). The dendritic cell receptor Clec9A binds damaged cells via exposed actin filaments. Immunity *36*, 646-657.

Zhang, Z., Zhang, Y., Xia, S., Kong, Q., Li, S., Liu, X., Junqueira, C., Meza-Sosa, K.F., Mok, T.M.Y., Ansara, J.*, et al.* (2020). Gasdermin E suppresses tumour growth by activating anti-tumour immunity. Nature *579*, 415-420.

Zhao, J., Wang, H., Dai, C., Wang, H., Zhang, H., Huang, Y., Wang, S., Gaskin, F., Yang, N., and Fu, S.M. (2013). P2X7 blockade attenuates murine lupus nephritis by inhibiting activation of the NLRP3/ASC/caspase 1 pathway. Arthritis Rheum *65*, 3176-3185.

Zhao, Y., Shi, J., Shi, X., Wang, Y., Wang, F., and Shao, F. (2016). Genetic functions of the NAIP family of inflammasome receptors for bacterial ligands in mice. J Exp Med *213*, 647-656.

Zhao, Y., Yang, J., Shi, J., Gong, Y.N., Lu, Q., Xu, H., Liu, L., and Shao, F. (2011). The NLRC4 inflammasome receptors for bacterial flagellin and type III secretion apparatus. Nature *477*, 596-600.

Zhivaki, D., Borriello, F., Chow, O.A., Doran, B., Fleming, I., Theisen, D.J., Pallis, P., Shalek, A.K., Sokol, C.L., Zanoni, I.*, et al.* (2020). Inflammasomes within Hyperactive Murine Dendritic Cells Stimulate Long-Lived T Cell-Mediated Anti-tumor Immunity. Cell Rep *33*, 108381.

Zhong, F.L., Mamai, O., Sborgi, L., Boussofara, L., Hopkins, R., Robinson, K., Szeverenyi, I., Takeichi, T., Balaji, R., Lau, A.*, et al.* (2016). Germline NLRP1 Mutations Cause Skin Inflammatory and Cancer Susceptibility Syndromes via Inflammasome Activation. Cell *167*, 187-202 e117.

Zhou, T., Damsky, W., Weizman, O.E., McGeary, M.K., Hartmann, K.P., Rosen, C.E., Fischer, S., Jackson, R., Flavell, R.A., Wang, J.*, et al.* (2020a). IL-18BP is a secreted immune checkpoint and barrier to IL-18 immunotherapy. Nature.

Zhou, Z., He, H., Wang, K., Shi, X., Wang, Y., Su, Y., Wang, Y., Li, D., Liu, W., Zhang, Y.*, et al.* (2020b). Granzyme A from cytotoxic lymphocytes cleaves GSDMB to trigger pyroptosis in target cells. Science *368*, eaaz7548.

Zhu, J. (2018). T Helper Cell Differentiation, Heterogeneity, and Plasticity. Cold Spring Harb Perspect Biol *10*.

1